ARYABHATTA RESEARCH INSTITUTE OF OBSERVATIONAL SCIENCES

(An Autonomous Institute under DST, Govt. of India)

Manora Peak, Nainital - 263 002, India

ACADEMIC REPORT

2013 - 2014

(1st April, 2013 to 31st March, 2014)

ARIES, Academic Report: 2013 - 2014
No. 9, 86 pages

Editor: Dr. M. Gopinathan

Editorial Assistance: Mr. Arjun Singh
Mr. Prashant Kumar
Mr. Satish Kumar

Phone	:	+91 (5942) 235136
EPABX	:	+91 (5942) 233727, 233734, 233735, 232655
Fax	:	+91 (5942) 233439
E-mail	:	krc@aries.res.in
URL	:	http://www.aries.res.in/

Front Cover:
3.6-m Enclosure building at Devasthal

Front Cover-Back Page
Remote view of 3.6m Telescope Building, ARIES (Devasthal)

Back Cover:
Panoramic view of the antenna array installed over the roof-top of ARIES ST Radar building.

September, 2014

Contents

Organizational Structure

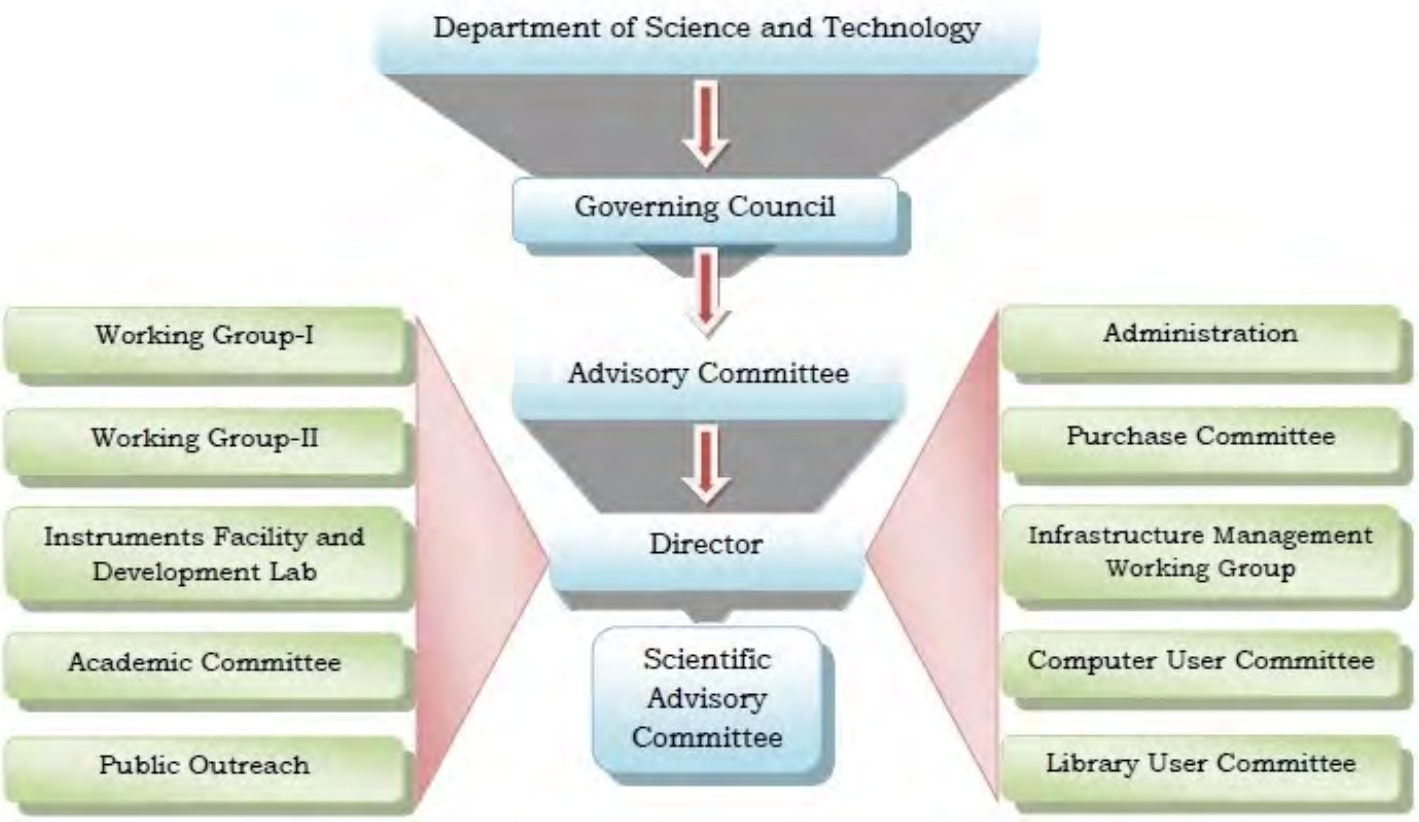

General Body and Governing Council

CHAIRPERSON

Prof. K. Kasturirangan *(till 10-10-2013)*
Member, Planning Commission,
Room No. - 119, Yojna Bhavan,
Parliament Street,
New Delhi - 110 001

Prof. S. K. Joshi *(from 11-10-2013)*
Former DG, CSIR, New Delhi

MEMBERS

Dr. T. Ramasami
Secretary, Ministry of Science and Technology, DST, Govt. of India,
New Delhi - 110 016

Mr. S. Kumar *(from 03-05-2013)*
Chief Secretary, Govt. of Uttarakhand,
Dehradun - 248 001

Ms. A. Mitra
Joint Secretary and Financial Advisor,
Ministry of Science and Technology,
DST, Govt. of India,
New Delhi - 110 016

Prof. J. V. Narlikar *(till 30-09-2013)*
Emeritus Professor, Inter University Centre for Astronomy and Astrophysics,
Pune University Campus, Ganeshkhind,
Pune - 411 007

Prof. P. C. Agrawal
405, Vigyan, Scientists CHS, Plot no.-23, Sector – 17, Vashi,
Navi Mumbai – 400 703

Prof. S. Hasan
Director, Indian Institute of Astrophysics,
Sarjapur Road,
Bangalore - 560 034

Prof. S. K. Ghosh
Director, National Centre for Radio Astrophysics, Pune University Campus,
Ganeshkhind, Pune - 411 007

Prof. D. Bhattacharya
Inter University Centre for Astronomy and Astrophysics, Pune University Campus,
Ganeshkhind,
Pune - 411 007

Prof. Ram Sagar *(till 21-05-2013)*
Dr. Wahab Uddin *(from 24-08-2013)*
(Member Secretary)
Acting Director, ARIES,
Manora Peak,
Nainital – 263 002

Mr. T. Bhattacharyya *(till 27-12-2013)*
(Non – Member Secretary)
Registrar, ARIES, Manora Peak,
Nainital - 263 002

Finance Committee

CHAIRPERSON

Prof. Ram Sagar *(till 21-05-2013)*
Dr. Wahab Uddin *(from 24-08-2013)*
Acting Director, ARIES,
Manora Peak,
Nainital - 263 002

MEMBERS

Ms. A. Mitra
Joint Secretary and Financial Advisor,
Ministry of Science and Technology,
DST, Govt. of India,
New Delhi - 110 016

Prof. P. C. Agrawal
405, Vigyan, Scientists CHS,
Plot no.- 23, ,
Sector – 17, Vashi,
Navi Mumbai – 400 703

Dr. Brijesh Kumar *(from 24-09-2013)*
Scientist-E, ARIES,
Manora Peak,
Nainital - 263 002

Mr. T. Bhattacharyya *(till 27-12-2013)*
Dr. A. Omar *(from 28-12-2013 to 02-03-2014)*
Dr. S. B. Pandey *(from 03-03-2014)*
(Member Secretary)
Acting Registrar, ARIES, Manora Peak,
Nainital - 263 002

Advisory Committee

CHAIRPERSON

Prof. S. K. Joshi
Former DG, CSIR
New Delhi

MEMBERS

Prof. P. C. Agrawal
405, Vigyan, Scientists CHS,
Plot no.- 23, ,
Sector – 17, Vashi,
Navi Mumbai – 400 703

Prof. G. Srinivasan
Former Professor,
RRI, Bangalore

Mr. Navin Chandra Sharma
Advisor, ARIES,
Manora Peak, Nainital

Representative of DST
New Delhi

Dr. Wahab Uddin
(Member-Convener)
ARIES, Manora Peak,
Nainital

Statutory Committee

The Scientific Advisory Committee (SAC)

Prof. Dipankar Bhattacharya
(Chairman)
IUCAA, Pune

Prof. D. K. Ojha
(Member)
TIFR, Mumbai

Prof. D. Banarjee
(Member)
IIA, Bangalore

Prof. A. Subramaniam
(Member)
IIA, Bangalore

Prof. B. Paul
(Member)
RRI, Bangalore

Prof. Jairam N. Chengalur
(Member)
NCRA, Pune

Prof. Vinayak Sinha
(Member)
ISSER, Mohali

3.6m Telescope Project Management Board (PMB)

Dr. P. C. Agrawal
(Chairman)
Mumbai

Prof. G. Srinivasan
(Vice Chairman)
Bangalore

Prof. T. G. K. Murthy
(Member)
ISRO, Bangalore

Prof. S. N. Tandon
(Member)
IUCAA, Pune

Prof. S. Anathakrishnan
(Member)
Pune University, Pune

Prof. T. P. Prabhu
(Member)
IIA, Bangalore

Mr. S. C. Tapde
(Member)
ECIL, Hyderabad

Prof. A. S. Kirankumar
(Member)
S. A. C., Ahmedabad

Prof. R. Srinivasan
(Member)
VIT, Bangalore

Prof. Pramesh Rao
(Member)
NCRA, Pune

Prof. Ram Sagar(till 21-05-2013)
(Convener)
ARIES, Nainital

Dr. Wahab Uddin
(Member - Convener)
ARIES, Nainital

Stratosphere Troposphere (ST) Radar Project Management Committee (PMC)

Prof. B. M. Reddy,
(Chairman)
NGRI, Hyderabad

Prof. Ram Sagar,
(Member)
ARIES, Nainital

Dr. P. Sanjeeva Rao
(Member)
DST, New Delhi

Mr. G. Viswanathan
(Member)
ISRAD, Bangalore

Dr. M. Satyanarayana
(Member)
Trivandrum

Dr. Manish Naja
(Convener)
ARIES, Nainital

Prof. A. Jayaraman
(Member)
NARL, Tirupati, AP

Prof. R. N. Keshavamurthy
(Member)
IITM, Pune

THE YEAR IN REVIEW

Wahab Uddin
Acting Director

It gives me immense pleasure to present the 9th Academic Report of ARIES. The highlights of the achievements made by ARIES in many fronts during the period of 2013-14 are presented. I am happy to say that ARIES has made significant progress in research and in setting up of the world class facilities for the astronomy and atmospheric science community. Progress has also been made in the human resource and infrastructure development, academic activities, instrumentation and public outreach.

ARIES scientists are actively engaged in research and development, providing guidance to the research scholars, collaborating with other national and international institutes in setting up new observing facilities and organizing workshops and meetings. Other than this they are also taking active participation in popularizing Astronomy & Astrophysics and Atmospheric Sciences among younger minds. The engineers are actively engaged in the in-house development of new software and hardware components for our existing and up-coming facilities. Currently, there are a total of 26 scientists, 14 engineers, 17 administrative and support staffs, 43 scientific and technical staffs, 14 laboratory assistants, 7 post doctoral fellows/research associates and 27 research scholars. The research activities of the institute are classified into three working groups, namely, Working group – I, Working group – II and the Instrument Facility and Design Laboratory (IFDL). The members of the respective groups have collectively published a total of 60 papers in refereed journals with majority of them being in relatively high impact factor journals. Extracts from some of the results published are presented in this issue of the annual report. A total of 6 Ph.D. theses have been awarded and two research scholar have submitted their thesis. ARIES scientists are also engaged in various national and international research projects. Highlights from their projects are also presented.

With regards to the status of the two major projects, the most significant development has been the near completion of the enclosure building for the 3.6 m telescope at Devasthal. The rolling shutters have been installed and the sheeting of the enclosure was also complete. The welding of the sheets on the dome structure was in progress. Ground trolleys also have been fabricated and placed. The dome structure was fabricated on the main ring beam of the structural building. Testing of the dome rotation, slit operation and wind screen movement is in

progress. Several tests were conducted on the telescope pier using geophones and piezoelectric sensors to measure various frequency modes. This measurement is important since the resonance frequency of the pier and the telescope have to be well separated to avoid the transfer of energy between the two. An observatory control software has been developed in-house to control the telescope, the instruments, the weather station and dome using single graphical user interface.

The Statosphere Troposphere Radar is currently being operated with 49 elements. Several experiments are being conducted and test profiles are generated for one cluster consisting of 49 TRMs and antennae to seven clusters. Fine tuning of the radar system is in progress. Recently, an uninterrupted power supply unit was installed.

ARIES is actively participating in the Thirty Meter Telescope project. Recently, a high level committee was constituted under the chairmanship of Prof. Ramesh Koul of BARC to evaluate the technical proposals submitted to manufacture Segmented Support Assemblies (SSAs) by various Indian manufacturers. Based on the recommendations of the committee, the contract for manufacturing the prototypes was awarded to two companies, M/s Avasarala Tech Ltd. and M/s Godrej. ARIES scientists are participating in various other work packages of the project. For instance, we are modeling the contribution of the polarization by the mirror, manufacturing of the leaf-springs for SSAs and in the development of the back-end instruments.

It has been ten years since the commissioning of one of the backend instruments, AIMPOL, which was built by ARIES team back in 2004. The instrument has produced one Ph.D. and 15 publications in the refereed journals. The demand for the instrument is growing as the year progresses.

A number of new instruments are either in design stage (Near Infrared Spectrograph) or in the fabrication stage (ADFOSC). The near infrared spectrograph will be jointly build by TIFR and ARIES. A formal contract was signed between two institutes.

In March 2004, ARIES became an autonomous institute under the administrative control of the Department of Science and Technology. Since then, ARIES has made significant contributions in the fields of Astronomy & Astrophysics and Atmospheric Sciences both in terms of research and in setting up state-of-the-art facilities. Over the past ten years, there has been a consistent increase in the number of faculties and research scholars who have jointed the institute. ARIES has produced a total of 403 publications from March, 2004 to March, 2014. A good number of them are in journals with relatively high impact factor. ARIES has produced 34 Ph.Ds over the last ten year period. The decadal report card of ARIES is shown graphically here.

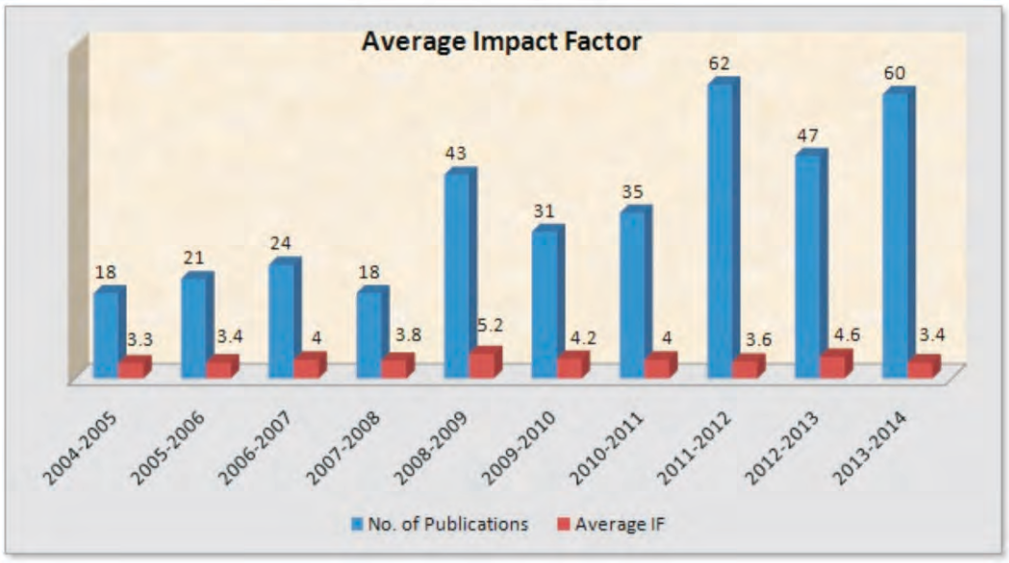

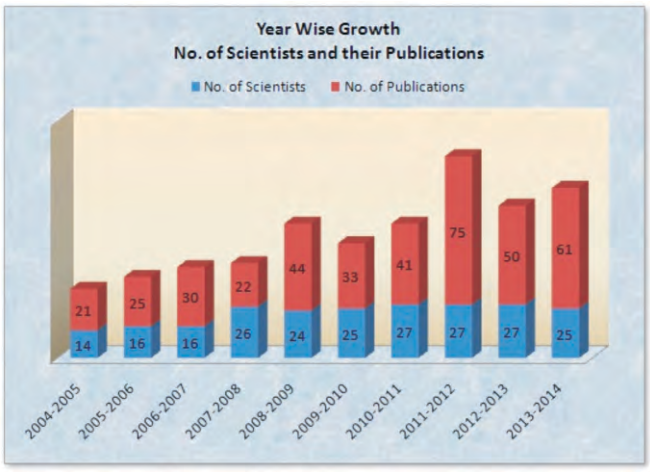

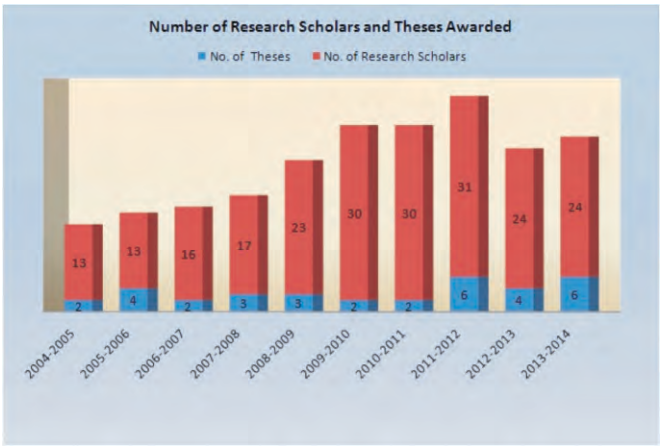

Year wise average impact factor of the publications, number of scientists and research scholars, and theses awarded are shown. The publications with no information on their impact factor are excluded from the analysis.

Astronomers and other staff members of ARIES are committed to disseminate the knowledge gathered by us to the general public. We have a very active public outreach program under which we conduct slide shows, sky watch programs etc., for the public. We visit schools to inculcate scientific temper in the minds of younger generation. Recently, a planetarium has been installed in the campus for the general public to simulate virtual sky.

ARIES continued its efforts in the implementation of the official language. The institute continues to provide a constructive and essential role in building an equitable work environment by safeguarding the interests of SCs and STs as well as women. All the necessary steps have been taken at appropriate instances in the implementation of important schemes as directed by the Government of India.

Research Highlights

The scientists of ARIES carry out research mainly on topics related to Astronomy and Astrophysics, Atmospheric Sciences and Instrumentation related to both the above fields. The research activities of the institute are classified into three working groups. The groups are

1. Working Group – I (WG I) – Galactic & Extragalactic Astronomy
2. Working Group – II (WG II) – Solar Physics & Atmospheric Sciences
3. Instruments Facility and Design Laboratory (IFDL)

The working group members are responsible for the annual planning and monitoring of the activities on the academic and technical matters. In this section, a brief account of the scientific and instrument related achievements of the institute, during the period of 2013-14, are presented.

Research Working Group – I

All the scientists working on the topics related to the Galactic and Extragalactic astronomy are the members of WG – I. The group consists of 19 scientists. The group members are actively involved in collaboration with scientists of national and international institutions in the fields of near earth objects, individual stars, star formation, open cluster systems, globular cluster systems, LMC, quasars, supernovae and numerical simulations. The extracts of the publications made by the members are briefly presented below.

Galactic Astronomy

1. Study of near earth objects

Polarimetric studies of Comet C/2009 P1(Garradd)

In an interesting study carried out on the comet C/2009 P1 (Garradd), it was concluded that this comet belongs to a dusty comet family. The conclusions were made based on the imaging polarimetry of the comet phase angles 28°.2, 28°.1 and 21°.6 using the IUCAA Faint Object Spectrograph (IFOSC) mounted on the 2m telescope of IUCAA, Pune on 21st and 22nd March 2012 and the ARIES Imaging Polarimeter (AIMPOL) mounted on the 1.04-m Sampurnanand Telescope of ARIES, Naintital on 23rd May, 2012. Both narrow-band filters (Red: λ = 0.684μm, $\triangle\lambda$ = 0.009μm) and broadband filters (Red: λ = 0.630μm, $\triangle\lambda$ = 0.120μm) were used in the observations. Jet activity was observed in the treated intensity map of the comet Garradd in the March observation runs. These jets were mainly seen towards the solar direction and extend up to 5100 km from the photocenter. The tail-ward extension is 1800 km and seems to be fainter. Like other comets, Garradd shows negative polarization at phase angle 21°.6. The observed linear polarization data of comet Garradd was compared with other comets observed by different investigators in the past at the same phase angles. It was found that the comets 67P/Churyumov –Gerasimenko, 22P/Kopff, 1P/Halley, C/1990 K1(Levy), 4P/Faye, and C/1995 O1 (Hale-Bopp) were also observed at phase-angle close to 28° and comet 47P/Ashbrook-Jackson at 21°.6. The polarization values coming out from the present analysis matched well with the results obtained for the dusty comets at such phase angles. It was also noticed that the linear polarization of the

dust coma showed a high degree of linear polarization at 28°, but not exceptionally high as comet Hale-Bopp.

2. Study of individual stars

Evidence of multiple slow acoustic oscillations in the stellar flaring loops of Proxima Centauri

The detection of magnetohydrodynamic (MHD) waves and oscillations may be very important in diagnosing the local plasma conditions of the coronae of the Sun and the Sun-like stars by implying the principle of MHD seismology. Detection of MHD waves is gaining sufficient importance in the development of refined MHD seismology techniques to understand the properties of solar as well as stellar coronae. The origin of such oscillations is still under debate, however, it has recently been proposed that they can be produced by several mechanisms during flaring activities in the magnetized coronae of stars. With this aim the first observational evidence of multiple slow acoustic oscillations in the post-flaring loops of the corona of Proxima Centauri using XMM-Newton observations was shown. The signature of periodic oscillations localized in the decay phase of the flare in its soft (0.3–10.0 keV) X-ray emissions was found. Using the standard wavelet tool, multiple periodicities of 1261 s and 687 s were found. These bursty oscillations persist for durations of 90 minutes and 50 minutes, respectively, for more than three cycles. The intensity oscillations with a period of 1261 s may be the signature of the fundamental mode of slow magnetoacoustic waves with a phase speed of 119 km s^{1} in a loop of length 7. $5x10^{9}$ cm, which is initially heated, producing the flare peak temperature of 33 MK and later cooled down in the decay phase and maintained at an average temperature of 7.2 MK. The other period of 687 s may be associated with the first overtone of slow magnetoacoustic oscillations in the flaring loop. The fundamental modes of oscillations show dissipation with a damping time of 47 minutes. Figure 1 shows the variation of the exponentially decaying harmonic function along with the detrended light curve of Proxima Centuri . The period ratio P1/P2 is found to be 1.83, indicating that such oscillations are most likely excited in longitudinal density stratified stellar loops. The density scale height of the stellar loop system was estimated as 23 Mm, which is smaller than the hydrostatic scale height of the hot loop system, and implies the existence of non-equilibrium conditions.

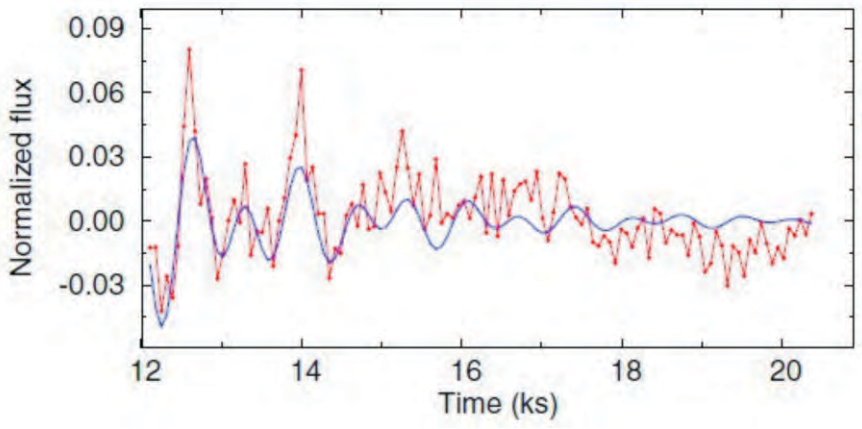

Figure1. *X-ray light curve of Proxima Cetauri during the post-flare phase as observed from XMM-Newton satellite along with the best fit damped harmonic function.*

Additional polarised standards in the fields of known bright standard stars

Broad-band (VRI) polarimetric observations of a number of stars that are present towards the fields of already known bright polarised standard stars namely BD+59° 389, HD 19820, and HD 25443 were carried out. These three relatively bright stars were observed continuously for various observing programs using ARIES Imaging Polarimeter (AIMPOL) attached with 104-cm Sampurnanand Telescope since 2006 to correct for any polarisation position angle offset. Since AIMPOL is an imaging polarimeter with a field-of-view of ~8 arcmin diameter, it is possible to get polarisation measurements of a number of relatively faint stars that are present within the field-of-view of the AIMPOL towards the above three bright polarised standards. Based on these compiled observations for a relatively long duration, the constancy of the degree of polarisation and position angles of these stars were monitored. With the help of some statistical tests, five stars in the field of BD+59° 389 and two stars in the field of HD 19820 have been identified as stars that could be used as additional polarised standard stars. Since these additional stars are relatively fainter than the known polarised standards, they could be observed with bigger aperture telescopes (like 2-m) without them getting saturated.

3. Study of star forming regions

Stars are formed in molecular clouds that are classified according to their masses. While low mass stars are formed in all types of molecular clouds, massive stars are formed in Giant molecular clouds. The star formation process is classified into two modes - spontaneous and triggered. Massive stars can both terminate and trigger star formation in their vicinity. Triggered star forming regions are actively studied by the scientists of ARIES to understand the process involved.

Magnetic fields in cometary globules – IV. LBN 437

Cometary globules (CGs) are molecular clouds that show a compact bright-rimmed head and a faint tail geometry that extends from the head and points away from a nearby photoionizing source. Pre-existing small, dense cores distributed in giant molecular clouds when exposed to the radiation from newly formed OB-type stars in a central OB association can develop cometary head–tail morphology. Thus, a compression of non-collapsing clumps by shock waves driven by the warm surface gas could possibly drive the inner cores to instability and gravitational collapse, triggering star formation. The effects of magnetic fields of various strengths and orientations on the formation and evolution of dense pillars and CGs at the boundaries of H II regions were investigated by various authors using 3D hydrodynamical simulations including photoionizing radiative transfer simulations. As a part of an ongoing effort to map the magnetic geometry in Galactic CGs, optical polarimetry of LBN 437 was carried out. LBN 437 is considered to be at a distance of 460 pc on the basis of spatial and kinematic coincidence with the Lac OB1 association.

Background starlight while passing through molecular clouds gets polarized due to the aligned, aspheric dust grains present in them. The polarization is produced because of the selective extinction suffered by the light as it passes through the aspheric dust grains that are aligned to the magnetic field of the clouds. The selective extinction due to aligned, aspherical dust grains would make the polarization vectors trace the direction of the plane-of-the-sky magnetic field of the molecular clouds. The contribution to the observed polarization depends on the amount of dust grains with sizes comparable to the wavelength of background starlight being observed. The magnetic

field geometry of LBN 437 is found to follow the curved shape of the globule head (as shown in **Figure 2**). This could be due to the drag that the magnetic field lines could have experienced because of the ionization radiation from the same exciting source that caused the cometary shape of the cloud. The orientation of the outflow from the Herbig A4e star, LkHα 233 (or V375 Lac), located at the head of LBN 437, is found to be parallel to both the initial (prior to the ionizing source was turned on) ambient magnetic field (inferred from a star HD 214243 located just in front of the cloud) and the Galactic plane.

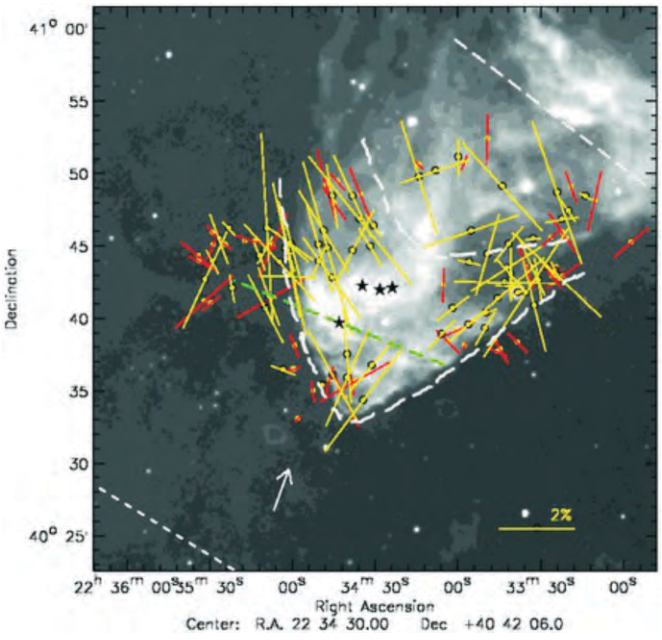

Figure 2. *Polarization vectors plotted on the 0∘.65 × 0∘.65 WISE 12 μm image of LBN 437 after subtracting the foreground polarization contribution. The red vectors correspond to the values with P/σp ≥ 1 and the yellow vectors show the values with P/σp ≥ 2. The dashed line vector in green colour shows the direction of outflow from the star LKHα 233. The white dashed line shows the Galactic plane at b = −15°. Positions of LKHα 230, LKHα 231 and LKHα 232 are identified using star symbols in black colour. The thick broken curve represents the inferred magnetic field orientation from the polarization vectors. An arrow is drawn to show the spatial direction of 10 Lac. A vector with 2 per cent polarization is shown as reference.*

Young stellar population and ongoing star formation in the HII complex Sh2-252

An extensive survey of the star-forming complex Sh2-252 with an aim to explore its hidden young stellar population as well as to understand the structure and star formation history has been carried out for the first time. This complex is composed of five prominent embedded clusters associated with the subregions A, C, E, NGC 2175s and Teu 136. Using the IR colour-colour criteria, they identified 577 YSOs, of which, 163 are Class I, 400 are Class II and 14 are transition disc YSOs, suggesting a moderately rich number of YSOs in this complex. Spatial distribution of the candidate YSOs shows that they are mostly clustered around the subregions in the western half of the complex, suggesting enhanced star formation activity towards its west. Morphology of the region in the 1.1 mm map shows a semicircular shaped molecular shell composed of several clumps and YSOs bordering the western ionization front of Sh2-252. Detailed analyses suggest that next generation star formation is currently under way along this border and that possibly fragmentation of the matter collected during the expansion of the H II region as one of the major processes is responsible for such stars. The densest concentration of YSOs (mostly Class I, ~0.5 Myr) was found at the western outskirts of the complex, within a molecular clump associated with water and methanol masers and it was also suggested that this site is indeed a site of cluster formation at a very early evolutionary stage, sandwiched between the two relatively evolved H II regions A and B.

4.Study of star clusters

Stars rarely form in isolation. Observations suggest that most of the stars in a galaxy form in star clusters or groups. Young open star clusters constitute samples of stars of different masses with approximately the same age, distance and chemical composition, and these are homogeneous with respect to these properties. The stellar initial mass function is considered a fundamental property of any population and it is a key observational input to the theory of star formation as well as evolution of star clusters and galaxies.

Structure and mass function of three young open clusters

Using newly obtained photometric data from 104-cm Sampurnanand telescope, a study was initiated to determine fundamental parameters (age, distance, mass function), to probe star formation processes and the dynamical evolution of three open clusters NGC 2129, NGC 1502 and King 12. Deep photometry reaching down to V = 22 magnitude, in conjunction with UBVRI data for these clusters were analysed to determine reddening E(B-V) of 0.77±0.05, 0.68±0.05 and 0.63±0.05 magnitude respectively, and distances of 2.1±0.1, 1.0±0.1 and 2.5±0.1 kpc. The ages of the clusters have been obtained after fitting theoretical stellar evolutionary models for solar metallicity isochrones with the observed color magnitude diagrams. This gives an age of 10.0±0.1 Myr for all the three clusters. Photometric as well as astrometric criteria were used to ascertain membership of stars in the direction of star clusters. Subsequently, luminosity function was constructed which was further used to estimate the mass functions by employing theoretical stellar evolutionary isochrones. The entire cluster region mass function slopes were obtained. It was found that the changes in the mass function slope of King12 are significantly different

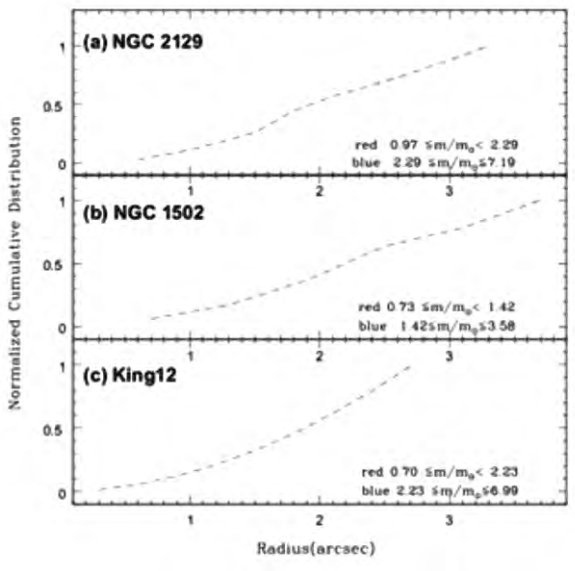

Figure 3. *Cumulative radial distribution of stars in different mass regions.*

compared to NGC 2129 and NGC 1502 from inner region to outer region. The mass function slope for King 12 is steeper at larger radii. The dynamical relaxation times for all the three clusters were found to be less than the age of the clusters. This indicates that all these clusters are dynamically relaxed. It was further shown that for NGC 1502 and King 12, passing off of low mass stars from the inner region of the clusters to the halo occurred during the course of evolution (see **Figure 3**).

X-ray Observations of Eight Young Open Star Clusters

The physical origin of X-ray emission from pre-main sequence low mass stars is poorly understood. X-ray studies of low mass pre-main sequence stars in young clusters with ages less than 5 Myrs and in between 30 to 100 Myrs are studied by many authors in past. Due to the lack of study of stars of age between 5-50 Mys, it is still not clear at which stage of the pre-main sequence evolution, the low mass stars deviate from the X-ray saturation level

(L_X/L_{bol} ~ 3.0), and which fundamental parameters govern their X-ray emission. To understand this, eight young open clusters with age spread of 4-46 Myrs were studied. Using X-ray data of these clusters obtained from XMM-Newton satellite, the probable cluster memberships of the X-ray sources have been established on the basis of multi-wavelength archival data, and samples of 152 pre-main sequence low mass (<2$M_\odot$), 36 intermediate mass (2–10$M_\odot$) and 16 massive (>10$M_\odot$) stars have been generated. X-ray spectral analyses of high

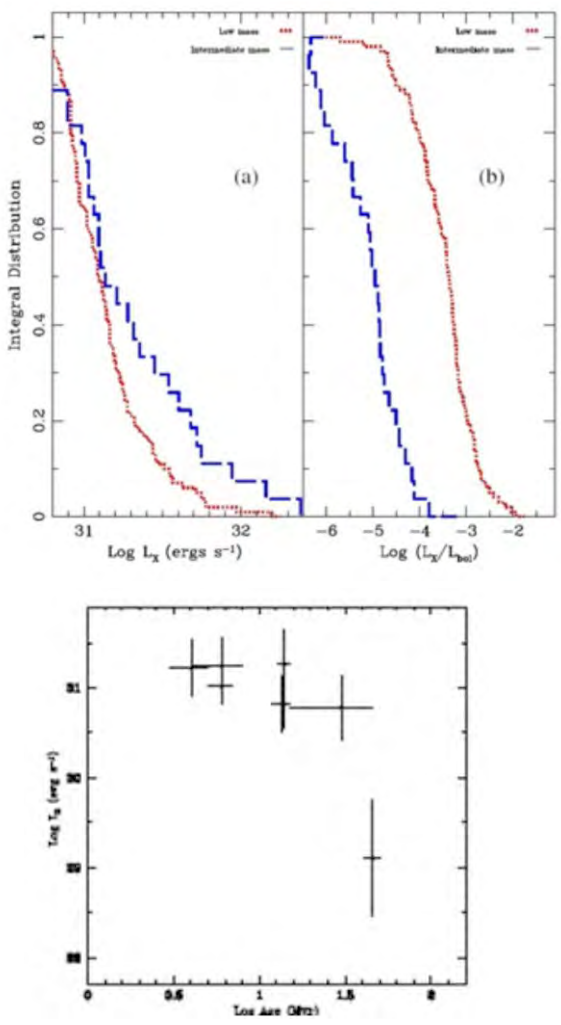

Figure 4. *(a) X-ray luminosity distribution (b) X-ray as function of of age.*

mass stars revealed the presence of high temperature plasma with temperature <2 keV, and mean L_X/L_{bol} of $10^{-6.9}$. In the case of pre-main sequence low mass stars, the plasma temperatures have been found to be in the range of 0.2 keV to 3 keV with a median value of ~1.3 keV, with no significant difference in plasma temperatures during their evolution from 4 to 46 Myrs. The X-ray luminosity and L_X/L_{bol} distribution of low an intermediate mass stars is shown in **Figure 4(a)**, indicating that the strength of X-ray activity in intermediate mass stars is weaker than in the low mass stars. Another possibility is that the origin of X-ray emission from intermediate mass stars might be as a result of X-ray emission coming from an unresolved nearby low mass PMS star. **Figure 4(b)** shows the L_X/L_{bol} as function of age indicating that a deviation of L_X/L_{bol} for low mass stars with masses greater than 1.4$M_\odot$ from X-ray saturation may occur at an age of 4 - 8 Myrs.

X-ray flares observed from six young stars located in the region of star clusters NGC 869 and IC 2602

Using XMM-Newton observations, seven intense X-ray flares from six stars (LAV 796, LAV 1174, SHM20023734, 2MASS 02191082+5707324, V553 Car, V557 Car) located in the region of young open star clusters NGC 869 and IC 2602 were detected. These flares showed a rapid rise (10–40 min) and a slow decay (20–90 min) feature. **Figure 5** shows the X-ray light curve of these six stars showing flaring event. The X-ray luminosities during the flares in the energy band 0.3–7.5 keV were found to be in the range of $10^{29.9\text{-}31.7}$ erg s^{-1}. The strongest flare was observed with peak of the flare to the quiescent intensity ratio of ~13. The maximum temperature during the flares has been found to be ~100 MK. The semi-loop lengths for the flaring loops were estimated to be of the order of 10^{10} cm. The physical

parameters of the flaring structure, the peak density, pressure and minimum magnetic field required to confine the plasma have been derived and found to be consistent with flares from pre-main sequence stars in the Orion and the Taurus-Auriga-Perseus region.

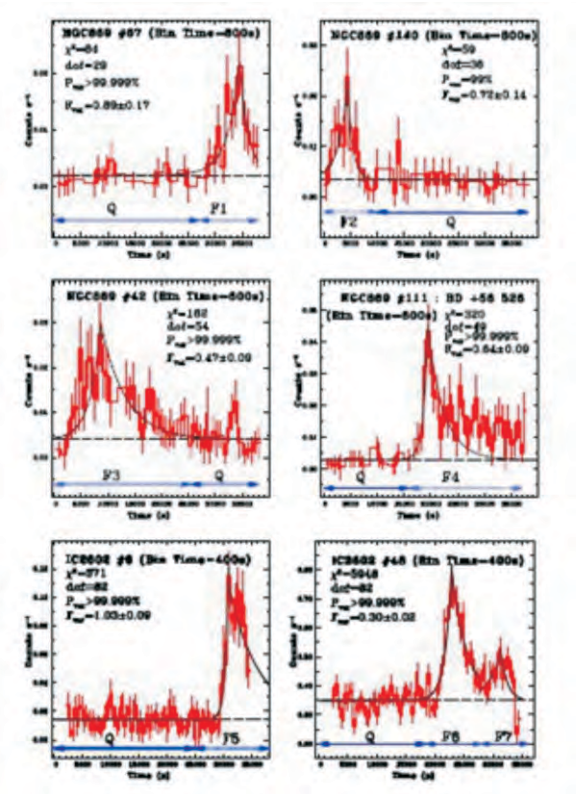

Figure 5. *X-ray light curve of the six pre-main-sequence stars in the cluster NGC 869 and IC 2602 showing flare characteristics. The best fit exponential rise and decay times are also shown.*

Apex determination and detection of stellar clumps in the open cluster M 67

Using the proper motion catalogue of M67 made by Yadav et al. 2008, the cluster apex coordinates, the substructures and membership analysis in the central part (34'X33') of the cluster were carried out. The individual stellar apexes method developed earlier and classical technique of proper motion diagrams in coordinate system connected with the apex were used. The neighbour-to-neighbour distance technique was applied to detect space details. The membership list was corrected and some stars were excluded from the most probable membership list. The apex coordinates have been determined as: A0=132.97+/-0.81 deg and D0=11.85+/-0.90 deg. The 2D-space star density field was analysed and high degree of inhomogeneity was found.

Photometric studies of open star clusters Haffner 11 and Czernik 31

Using broadband UBVI CCD photometric observations, two open clusters Haffner 11 and Czernik 31 were selected and studied. The radii of the clusters are determined as 3'.5 and 3'.0 for Haffner 11 and Czernik 31 respectively. Using two colour (U-B) versus (B-V) diagram they determined the reddening E(B-V)=0.50±0.05 magnitude and 0.48 ± 0.05 magnitude for the cluster Haffner 11 and Czernik 31 respectively. Using 2MASS JHKs and optical data, E(J-K)= 0.27±0.06 magnitude and E(V-K)=1.37±0.06 magnitude for Haffner 11 and E(J-K)=0.26±0.08 magnitude and E(V-K)= 1.32±0.08 magnitude for Czernik 31 were determined. The analysis indicated normal interstellar extinction law in the direction of both the clusters. Distance of the clusters was determined as 5.8 ± 0.5 kpc for Haffner 11 and 3.2 ± 0.3 kpc for Czernik 31 by comparing the ZAMS with the color-magnitude diagram of the clusters. The age of the cluster has been estimated as 800 ± 100 Myr for Haffner 11 and 160 ± 40 Myr for Czernik 31 using the stellar isochrones of metallicity Z=0.019.

Photometric study of five open star clusters

UBVRI photometry of the five open clusters Czernik 4, Berkeley 7, NGC 2236, NGC 7226 and King 12 were made using 104-cm Sampurnanand

telescope, Nainital. Fundamental cluster parameters such as foreground reddening E(B-V), distance, and age have been derived by means of the observed two colour and colour-magnitude diagrams, coupled to comparisons with theoretical models. E(B-V) values range from 0.55 to 0.74 mag, while ages derived for these clusters range from ~ 10 to ~ 500 Myr. The spatial structure, mass function and mass segregation effects were also examined. This study shows that evaporation of low mass stars from the halo of the clusters increases as they evolve. The cluster extents are 3.5 arcmin for Czernik 4, 4.1 arcmin for Berkeley 7, 4.4 arcmin for NGC 2236, 3.7 arcmin for NGC 7226 and 4.0 arcmin for King 12. The mass function slope for whole cluster region of the presented cluster sample was found to be comparable to the Salpeter value. All the clusters show effects of mass segregation.

Photometric study of open clusters - II. Stellar population and dynamical evolution in NGC 559

In order to investigate the occurrence of pulsations in A- and F-type stars in different galactic environments, UBVRI photometry of stars in the field of the NGC 559, a moderately populated and heavily reddened intermediate-age open cluster was performed. The fundamental parameters of this cluster was accurately determined by identifying 22 most probable members using photometric and kinematic criteria. The luminosity function and the mass function for the cluster main sequence were also constructed and found evidence of mass segregation in this dynamically relaxed cluster.

Characterization of the Praesepe star cluster by photometry and proper motion with 2MASS, PPMx2 and Pan-stars

Membership identification, specially of low mass stars, is vital in determining the properties of a star cluster. The low-mass members could be used to trace the dynamical history, such as mass segregation, stellar evaporation, or tidal stripping, of a star cluster in its Galactic environment. The member candidates of the intermediate-age Praesepe cluster (M44) with stellar masses ~ 0.11–2.4 $M_{\odot}$ were identified using Panoramic Survey Telescope And Rapid Response System and Two Micron All Sky Survey photometry, and PPMXL proper motions. Within a sky area of 3 degree radius, this most complete and reliable membership determination yield 872 members. The cluster shows a distinct binary track above the main sequence, with a binary frequency of 20%–40%, and a high occurrence rate of similar mass pairs. The mass function is consistent with that of the disk population but shows a deficit of members below 0.3 $M_{\odot}$ (**Figure 6**). A clear mass

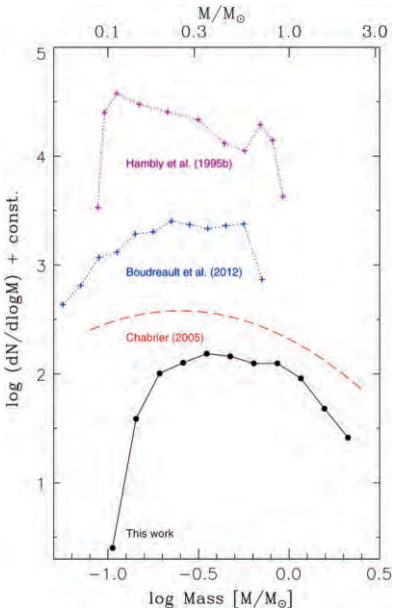

Figure 6. *Mass function of Praesepe (solid line). The mass function of the disk population by Chabrier (2005; long-dashed line) and the mass function of Praesepe as found by Hambly et al. (1995b; representing a rising mass function) and Boudreault et al. (2012; representing a falling mass function) (representing a falling mass function; dashed lines) are also shown. Each is shifted vertically for clarity.*

segregation is evident, with the lowest-mass members in the present sample being evaporated from the cluster.

5. Study of globular cluster systems

Galactic globular clusters are among the oldest population of the Universe. Their studies are of particular interest to know about the evolution history of the Milky Way. In a globular cluster, most commonly found variables are RR Lyrae stars ("cluster-type" variables). RR Lyrae being short period variables are easy to detect by means of observational data of few hours. They have long been used as standard candles, making the distance estimation of a cluster possible. Studying their pulsational properties enables the astronomers to probe the internal structure of the stars. They are particularly important to study the evolution of low mass stars. RR Lyrae also play important role in studying the horizontal branch (HB) morphology of the globular cluster.

Variable stars in the globular cluster NGC 4590 (M68)

Observations of NGC 4590 in Johnson *V* filter using 104-cm Sampurnanand telescope were carried out to identify possible variable stars. The cluster was observed for 10 nights during January–March, 2011. Time series photometry of the globular cluster NGC 4590 using images in *V* band for 10 nights were carried out. Phased light curves and periods for 40 known variables have been revised. No significant change in the periods or in the variability type was observed. RRab stars show some change in Blazhko effect. Nine new probable variables were identified. Phased light curves and periods of the variable stars were determined. Five new probable variables were categorized as Bailey type RRc stars, while for 4 variables only periods and phased light curves were provided. The classification for these 4 variables remains undetermined. The status of membership of variable stars has been assigned on the basis of comparison with Lane et al. (2011).

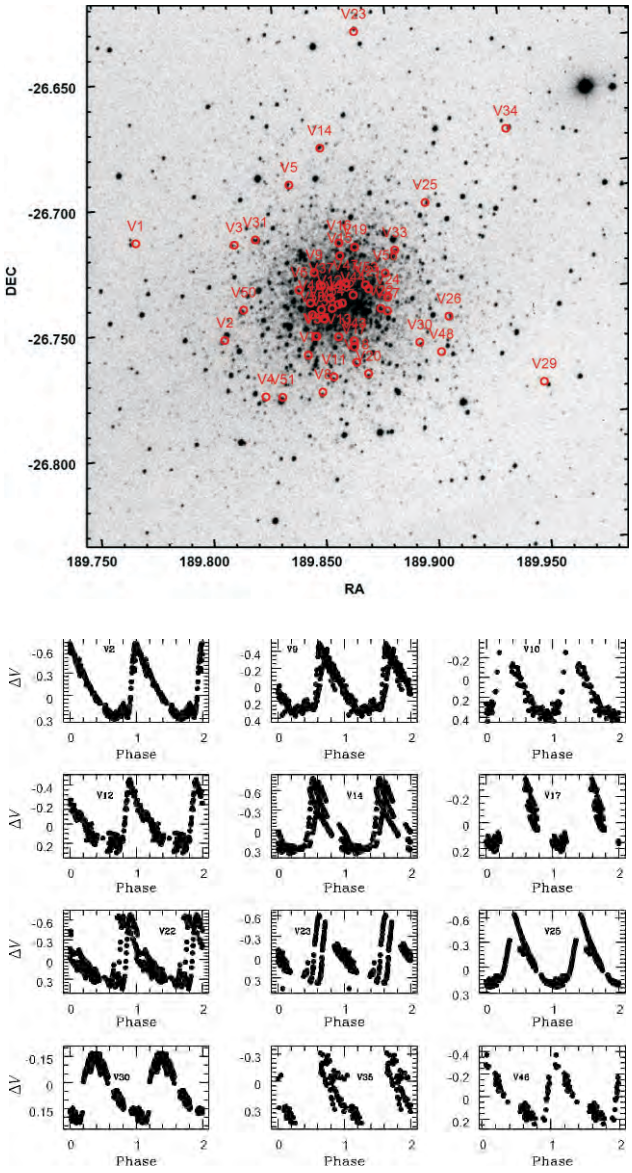

Figure 7. *Top panel: The observed region of NGC 4590 in V band. The open circles represent the variables identified in the present work. RA and DEC are given in degree. Bottom panel: Phased light curves for known RRab type stars. The ΔV shows differential instrumental magnitude.*

Extragalactic Astronomy

1. Study of local galactic group

Star formation history of the Large Magellanic Cloud

Cepheids have been used to understand the history of star formation as they are intrinsically bright, easily observable and ubiquitous in the Large Magellanic Cloud (LMC). They are very good candidates to understand the star formation activity during the last 30 – 600 Myrs as typical life of the Population I Cepheids lie in this time span. The use of Cepheids as tracers of young stellar populations comes from the fact that they obey a period-luminosity and a mass-luminosity relation. OGLE has detected thousands of new Cepheid and determined very accurate parameters like periods, magnitudes and amplitudes.

With the aim to understand the Cepheids period and age distributions in the LMC and to study the spatial distribution of the Population I Cepheids in order to examine the star formation scenarios in the LMC, a study was initiated using high quality photometric data from the OGLE-III survey. This survey acquired high quality photometric data in the V and I bands for stars in a 40 square degree region of the LMC using the 1.3-m Warsaw telescope at the Las Campanas Observatory, Chile. In this work, a sample of 3087 CCs was taken including 1849 FU and 1238 FO Cepheids as their ages can be determined accurately from their pulsation periods. Taking advantage of a large and homogeneous sample of CCs in the OGLE catalogue, the period distribution of CCs was studied and found a bimodal period distribution. The study showed that these two peaks actually correspond to FU and FO mode Cepheids showing maxima in the distribution at log P = 0.49±0.01 and 0.28±0.01, respectively. When the two class of pulsating stars were combined together, after converting periods of FO Cephieds to that of the corresponding FU Cepheids, and employing a period-age relation derived through the LMC cluster Cepehids, an age distribution comprising of only a single age maxima with a pronounced peak at the log (Age) =8.2±0.1 was identified. The study showed that the Cepheids are not homogeneously distributed throughout the LMC bar but lie in the clumpy structures. The clumps are more prominent in the southeast region, far-off from the optical center of the LMC. The enhanced population of Cepheids suggests that a major star formation episode has

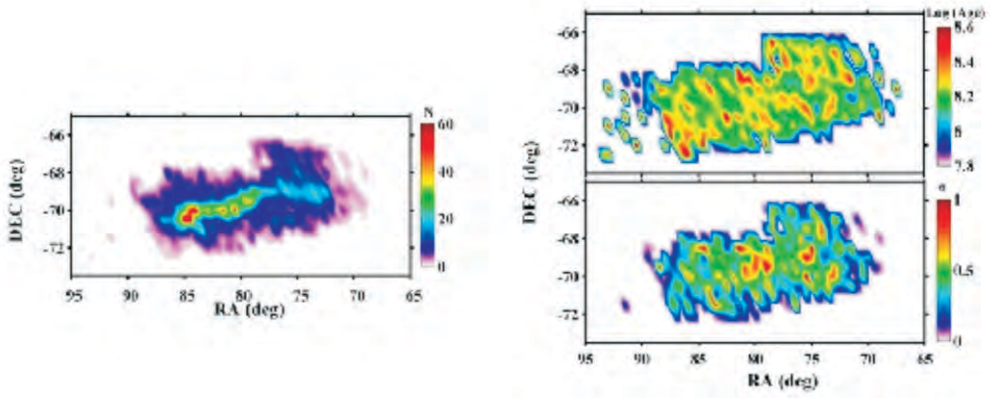

Figures 8: *The map of CC distribution in the RA-DEC plane with bin sizes of 0.5x0.5 deg^2. The left panel shows frequency distribution, top-right panel shows the log(Age) distribution, and bottom-right panel shows map for the dispersion in log(Age).*

taken place at around 125 – 200 Myr ago in the LMC. However, a combined analysis of CCs and star clusters put this value at around 125 Myr. It is believed that star formation episode at this time scale was triggered due to close encounter between the SMC and the LMC. On a comparison of spatial distribution of CCs and star clusters, a mutual avoiding of clumps of the CCs and star clusters was noticed in the LMC (**Figure 8**).

2. Study of Active Galactic Nuclei

Dependence of Residual Rotation Measure (RRM) on Intervening MgII Absorbers at Cosmic Distances

Magnetic field plays a key role in the structural and dynamical evolution of the Universe, but there are no methods for its direct measurement. Faraday Rotation (FR) is one of the powerful probes to measure the strength of magnetic field over the cosmic time scale. Such investigation till now has been done with few dozen of sources using rotation measure at 6cm. With the aim to extend such investigation using larger sample size (few hundred) and to test whether the influence of intervening system seen on the rotation measure at 6cm do also persist on the rotation measure carried at 21cm or not?, A sample of source for which both rotation measure and SDSS spectra are available was compiled. The sample was then divided into two groups - one consisting of intervening MgII absorber and another without such intervening systems. These sub-samples, with and without MgII systems, allow to quantify the effect of intervening absorbers on the rotation measure. From this study an excess of extragalactic contribution in the standard deviation of residual rotation measure (RRM i.e., the

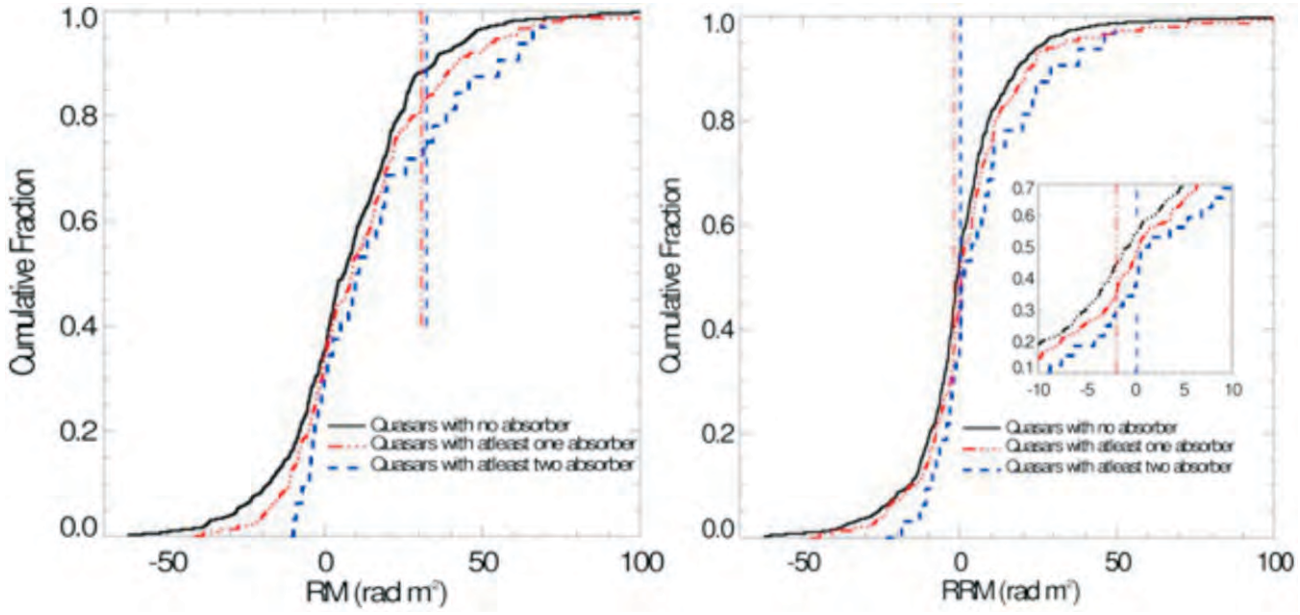

Figure 9. *Left panel: Cumulative distribution of the Rotation Measure (RM), for the quasar with no absorber (thick line), with at least one absorber (dashed-doted line) and with at least two absorber (dashed line). right panel: same as left, for the Residual Rotation Measure (RRM) measurements, the inset displays the zoom-in on the maximum distance between the distribution functions.*

rotation measure after subtracting contribution from our own galaxy), of about 8.11 ± 4.83 rad m^{-2} in the sample with an intervening Mg II absorber as compared to the sample without an Mg II absorber was found. Based on the results it was concluded that the intervening absorbers could contribute to the enhancement of RRM at around 21 cm wavelength, as was found earlier for rotation measure measurements at around 6 cm wavelength (see **Figure 9**).

Incidence of strong Mg II absorbers towards different types of quasars

A comparative study, first of its kind, of strong Mg II absorbers (W_r ~ 1.0 Å) seen towards radio-loud quasars of core-dominated (CDQ) and lobe-dominated (LDQ) types and normal quasars (QSOs) was performed. The CDQ and LDQ samples were derived from the Sloan Digital Sky Survey Data Release 7 after excluding known `broad-absorption-line' quasars and blazars. The Mg II associated absorption systems having a velocity offset v < 5000 km s^{-1} from the systemic velocity of the background quasar were also excluded. Existing spectroscopic data for redshift-matched sightlines of 3975 CDQs and 1583 LDQs, covering an emission redshift range 0.39-4.87, were analysed and 864 strong Mg II absorbers were found, covering the redshift range 0.45-2.17. The conclusions reached using this well-defined large data set of strong Mg II absorbers are:

(i) the number density, dN/dz, towards CDQs shows a small, marginally significant excess (~9 per cent at 1.5σ significance) over the estimate available for QSOs.

(ii) in the redshift space, this difference is reflected in terms of a 1.6σ excess of dN/dz over the

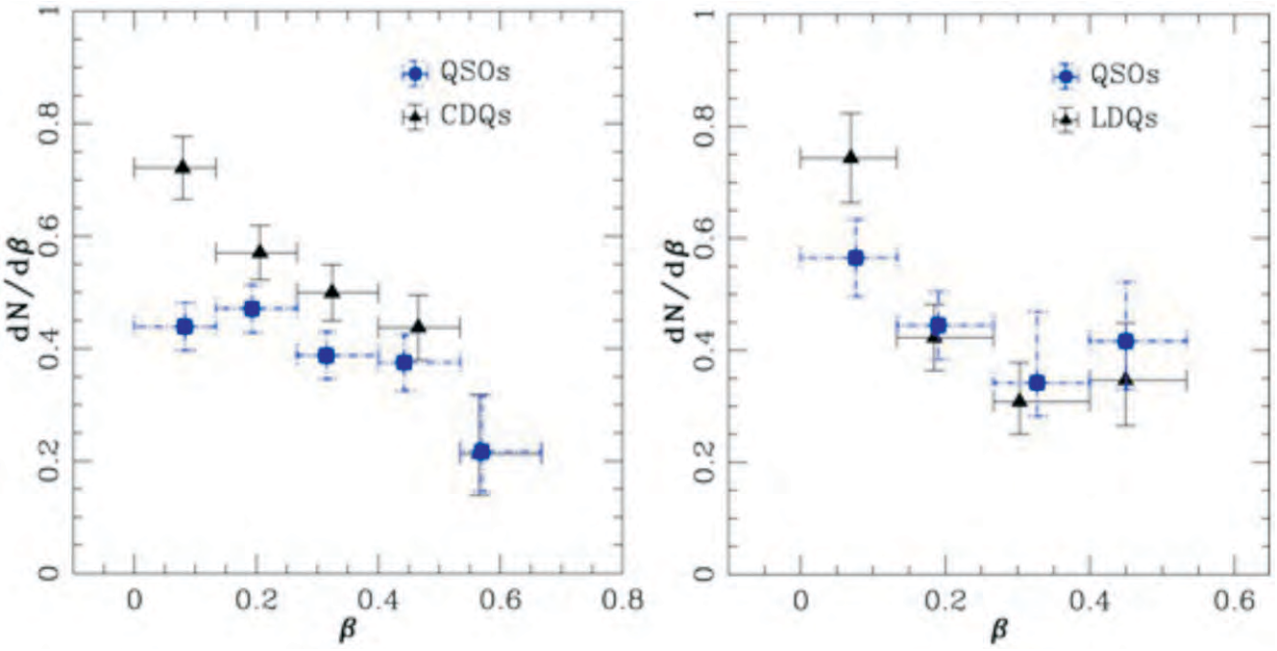

Figure 10. *Left: the incidence of MgIIstrong absorbers as a function of offset velocity, v = βc, measured relative to the quasar rest frame, for CDQs and QSOs. Right: same for LDQs and QSOs. The horizontal bars indicate the velocity bins and vertical bars the 1σ uncertainty from counting statistics.*

QSOs, within the narrow redshift interval 1.2-1.8.

(iii) the dN/dβ distribution (with β = v/c) for CDQs shows a significant excess (at 3.75σ level) over the distribution found for a redshift- and luminosity-matched sample of QSOs, at β in the range 0.05-0.1(see **Figure 10**).

Based on these results it was inferred that a significant fraction of strong Mg II absorption systems seen in this offset velocity range are probably associated with the CDQs and might be accelerated into the line of sight by their powerful jets and/or due to the accretion-disc outflows close to the line of sight. Support to this scenario comes from a consistency check in which only the spectral range corresponding to β > 0.2 were considered. The computed redshift distribution for strong Mg II absorbers towards CDQs now shows excellent agreement with that known for QSOs, as indeed is expected for purely intervening absorption systems. Thus, it appears that for CDQs (and blazars) the associated strong Mg II absorbers can be seen at much larger velocities relative to the nucleus than the commonly adopted upper limit of 5000 km s^{-1}.

Signature of outflows in strong Mg II absorbers in quasar sightlines

The excess absorber seen towards blazars (about a factor of 2) and core dominated quasars (about 10 per cent) vis-a-vis normal QSOs, give rise to the possibility of cool gas outflows associated to their jets. The firm conclusion for jet based above excess still await the realistic numerical modelling of jet–ambient gas interaction, however, an alternative scenario, which could be more plausible, is the dust- or radiation-driven outflows. For instance, if there is some contribution to dN/dz of strong Mg II absorber from these outflows, then one would expect the AGN luminosity to be statistically correlation with the velocity offset of the strong Mg II absorber relative to the background AGN. With this aim, a large sample of QSOs was extracted from the SDSS and determined number density of MgII absorbers to search for any correlation with the bolometric luminosity of the background sources. The velocity offset (β = v/c) showed a power-law increase with L_{bol}, with a slope ~1/4. Further, such a relation of β with L_{bol} is expected for outflows driven by scattering of black hole radiation by dust grains and which are launched from the innermost dust survival radius. Based on these findings, it was concluded that a significant fraction of the strong Mg II absorbers, in the range of β = 0-0.4, may be associated with the quasars themselves.

Intra-night optical variability of radio-quiet weak emission line quasars

Recently with the advent of large surveys such as SDSS, a sample of dozens of WLQs marked by abnormally weak broad emission lines (i.e. rest-frame EW < 15.4 Å for the Lyα+NV emission-line complex) have been reported, similar to BL Lac objects (BLOs). However, in contrast to BLOs (and much like RQQSOs) radio-quiet WLQs (RQWLQs) are found to exhibit low optical polarization, as a result they may be the, long sought, radio-quiet BLOs in which optical emission arises predominantly from a relativistic jet of synchrotron radiation. In this scenerio, RQWLQs are expected to be more variable, therefore one strategy to confirm or verify such a possibility is to characterize the intranight optical variability (INOV) of RQWLQs. Based on a recently started programme, a search for intranight optical variability (INOV) among radio-quiet `weak-line-quasars' (RQWLQs) was initiated for the first time. Eight members of this class were observed on 13 nights in the R band, such that each source was monitored continuously at least once for a minimum duration of about 3.5 hours, using the recently installed 130-cm telescope at Devasthal. Statistical analysis of the differential light curves was carried out using two versions of the F test.

Based on the INOV data acquired so far, the RQWLQ population appears to exhibit stronger INOV activity as compared to the general population of radio-quiet quasars, but similar to the INOV known for radio-loud quasars of non-blazar type. To improve upon this early result, as well as to extend the comparison to blazars, a factor of ~2 improvement in the INOV detection threshold would be needed. Such efforts are underway, motivated by the objective to search for the elusive radio-quiet blazars using INOV observations. Based on the INOV data acquired so far, the RQWLQ population appears to exhibit stronger INOV activity as compared to the general population of radio-quiet quasars, but similar to the INOV known for radio-loud quasars of non-blazar type.

Anti-correlated optical flux and polarization variability in BL Lac

The results of photometric (V band) and polarimetric observations of the blazar BL Lac during 2008–2010 using TRISPEC attached to the KANATA 1.5 m telescope in Japan were presented. The data reveal a great deal of variability ranging from days to months with detection of strong variations in fractional polarization. The V band flux strongly anticorrelates with the degree of polarization during the first of two observing seasons but not during the second. The direction of the electric vector, however, remained roughly constant during all of our observations. These results are consistent with a model with at least two emission regions being present, with the more variable component having a polarization direction nearly perpendicular to that of the relatively quiescent region so that a rising flux can produce a decline in degree of polarization. We also computed models involving helical jet structures and single transverse shocks in jets and show that they might also be able to agree with the anticorrelations between flux and fractional polarization.

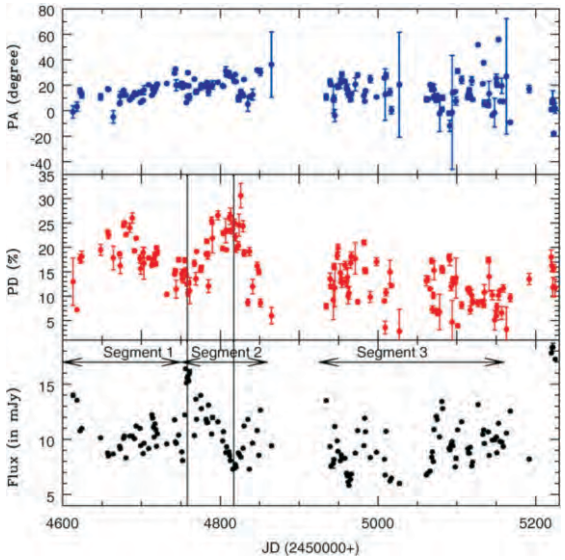

Figure 11. *V passband light curve of the BL Lac over the two observing seasons during the period May 2008–Jan 2010 from KANATA telescope (lower panel), its percentage polarization (middle panel), and polarization angle (in upper panel). Segments 1, 2, and 3 are marked in the bottom panel of the figure.*

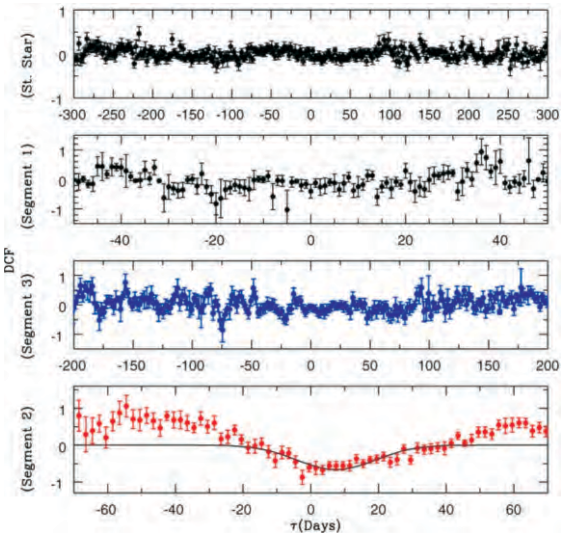

Figure 12. *DCF for an unpolarized standard star is shown in the top panel. The DCF between optical flux and polarization degree for the portions of the observations presented and marked in Figure 1 as Segment 1, Segment 3, and Segment 2 are shown moving downward; the solid line represents the fitted Gaussian function in Segment 2.*

The 72-h WEBT microvariability observation of blazar S5 0716 + 714 in 2009

The international Whole Earth Blazar Telescope (WEBT) consortium planned and carried out three days of intensive micro-variability observations of S5 0716 + 714 from February 22, 2009 to February 25, 2009. This object was chosen due to its bright apparent magnitude range, its high declination, and its very large duty cycle for micro-variations. The long continuous optical micro-variability light curve of 0716+714 obtained during the multi-site observing campaign is presented. During this period the Blazar showed almost constant variability over a 0.5 mag range. Thirty-six observatories in sixteen countries participated in this continuous monitoring program and twenty of them submitted data for compilation into a continuous light curve. The resulting light curve is presented here for the first time. Observations from participating observatories were corrected for instrumental differences and combined to construct the overall smoothed light curve. The light curve was analyzed using several techniques including Fourier transform, Wavelet and noise analysis techniques. Those results led us to model the light curve by attributing the variations to a series of synchrotron pulses. The observed microvariations in this extended light curve is interpreted in terms of a new model consisting of individual stochastic pulses due to cells in a turbulent jet which are energized by a passing shock and cool by means of synchrotron emission. An excellent fit was obtained to the 72-hour light curve with the synchrotron pulse model.

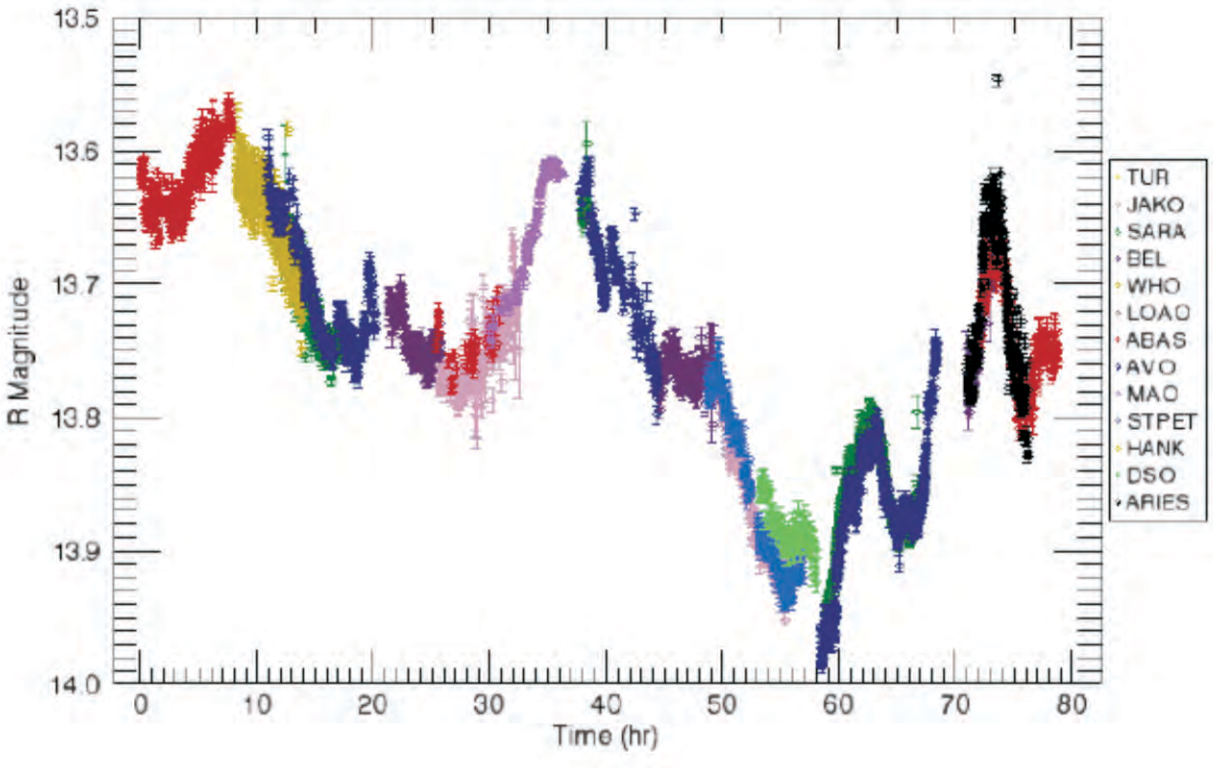

Figure 13. *Raw light curve of S5 0716+714 obtained by the compilation of some of the high quality data by major contributors. The light curves contributed from each observatory is plotted together with different symbols indentifying the observatory according to the codes given in Table 1.*

Radio to gamma-ray variability study of blazar S5 0716+714

The results of a series of radio, optical, X-ray, and γ-ray observations of the BL Lac object S5 0716+714 carried out between April 2007 and January 2011 are presented. The multifrequency observations were obtained using several ground and space based facilities. The intense optical monitoring of the source reveals faster repetitive variations superimposed on a long-term variability trend on a time scale of ~350 days. Episodes of fast variability recur on time scales of ~60−70 days. The intense and simultaneous activity at optical and γ-ray frequencies favors the synchrotron self-Compton mechanism for the production of the high-energy emission. Two major low-peaking radio flares were observed during this high optical/γ-ray activity period. The radio flares are characterized by a rising and a decaying stage and agrees with the formation of a shock and its evolution. It was found that the evolution of the radio flares requires a geometrical variation in addition to intrinsic variations of the source. Different estimates yield robust and self-consistent lower limits of $\delta \geqslant 20$ and equipartition magnetic field $B_{eq} \geqslant 0.36$ G. Causality arguments constrain the size of emission region $\theta \leqslant 0.004$ mas. We found a significant correlation between flux variations at radio frequencies with those at optical and γ-rays. Theoptical/GeV flux variations lead the radio variability by ~65 days. The longer time delays between low-peaking radio outbursts and optical flares imply that optical flares are the precursors of radio ones. An orphan X-ray flare challenges the simple, one-zone emission models, rendering them too simple. Here we also describe the spectral energy distribution modeling of the source from simultaneous data taken through different activity periods.

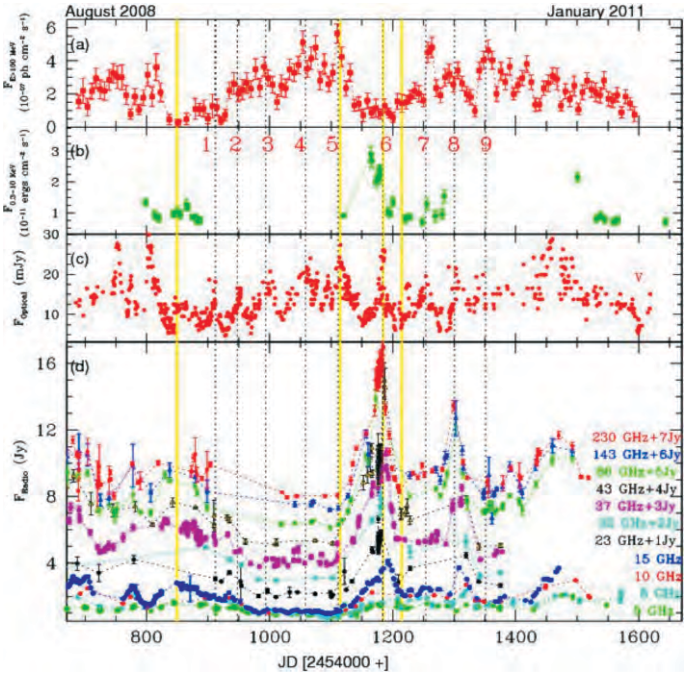

Figure 14. *Light curves of 0716+714 from γ-ray to radio wavelengths a) GeV light curve at E > 100 MeV; b) X-ray light curve at 0.3−10 KeV; c) optical V passband light curve and d) 5 to 230 GHz radio light curves. Vertical dotted lines are marked w.r.t. different optical flares labeling the broadband flares as "G" for γ-rays, "X" for X-rays, "O" for optical and "R" for Radio followed by the number close to flare. The yellow area represents the period for which we construct the broadband SEDs of the source (see Sect. 3.5 for details).*

3. Study of core-collapse supernovae

It is understood that the core-collapse supernovae explosions mark end stages in the life of massive stars having initial masses greater than about eight solar masses. Majority of the core-collapse events are classified as Type II SNe, which show presence of hydrogen lines in their spectra, and their progenitors are thought to have retained enough hydrogen until time of explosion. About 90% of all Type II are sub-classified as Type IIP, which displays plateau of about hundred days in its V-band light curves. On the other hand, Type Ibc events are commonly referred as stripped-envelope supernovae, as their outer layers of hydrogen and/or helium are stripped off before the explosion.

The observed physical parameters derived from light curves and spectra of SNe provide important clues to the understanding of the explosion mechanism as well as to the nature of progenitor stars. Several questions on SNe remain unanswered. For example, the stellar evolution models suggest that type IIP SNe originate from red supergiants having initial masses between 9-25$M_{\odot}$, having an upper mass cut of 32$M_{\odot}$, for solar metallicity stars, however, the observational constraints are ambiguous and the mass of progenitors recovered from the analysis of pre-explosion archival HST images for 20 IIP SNe lie in the range 9-17 $M_{\odot}$, while the hydrodynamical modelling of light curves for a handful of well studied IIP SNe indicate that they primarily originate from 15-25 $M_{\odot}$, progenitors. Some of the problems in inferring physical properties are the lack of good quality data for nearby SNe. The explosion geometry in cases of type Ibc are still debatable.

Supernova 2012aw - a high-energy clone of archetypal Type IIP SN 1999em

Supernova 2012aw was discovered in a nearby (~ 9.9 Mpc) galaxy, M95, on 16.1 March, 2012 and it was one of the brightest events of that year. Dense UBVRI/griz photometric follow-up observations spanning 4 to 270 days were carried out using 104-cm and 130-cm telescopes of ARIES, see **Figure 15**. Low-resolution optical spectroscopic observations were also collected using 2m HCT and

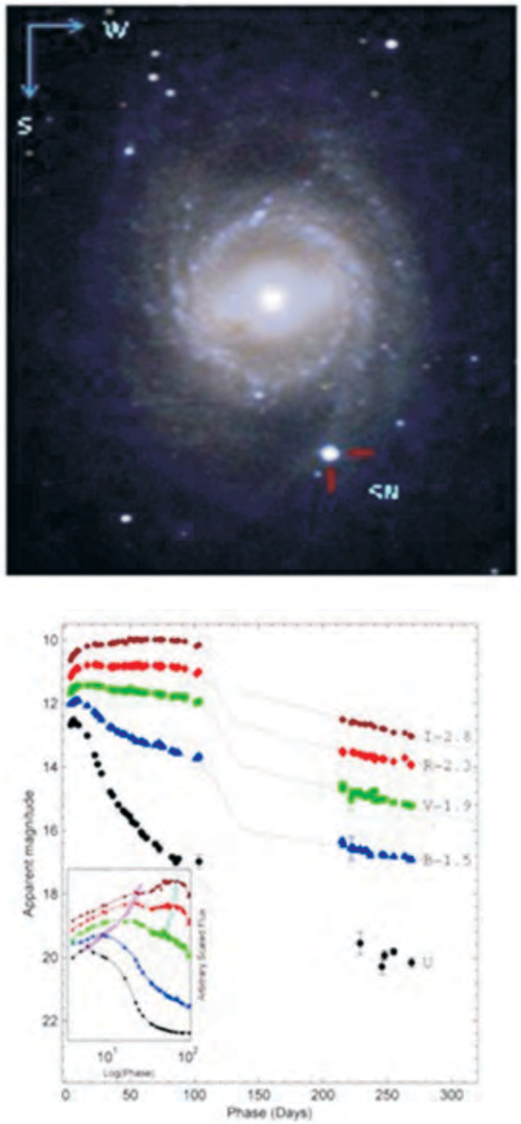

Figure 15. *SN 2012aw in M95. The BVR composite image taken from 104-cm ST telescope is shown. The photometric light-curve in UBVRI system. The evolution of early time light-curve is shown in inset.*

2m IGO telescope. The light-curve characteristics, colors, bolometric luminosity and the presence and evolution of prominent spectral features are found to have striking similarity with the archetypal IIP SN 1999em. The early time observations of SN 2012aw clearly showed minima in the light-curve of V, R and I bands near 37 days after explosion and this was suggested to be first observational evidence for emergence of recombination phase. Detailed SYNOW modelling has been done to study the spectral evolution, line identification and expansion velocity profile. The velocity profile is similar to other archetypal IIP SN but about ~ 600 km/s, higher than its clone SN 1999em. A comparison of ejecta velocity properties with that of existing radiation-hydrodynamical simulations indicate that the energy of explosion lies in the range 1 to $2x10^{51}$ erg; a further comparison of nebular phase OII doublet luminosity with SNe 2004et and 1987A indicate that the mass of progenitor star is about 14-15$M_{\odot}$. The presence of high-velocity absorption features in the mid-to-late plateau and possibly in early phase spectra show signs of interaction between ejecta and the circumstellar matter; being consistent with its early-time detection at X-ray and radio wavebands.

Distance Determination to Eight Galaxies Using Expanding Photosphere Method

Type II SNe are also recognized as independent extragalactic distance indicators. However, in view of diverse nature of their properties as well as availability of good quality data, more and newer events need to be tested for their applicability as reliable distance indicators. Early photometric and spectroscopic data of Type IIP SNe 1999em, 1999gi, 2005cs, 2006bp, 2008in, 2009bw, and 2012aw are used to derive distances to their host galaxies using the expanding photosphere method (EPM). For five of these, EPM is applied for the first time. In this work, EPM application was improved by using SYNOW, estimated velocities and by semi-deconvolving the broad-band filter responses while deriving color temperatures and black-body angular radii. **Figure 16** shows the EPM fitting plot for SN 2012aw using two dilution factors. It was found that the derived EPM, distances are consistent with that derived using other redshift independent methods.

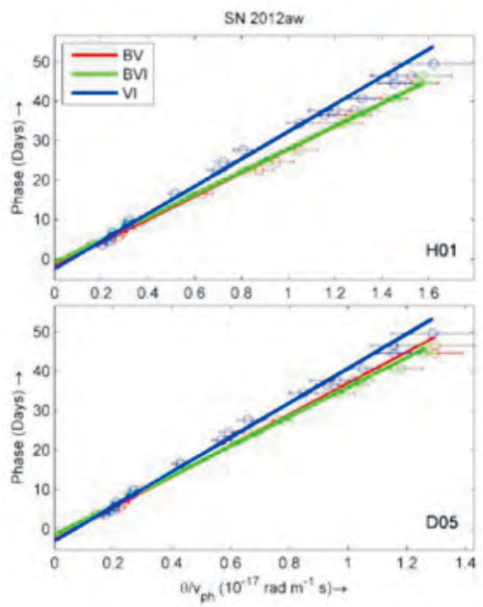

***Figure 16.**: EPM fitting for SN 2012aw using two sets of dilution factors, in combination with three filter sets.*

SN 2007uy - metamorphosis of an aspheric type Ib explosion

The supernova 2007uy was discovered in the galaxy NGC 2770 on 31.7 Dec 2007. The photometric observations were collected from 104-cm telescope. Analysis of the photometric observations revealed this explosion as an energetic event with peak absolute R-band magnitude −18.5 ± 0.16, which is about 1 magnitude brighter than the mean value (−17.6 ± 0.6) derived for well observed Type Ibc events. The SN is highly extinguished, E(B − V) = 0.63 ± 0.15 magnitude, mainly due to foreground material present in the host galaxy. From optical light curve modeling,

researchers determined about 0.3 $M_\odot$ radioactive 56 Ni is produced and roughly 4.4 $M_\odot$ material was ejected during this explosion with liberated energy $\sim 15 \times 10^{51}$ erg, indicating the event to be an energetic one. Through optical spectroscopy, a clear aspheric evolution of several line-forming regions was noticed, but no dependency of asymmetry was seen on the distribution of 56 Ni inside the ejecta. The SN shock interaction with the circumstellar material is clearly noticeable in radio follow-up observations, presenting a synchrotron self-absorption dominated light curve with a contribution of free–free absorption during the early phases.

Broad - band polarimetric follow-up of Type IIP SN 2012aw

In an interesting study, results of R-band polarimetric follow-up observations of the nearby (~10 Mpc) Type II-plateau SN 2012aw were presented. Starting from ~10th day after the supernova (SN) explosion, these polarimetric observations cover ~90 days (during the plateau phase) and are distributed over nine epochs. To characterize the Milky Way interstellar polarization (ISP_{MW}), 14 field stars lying in a radius of 10º around the SN were observed. The host galaxy dust polarization component was subtracted assuming that the dust properties in the host galaxy are similar to that observed for Galactic dust and the general magnetic field follows the large-scale structure of the spiral arms of a galaxy. After correcting the ISP_{MW}, it was inferred that the SN 2012aw has maximum polarization of 0.85 ± 0.08 per cent but polarization angle does not show much variation with a weighted mean value of ~138º. However, if both ISP_{MW} and host galaxy polarization components are subtracted from the observed polarization values of SN, maximum polarization of the SN becomes 0.68 ± 0.08 per cent. The distribution of Q and U parameters appears to follow a loop-like structure. The evolution of polarimetric light curve properties of this event was also compared with other well-studied core-collapse SNe of similar type.

4. Numerical Studies

Effect of the fluid composition on outflow rates from accretion discs around black holes

Flow is relativistic on account of its speed or temperature. It has been shown that the composition of the flow, dynamically affects the solution of the flow. Thermally it has been showed that electron-positron flow is the least relativistic. Based on a semi-analytical work, a study was conducted to investigate whether the composition of the flow in the accretion disc also affect the outflow. This was also the first work which combined relativistic equation of state with the dynamics of pseudo-Newtonian potential. The relevant fluid equations for Paczynski-Wiita potential, in the form of spatial derivative of radial velocity, and non-dimensional temperature were transformed and integrated the equations numerically by Runge Kutta method to find the solutions.

The entropy equation for adiabatic conditions was integrated and obtained, for the very first time, the expression of adiabatic equation of state for relativistic fluid. Using this the entropy-accretion rate of the flow was redefined, and is given by,

$$\dot{\mathcal{M}} = \frac{\dot{M}_{\rm in}}{4\pi\mathcal{K}} = \vartheta H x \exp(k_3)\, \Theta^{3/2}(3\Theta+2)^{k_1}(3\Theta+2/\eta)^{k_2}$$

Here, H is the local height of disc, ξ is the ratio between proton to electron number density, υ is the flow-velocity. Moreover,

$$k_1 = 3(2-\xi)/4, k_2 = 3\xi/4 \text{ and } k_3 = (f-K)/(2\Theta)$$

$$K = [2-\xi(1-1/\eta)] \qquad \Theta = kT/(m_e c^2)$$

It was shown that the bipolar jets do form from shocked disc even for relativistic equation of state. Since pair plasma is thermally the least relativistic, an accretion disc made of such light leptons, neither shows any shock nor any bipolar jets. The flow is thermally most relativistic for ξ = 0.27, and consequently the maximum outflow rates can be obtained for a shocked disc for such values of ξ.

Radiatively and thermally driven self-consistent bipolar outflows from accretion discs around compact objects

In the past there have been separate studies of jet generation from advective discs, and radiative acceleration of jets. With the aim to investigate what happens if the disc radiation deposits momentum onto the emanating jets, and how disc viscosity affects the jets, the study was initiated which followed a semi analytical solution procedure, and a fourth order Runge Kutta method to integrate the governing equations. The motivation for the present work came from the results previous works where it was seen that the accretion shocks move closer towards the black hole as the viscosity parameter is increased for flows starting with the same outer boundary condition. In the present work it was shown that as the viscosity parameter α is increased, shock location decreased. Simultaneously, the disc moved from low-intensity disc to brighter disc, and the jet also became stronger and faster. Although, the Keplerian disc component is not considered in the solution, the result resembles qualitatively the transition of the disc from hard to intermediate-hard states with associated strengthening of the jet from slow jets to faster and stronger jets, as has been reported in observations.

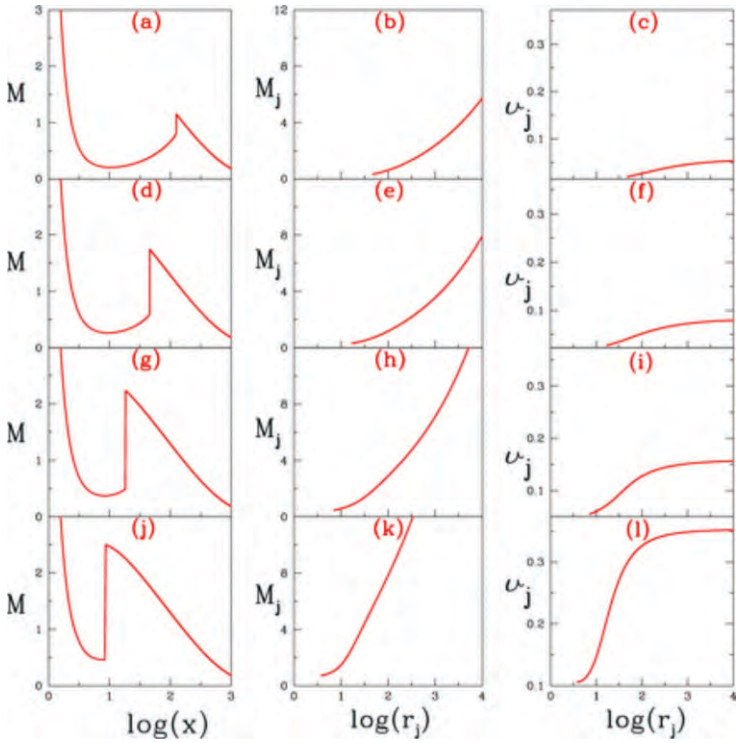

Figure 17. *Variations of accretion Mach number M (a, d, g and j) with log□(x), Mj (b, e, h and k) and vj (c, f, i and l) with log□(rj). The disc solutions are for parameters E = 0.001,□λinj = 18.592 at outer boundary xinj = 104, and for α = 0.009115 (a–c), 0.009315 (d–f), 0.009626 (g–i) and 0.009875 (j–l). Plots (a–c) are characterized by (xs, Rm˙, ℓps, ℓs=125.8964, 0.0091, 0.0054, 0.0346); for (d–f) (xs, Rm˙, ℓps, ℓs=45.9986, 0.0208, 0.0103, 0.0438); for (g–i) (xs, Rm˙, ℓps, ℓs=18.2871, 0.0504, 0.0380, 0.0585) and for (j–l) (xs, Rm˙, ℓps, ℓs=8.5741, 0.0991, 0.2337, 0.0948), and the jet terminal velocities are v∞ = 0.0534,□0.0793,□0.1566, 0.3519, respectively.*

Research Working Group – II

All the scientists working on the Sun and Atmospheric Sciences are members of WG – II. The group consists of 6 scientists. The solar physics research group (consisting of 2 scientists) is basically concentrated on the observations and modeling of the transients (e.g., flares and associated plasma processes, jets, spicules, etc.), space weather phenomena, and magneto-hydrodyanmic waves in the solar atmosphere. Atmospheric Science group (consisting of 4 scientists) is mainly engaged in the investigation of aerosols, trace gases, dynamics, meteorology etc., of the lower atmosphere. The extracts of the publications made by the members are briefly presented below.

Solar Physics

Observations of intensity oscillations in a prominence-like cool loop system as observed by SDO/AIA: evidence of multiple harmonics of fast magnetoacoustic waves

The evolution of weak intensity oscillations in a prominence like cool loop system was observed at the North-West limb on 7 March 2011 using *Solar Dynamics Observatory/Atmospheric Imaging Assembly (SDO/AIA)* 304 Å channel. Standard wavelet tool was used to produce statistically significant power spectra of AIA 304 Å normalized fluxes derived respectively near the apex and footpoint of the fluxtube. Periodicities of ≈667 s and ≈305 s respectively near apex and above footpoint

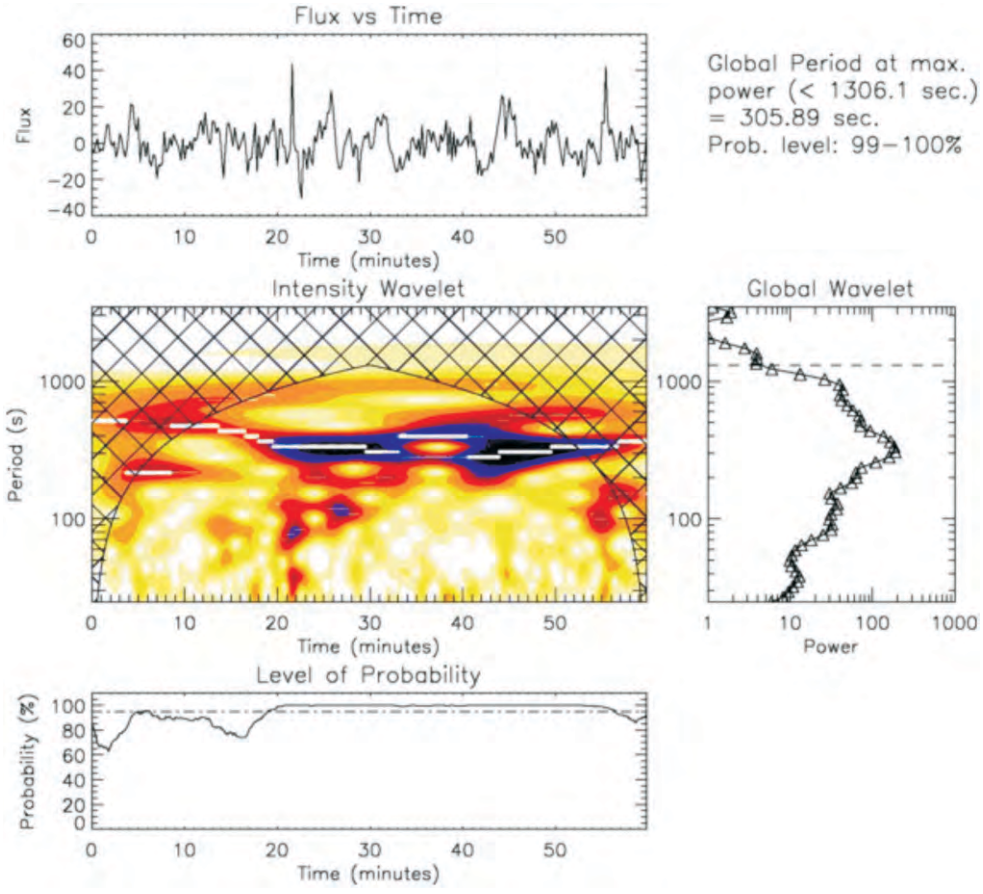

Figure 18. *Wavelet result of the SDO/AIA 304 Å time series derived near the footpoint of the cool prominence-like cool loop system. The top panel shows the flux vs time profile, the middle-left panel shows the intensity wavelet and power distribution, while the middle-right panel displays the global power centered around 305 s with a probability 99–100%. The bottom panel shows the temporal probability*

with significance level >98 % were identified. Observed statistically significant periodicities in the tube of projected length ≈ 170 Mm and width ≈ 10 Mm, are interpreted as most likely signature of evolution of various harmonics of tubular fast magnetoacoustic waves. Sausage modes are unlikely, though they are compressible, as they need bulky and highly denser loop system for their evolution for sustaining such large periods. The observed periodicities are interpreted as multiple harmonics (fundamental and first) of fast magnetoacoustic kink waves that can generate some weak density perturbations (thus intensity oscillations) in the tube and can be observed pertaining to periodic variation in plasma column depth as tube is oblique in projection with respect to the line-of-sight. The period ratio P_1/P_2=2.18 is observed in the flux tube, which is the signature of the magnetic field divergence of the cool loop system. Tube expansion factor was estimated as 1.27 which is typical of EUV bipolar loops in the solar atmosphere. The lower bound average magnetic fields was also estimated and found to be in the range of ≈ 9 to 90 Gauss depending upon typical densities as 109–1011 cm−3 in the observed prominence-like cool loop system. The first signature of lowering fundamental mode period by a factor 0.85 due to cooling of this loop system was also observed (see **Figure 18**).

X6.9-class Flare-induced Vertical Kink Oscillations in a Large-scale Plasma Curtain as Observed by the Solar Dynamics Observatory/Atmospheric Imaging Assembly

Kink MHD waves are thought to be responsible for the displacement of the axis of a magnetic tube and the tube as a whole. For that reason the standing transverse MHD waves observed in coronal loops are interpreted as standing MHD kink waves. Apart

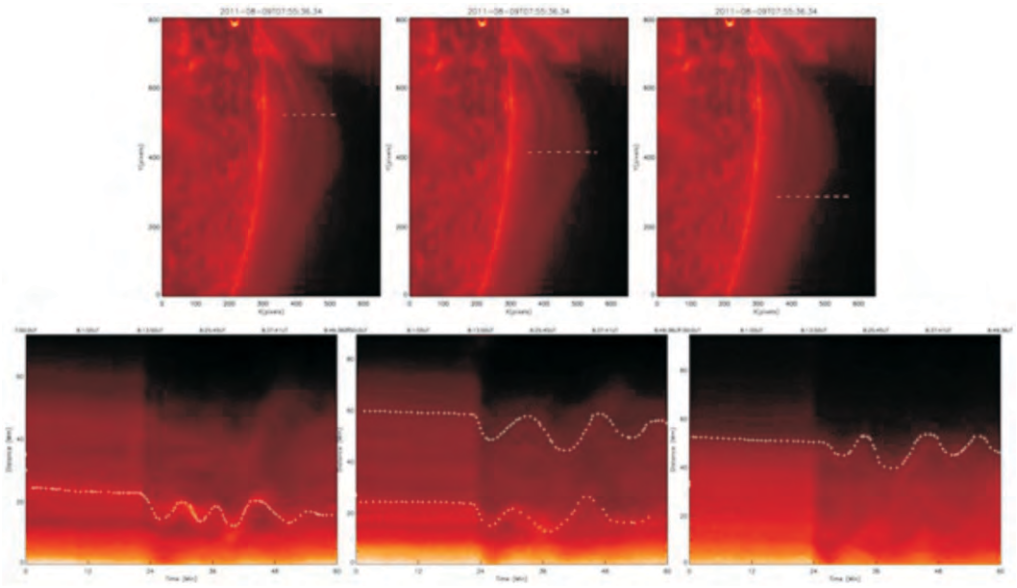

Figure 19 . *Top three panels show the position of vertical slits over the plasma curtain, while the bottom panels show the corresponding distance–time diagrams. From left to right, the slit positions are shifting away from the flare energy release site.*

from the transverse kink waves, there are claims that torsional Alfvén waves have been detected in various magnetic structures at diverse spatial scales in the solar atmosphere.

While horizontal kink oscillations triggered by flares have been observed in imaging observations of solar loops since the era of TRACE followed by Hinode, STEREO, and the Solar Dynamics Observatory, only a few cases of vertical kink waves are reported so far. Horizontal and vertical kink oscillations can be a useful tool for constraining important properties of the localized corona using MHD seismology. The damping/growth of these waves may also provide clues about the role of dynamic ambient plasma. A rare observational evidence of vertical kink oscillations in a laminar and diffused large-scale plasma curtain as observed by the SDO/AIA. The X6.9-class flare in active region 11263 on 2011 August 9 induces a global large-scale disturbance that propagates in a narrow lane above the plasma curtain and creates a low density region that appears as a dimming in the observational image data. This large-scale propagating disturbance acts as a non-periodic driver that interacts asymmetrically and obliquely with the top of the plasma curtain and triggers the observed oscillations. In the deeper layers of the curtain, evidence of vertical kink oscillations with two periods (795 s and 530 s) was found. On the magnetic surface of the curtain where the density is inhomogeneous due to coronal dimming, non-decaying vertical oscillations are also observed (period $\approx$ 763–896 s). The global large-scale disturbance is inferred as responsible for triggering the vertical kink oscillations in the deeper layers as well as on the surface of the large-scale plasma curtain. The properties of the excited waves strongly depend on the local plasma and magnetic field conditions (see **Figure 19**).

A multiwavelength study of eruptive events on January 23, 2012 associated with a major solar energetic particle event

Solar flares and coronal mass ejections (CMEs) involve a sudden release of magnetic energy stored in complex active regions through magnetic reconnection. The several mechanisms could be responsible for the energy build-up in the flaring and eruptive regions that are later released in the form of bulk mass motion, heating, as well as acceleration of the energetic particles. These processes may involve magnetic instabilities, flux and helicity emergence, building of the magnetic field complexity, etc.

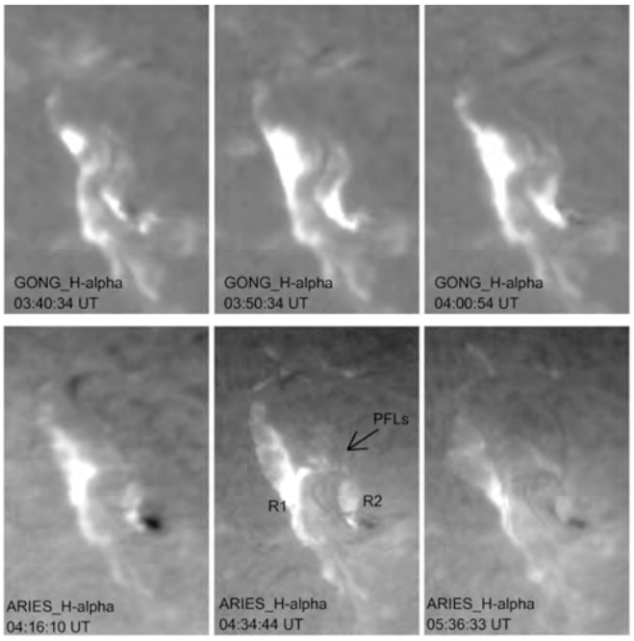

Figure 20. *Upper panel: GONG Hα images showing the rising phase of the M8.7 flare (FOV 200˝×300˝200″×300″). Bottom panel: ARIES Hα images showing the decay phase dynamics of the M8.7 flare. 'R1' and 'R2' in the bottom middle figure indicates the eastern and western flare ribbon respectively. Post Flare Loops (PFLs) are also indicated by the arrow in the middle panel at 04:34:44 UT. North is up and west is to the right (FOV 232˝×348˝232″×348″).*

Using multiwavelength data from space and ground based instruments, the solar flares and coronal CMEs on January 23, 2012 that were responsible for one of the largest solar energetic particle (SEP) events of solar cycle 24 was investigated. The eruptions consisting of two fast CMEs ($\approx$ 1400 km s^{-1} and $\approx$ 2000 km s^{-1}) and M-class flares that occurred in the active region 11402 located at $\approx$N28 W36. The two CMEs occurred in quick successions, so they interacted very close to the Sun. The second CME caught up with the first one at a distance of $\approx$ 11-12 $R_{\odot}$. The CME interaction may be responsible for the elevated SEP flux and significant changes in the intensity profile of the SEP event. The compound CME resulted in a double-dip moderate geomagnetic storm (Dst~-73 nT). The two dips are due to the southward component of the interplanetary magnetic field in the shock sheath and the ICME intervals. One possible reason for the lack of a stronger geomagnetic storm may be that the ICME delivered a glancing blow to Earth (see **Figure 20**).

Origin of Macrospicule and Jet in Polar Corona by a Small-scale Kinked Flux Tube

Macrospicules are giant spicules, mostly observed in polar coronal holes, reaching heights up to between 7 and 45 Mm above the solar limb with lifetimes of 3–45 minutes. The first evidence of the activation of a small-scale bipolar twisted flux tube in the lower polar corona, which undergoes internal reconnection and triggers a macrospicule and associated coronal jet was reported in a recent study. The aim was to study the relationship between the formation of a

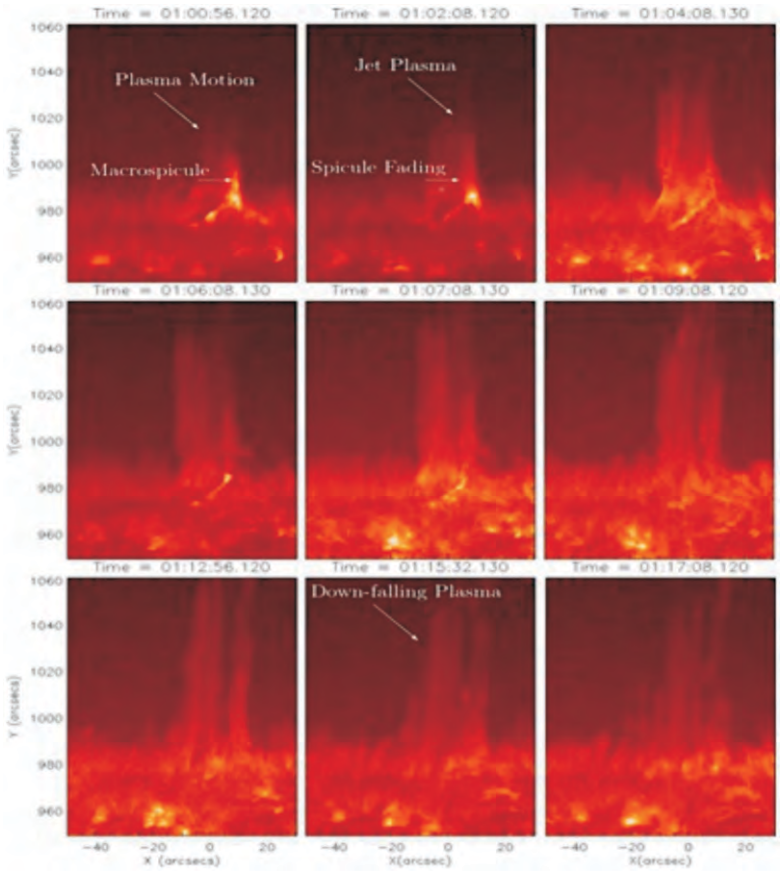

Figure 21. *Macrospicule triggers on 00:59:44 UT due to the reconnection between the opposite halves of flux tube and finally converts into a jet (cf. 01:02:08–01:06:08 UT snapshot). The comprehensive dynamics of the macrospicule and jet are shown in the online movie.*

macrospicule and its associated jet, as well as their most likely triggering mechanism. The study used SDO/AIA observations of a small-scale flux tube that undergoes kinking and triggers the macrospicule a jet on 2010 November 11 in the north polar corona and followed-up with the numerical simulations.

The small-scale flux tube emerged well before the triggering of the macrospicule and as time progresses the two opposite halves of this omega-shaped flux tube bent transversely and approach each other. After ~2 minutes, the two approaching halves of the kinked flux tube touch each other and an internal reconnection as well as an energy release takes place at the adjoining location and a macrospicule was launched which goes up to a height of 12 Mm. Plasma begins to move horizontally as well as vertically upward along with the onset of the macrospicule and thereafter converts into a large-scale jet in which the core denser plasma reaches up to ~40 Mm in the solar atmosphere with a projected speed of ~95 km s^{-1}. The fainter and decelerating plasma chunks of this jet were also seen up to ~60 Mm. A two-dimensional numerical simulation was performed by considering the VAL-C initial atmospheric conditions to understand the physical scenario of the observed macrospicule and associated jet. The simulation results showed that the reconnection-generated velocity pulse in the lower solar atmosphere steepens into slow shock and the cool plasma is driven behind it in the form of macrospicule. The horizontal surface waves also appeared with shock fronts at different heights, which most likely drove and spread the large-scale jet associated with the macrospicule (see **Figure 21**).

A study of a failed coronal mass ejection core associated with an asymmetric filament eruption

Filaments and prominences are composed of cool (10^4 K) and dense (10^{10}–10^{11} cm^{-3}) plasma material embedded in the magnetic field of the ambient solar atmosphere. These solar magnetic structures are the same intrinsically but appear different due to projection. Prominences, when observed on the disk, are known as solar filaments and lie along the polarity inversion line. Filaments may remain in the quiescent state for several days over the solar disk, while some filaments may exhibit an eruptive nature. Eruptive filaments are closely associated with coronal mass ejections (CMEs). CMEs are the propulsion of large-scale plasma outflows and magnetic fields into the outer corona and interplanetary space. In general, a CME has a three-part structure, i.e., a leading edge, a dark cavity, and a bright core associated with the eruptive filament. CMEs produce outward movement in the corona; this movement may be either driven by magnetic pressure or by a shock in the background of the ambient solar wind. The less dense outer corona sometime shows downflows of the plasma blobs, CME cores, etc. CME core exhibits downfall depending on the local magnetic field and plasma configurations. The most probable reason for the core exhibiting downfall may be the pre-settings of the large-scale reconnection in the outer corona. The CME itself can also produce several changes in the outer coronal magnetic fields in the form of deflection of coronal streamers, kink propagation in coronal rays, etc.

A multi-wavelength investigation of asymmetric filament evolution and eruption, associated CME, coronal downflows, and their relationships was carried out using the observations from the *Solar Dynamics Observatory*/Atmospheric Imaging Assembly (*SDO*/AIA), the *Solar Terrestrial Relations Observatory*/Sun Earth Connection Coronal and Heliospheric Investigation (*STEREO*/SECCHI) and the *Solar and Heliospheric Observatory*/Large Angle and Spectrometric Coronagraph (*SOHO*/LASCO) C2 instruments on 2012 June 17 and 18 during 20:00–05:00 UT. The *SDO*/AIA and *STEREO*-

B/SECCHI observations were used to understand the filament eruption scenario and its kinematics, while LASCO C2 observations are analyzed to study the kinematics of the CME and associated downflows. *SDO*/AIA limb observations show that the filament exhibits a whipping-like asymmetric eruption. *STEREO*/EUVI disk observations reveal a two-ribbon flare underneath the southeastern part of the filament that most probably occurred due to reconnection processes in the coronal magnetic field in the wake of the filament eruption. **Figure 22** shows selected EUV 171Å and 304Å images of the filament evolution as observed by *STEREO-B*/SECCHI and SDO/AIA..

The whipping-like filament eruption later produces a slow CME in which the leading edge and the core propagate, with an average speed of $\approx$ 540 km s^{-1} and $\approx$126 km s^{-1}, respectively, as observed by the LASCO C2 coronagraph. The CME core formed by the eruptive flux rope shows outer coronal downflows with an average speed of $\approx$ 56 km s^{-1} after reaching $\approx$ 4.33 $R_\odot$. Initially, the core decelerates at $\approx$ 48 m s^{-2}. The plasma first decelerates gradually up to a height of $\approx$4.33 $R_\odot$ and then starts accelerating downward. We present a high-resolution image of the filament during the evolutionary phase in the left panel of figure 2, schematics of the filament in the middle panel while the rise speed of the filament in the right panel.

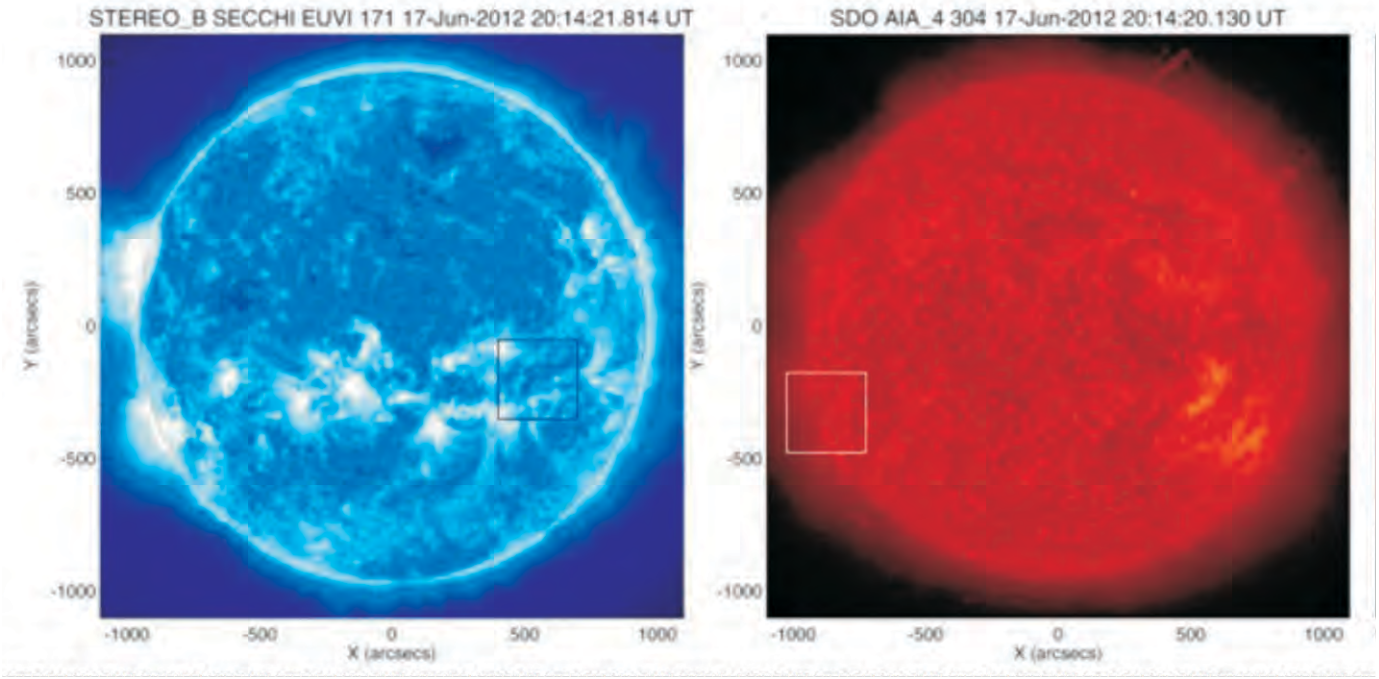

Figure 22. *STEREO-B*/SECCHI 171Å (left) and *SDO*/AIA 304Å (right) images showing the full disk of the Sun on 2012 June 17. The boxes show the location of the filament from two different angles.

From this study, It has been suggested that a self-consistent model of a magnetic flux rope representing the magnetic structure of the CME core formed by an eruptive filament. This rope loses its previous stable equilibrium when it reaches a critical height. With some reasonable parameters, and inherent physical conditions, the model describes

the non-radial ascending motion of the flux rope in the corona, its stopping at some height, and thereafter its downward motion (see **Figure 23**).

A summary of the results is as follows:

1. The observations show whipping-like, highly asymmetric filament eruption with an active (southeastern) leg and an anchored (northwestern) leg.

2. During the eruption, a two-ribbon flare occurred underneath the eastern part of the filament. This supports the standard flare model (CSHKP) of reconnection well.

3. The deceleration profile of the CME core shows that gravity is not the only force responsible for the downflow. The downflow of the CME core has been observed and may be due to the self-consistent evolution of the flux rope in the coronal magnetic field.

4. Coronal ray deflection occurs during the upward motion of the CME. However, it does not exhibit a precise correlation with the coronal downflows.

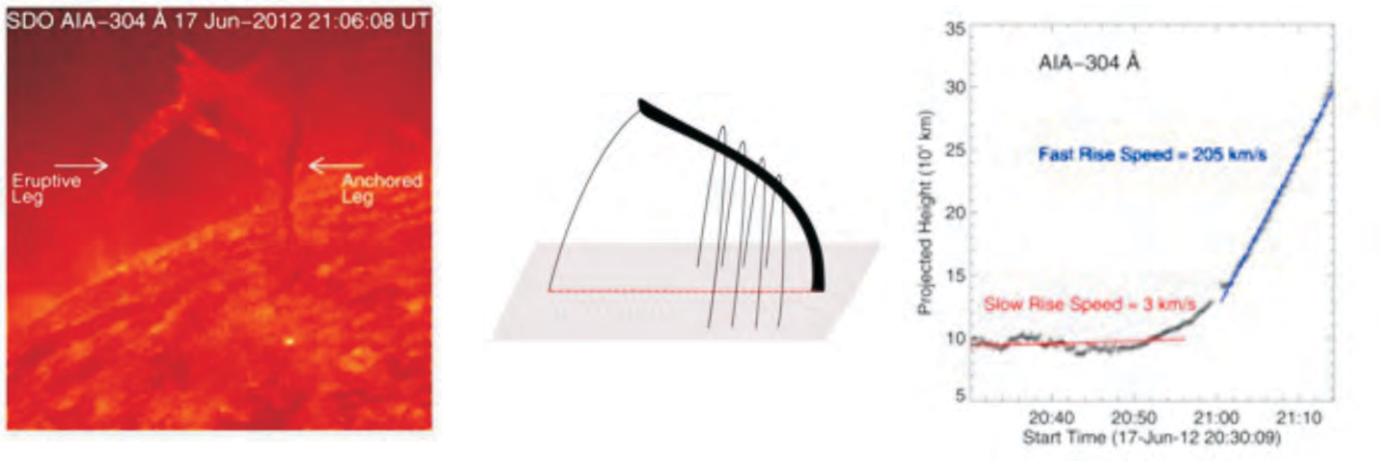

Figure 23: Left Panel - High-resolution image of the filament in SDO/AIA 304 Å during the evolutionary phase. Middle panel - Schematic of the whipping-like asymmetric filament eruption. The red line indicates the polarity inversion line. Right Panel - Rise speed of the filament.

Atmospheric Science

Dynamical aspects of aerosols over central Himalayan region

Recent studies showed a possible trend of increase of Aerosol Optical Depth (AOD) over central Himalayas region. The plausible reason for this could be that the long range transport of aerosols from distant locations as in-situ aerosol production is not significant over this region.

In this context, a study was conducted where it was tried to illustrate, for the first time, the direct aerosol radiative forcing which has large uncertainty due to diverse simulated vertical profile of aerosol over this free tropospheric site. Interestingly, the observations showed that there is an increment in surface radiative forcing due to the insertion of derived aerosol extinction profile for the same columnar properties of aerosols. Moreover, it has also been found that the higher the aerosol layer contribution to the total aerosol optical depth, the

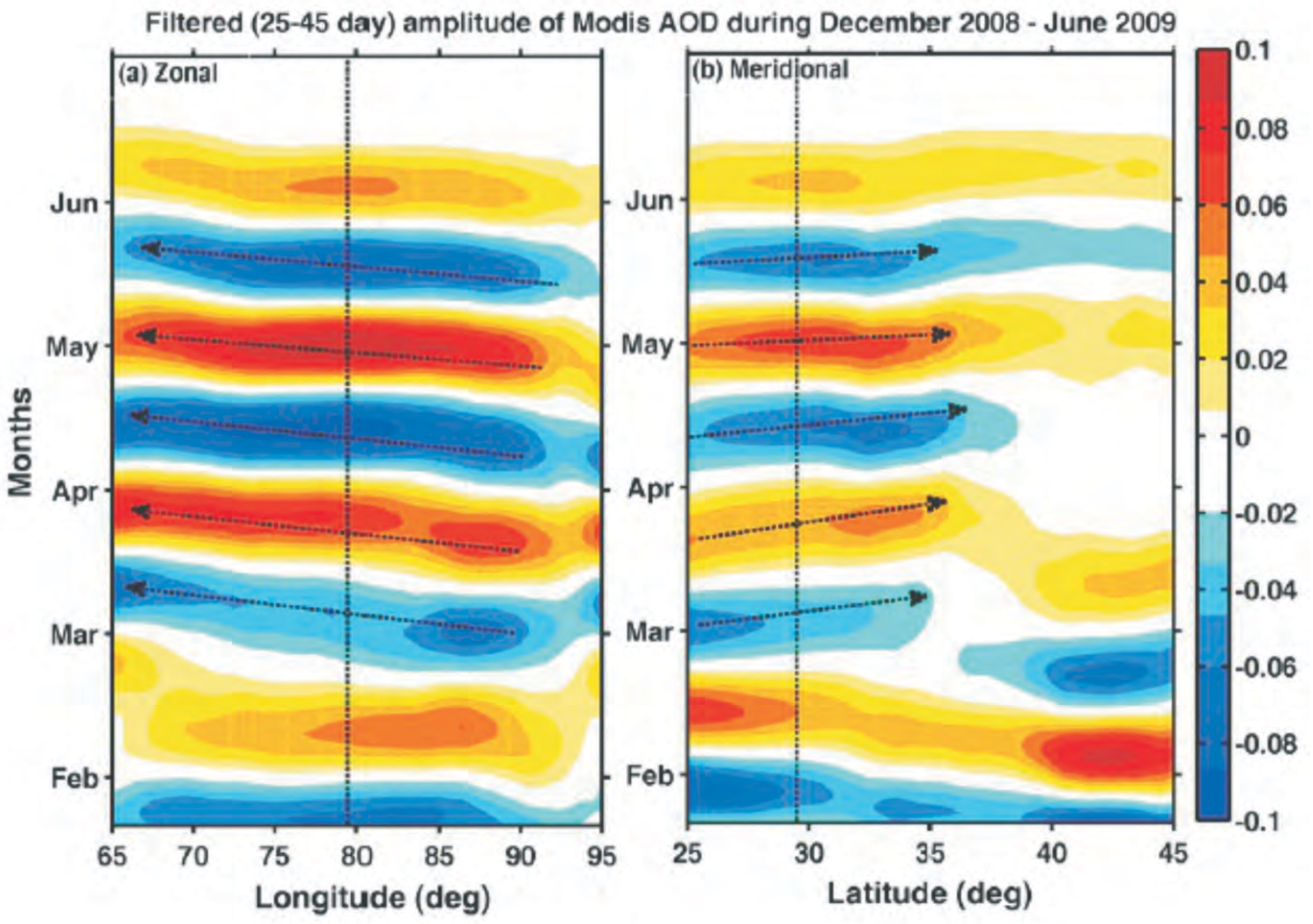

Figure 24. *Time–longitude section of filtered (25–45 day) amplitudes of MODIS AOD from December 2008 to June 2009 for* ***(a)*** *zonal propagation (longitude) and* ***(b)*** *meridional propagation (latitude). Dotted line represents the longitude and latitude of the observational site and arrows indicate the direction (westward/northward) of propagation.*

more the uncertainty in aerosol radiative forcing. Apart from this, significant differences were also found in the atmospheric forcing at each altitude due to variation in vertical profile of aerosol extinction, which leads to the modification of the thermal structure of the atmosphere. A study has been conducted to quantify the effect of cloud reflection on the aerosol radiative forcing and contribution of aerosol layers located above and below of the cloud layers over central Himalayan region. The results showed higher forcing values when the aerosol layer is above the cloud layer as compared to the aerosol layer below the cloud. Hence, the study emphasized the importance of the knowledge of cloud properties along with the aerosol vertical profiles in cloudy atmosphere. Apart from these, studies have also been conducted which concentrated on the affects of long-period 25-45 day modulations on aerosol optical depth, for the first time, over a high-altitude site the central Himalayan region. Further, Hovmoller diagram showed westward (northward) propagation at a different longitude (latitude) confirming that these modulations are associated with Rossby waves (Refer to **Figure 24**). It is also shown that inclusion of Rossby wave amplitude in aerosol radiative forcing causes a ~20% additional warming over the observational site. Hence, the present study illustrated the importance of wave-induced aerosol dynamics and the corresponding radiative effects.

The mixing layer height over Himalayan region has been estimated, for the first time, using three different instruments and with six different methods in post-monsoon season. Mixing layer height is found to be located ~0.57 ± 0.1 and 0.45 ± 0.05 km AGL during day and nighttime (Refer to **Figure 25**). Results showed that wavelet co-variance transform is a robust method for mixing layer height estimation over this region.

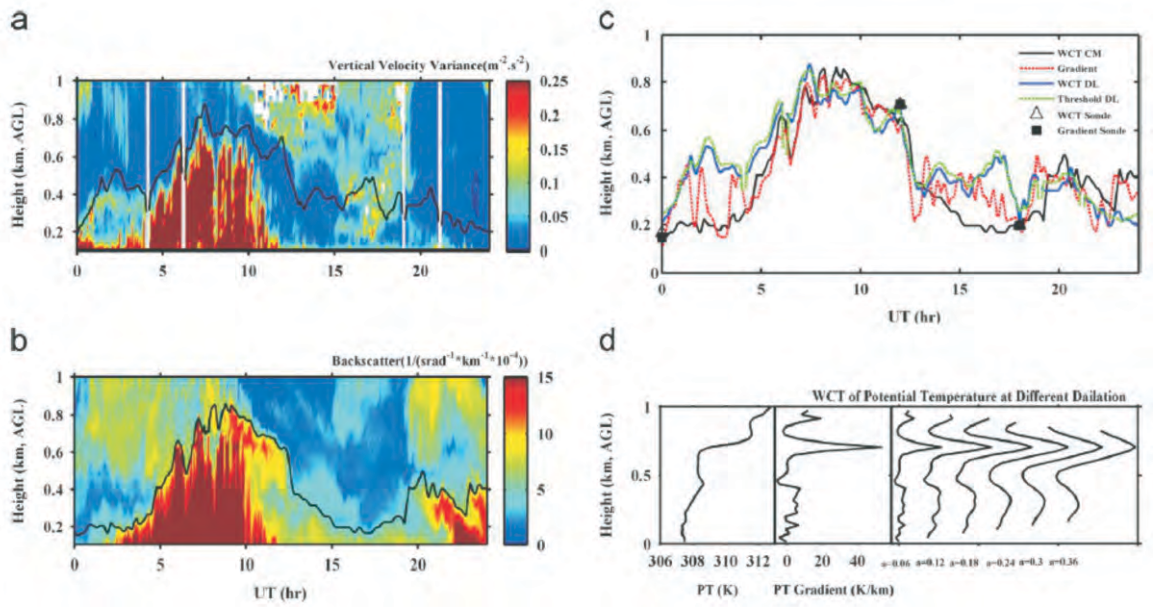

Figure 25. *Range-time intensity(RTI) plot showing the mixed layer evolution on 16 October2011 using (a) DL MLH with WCT plotted with black solid line and (b) CM MLH with WCT plotted with black solid line (c) diurnal variation of the MLH obtained using DL (threshold/WCT), CM(gradient/WCT) and RS (PT gradient/WCT) on the same day. (d) Identification of inversion layer height from Radiosonde Potential temperature profile at12UT by using WCT method at different dilations.*

Temporal variability and radiative impact of black carbon aerosol over tropical urban station Hyderabad

Aerosol black carbon (BC) or soot among the carbonaceous aerosols has become the subject of prime interest in the recent years because it is one of the most important absorbing aerosol species in the atmosphere, BC is a primary emission and it is not produced in secondary reactions and mainly arises due to man-made (or anthropogenic) activities and is emitted from the incomplete combustion processes of fossil fuel e.g. automobile exhaust, industrial and power plant exhaust, aircraft emission etc and bio fuel i.e. biomass burning and forest fires. The presence of BC aerosols in the atmosphere has not only adverse health effects, but its impact on the radiation balance in the tropics can have potential impact on the hydrological cycle and thereby a far reaching effect on the weather and the climate. Due to special significance of Asian region, considered as the biggest source of industrial exhaust, we made extensive measurements of aerosol black carbon mass concentration for two year period (January 2009 to December 2010) over Hyderabad, which a typical large tropical industrial town. The data were obtained using a seven channel portable Aethalometer procured from Magee scientific and are used to study the seasonal and diurnal variation of BC and their association with the prevailing atmospheric processes.

Figure 26 shows the monthly mean diurnal variation of black carbon mass concentration obtained from the hourly mean. A well defined diurnal variation is observed over Hyderabad with primary peak at around 8:00 LST and another moderate peak in the late evening around 20:00 LST. The primary and secondary peaks in the morning and late evening appear consistently throughout the year but with

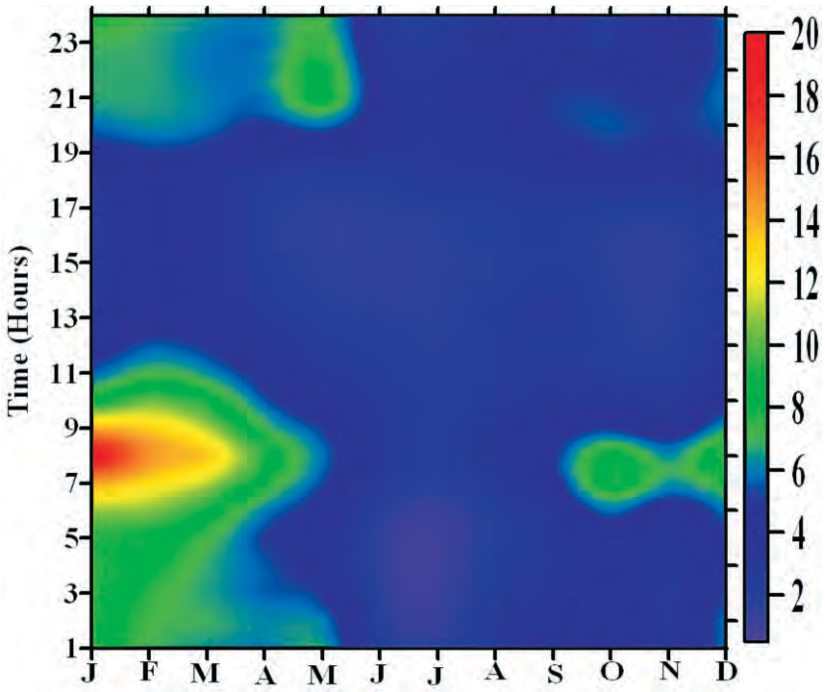

Figure 26. *Diurnal variation of BC mass concentration for each month over Hyderabad during January 2009–December 2010.*

varying magnitude. The diurnal variation of BC has shown a strong association with the local boundary layer dynamics as well as local anthropogenic activities. Also, the primary morning peak might also be associated with the fumigation effect in the atmospheric boundary layer, which brings aerosols and pollutants from the nocturnal residual layer shortly after the sun rise. As the day advances the BC mass concentration continuously decreases and reaches the diurnal minima at the local noon hours. As the day advances, increased solar heating leads to faster dispersion of aerosols and hence dilution of BC mass concentration occurs near the surface. The BC mass concentration continue to be lower until 17:00 hours and thereafter it is slowly start to increase and reach a secondary peak at 20:00 hours local time. This increase in the late evening peak is associated with the shallower nocturnal boundary layer during the night times, which leads to rapidly reduction in the ventilation effects and consistently confines the aerosols causing the secondary peak.

Figure 27, left panel shows the six main trajectory pathways along with the percentage contribution of each trajectory, whereas the **Figure 27** right panel shows the concentration weighted trajectory (CWT) map for black carbon mass concentration at Hyderabad during January 2009 to December 2010. **Figure 27** shows that the most important potential source for black carbon concentration is the central India and Indo-Gangetic Plain and some hot spots in Pakistan. Note also the larger value in the eastern costal India than the western one. Airmass backtrajectory originating from Arabian Peninsula and Persian Gulf traversing the northern Arabian Sea can also contribute to the medium black carbon mass concentration, while the air mass from the southern Arabian sea seem to be clear.

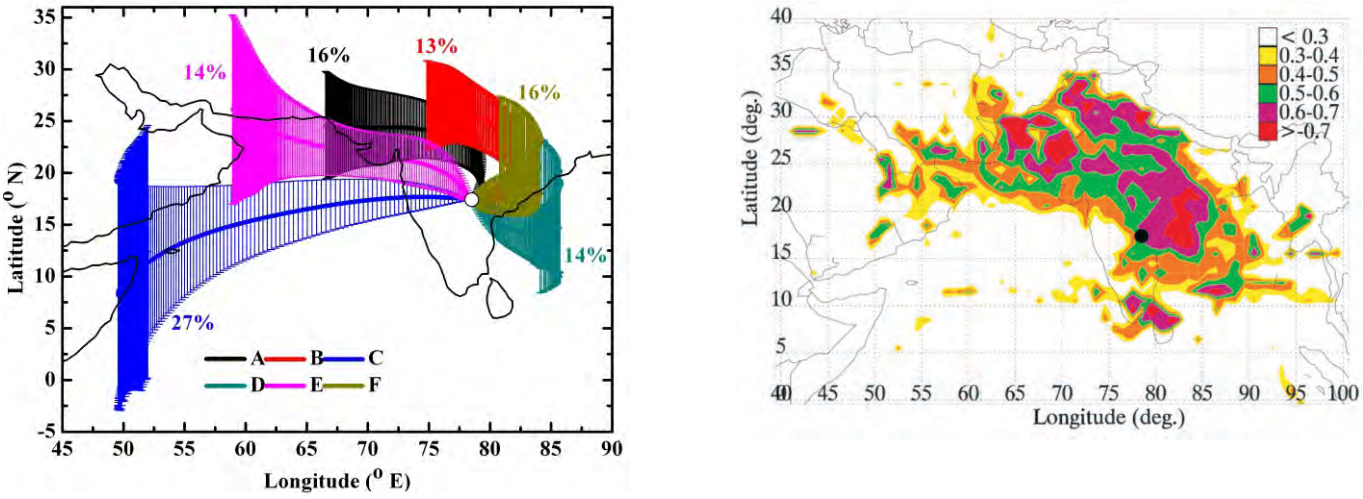

Figure 27. *Different mean advection pathways (trajectory clusters) that influence Hyderabad (open circle) during January 2009–December 2010. The error bars at each hourly point represent the latitudinal extent of trajectories in each cluster group. The percentage contribution for each cluster is also given in the figure (top panel). Concentration weighted trajectory (CWT) map for BC mass concentration (μg m^{-3}) at Hyderabad January 2009–December 2010. The black circle shows the location of the observational site (bottom panel).*

First simulations measurements of O3, CO, and NOy in the central Himalayas

First ever observations of NOy, together with ozone and CO, from Indian region were reported. CO and NOy show slight enhancement during daytime, unlike in ozone and diurnal patterns are attributed to mainly to the dynamical processes. Springtime higher levels of ozone (~58 ppbv), CO (~215 ppbv), and NOy (~1918 pptv) have been attributed mainly to regional pollution supplemented with northern Indian biomass burning. Additionally, downward transport from higher altitudes is estimated to enhance surface ozone levels over Nainital by 6–19 ppbv. The classification based on air mass residence time and boundary layer shows higher levels of ozone (~57 ppbv), CO (~206 ppbv), and NOy (~1856 pptv) in the continental air masses when compared with their respective values (~28 ppbv, ~142 ppbv, and ~226 pptv) in the regional background air masses. Ozone-CO and ozone-NOy slope values clearly show in-complete in-situ photochemistry and highlight the role of dynamical processes in controlling the levels of ozone and other pollutant in this central Himalayan region. The higher CO/NOy value also confirms minimal influence of fresh emissions in this region. Enhancements in ozone, CO, and NOy during high fire activity period are estimated to be 4–18%, 15–76%, and 35–51%, respectively. Despite higher CO and NOy concentrations, ozone levels in this region are nearly similar to those at other global high-altitude sites **(Figure 28)**.

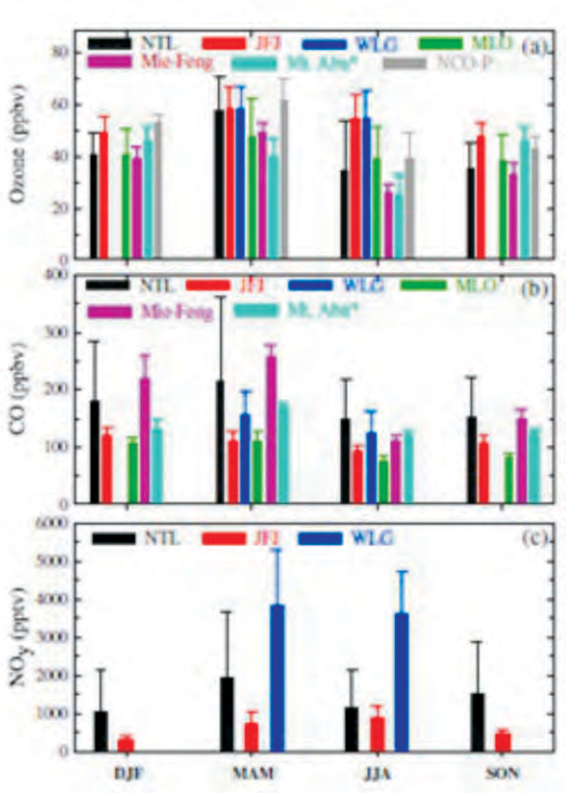

Figure 28. *Seasonal variations in ozone, CO and NOy at Nainital and other global high-altitude sites.*

Ozone and precursors over oceanic region

Observations of ozone and related gases over the Bay of Bengal (BoB) revealed large variability in ozone (11 to 60 ppbv) and CO (45 to 260 ppbv). Estimated south to north latitudinal gradients in ozone and CO were significantly higher than those observed during earlier studies. Back air trajectories were used to classify these measurements into pollution plumes from nearby sources (India-Bangladesh region and Southeast Asia), influenced by long-range transport and pristine marine air from the Indian Ocean. Interspecies correlations were used to identify emission signatures in these air masses. Principle component analysis indicated contributions of ship emissions to NOx levels over the BoB. Influences of fire from the Myanmar and Thailand regions are shown to be the potential contributor to enhanced CO levels (>250 ppbv) over the BoB. Diurnal variations in surface ozone revealed effects of advection, entrainment, and photochemistry.

Vertical ozone distribution over the central Himalayas

Observations of ozone vertical distribution and meteorological parameters are made for the first time in the central Himalayan region, which shows prominent seasonality in the lower troposphere. The lower tropospheric ozone minimum coincides with highest values of relative humidity (80-100%) during the summer-monsoon. However, ozone mixing ratios in the middle-upper troposphere show less pronounced and different seasonality. A stratospheric intrusion event during winter is observed, which enhances the ozone levels by ~180% in the middle-upper troposphere. Ozone levels in 2-4 km altitude range are higher by about 20 ppbv during the springtime high fire activity period over the northern India **(Figure 29)**. Moreover, a comparison with ozone profiles at Ahmedabad confirms the influences of pollution from IGP that is supplemented with the contribution of northern Indian biomass burning. It is suggested that regional photochemistry and biomass burning processes play controlling role in the lower troposphere, while, the middle-upper tropospheric variations are driven by dynamical processes including advection and stratospheric intrusion.

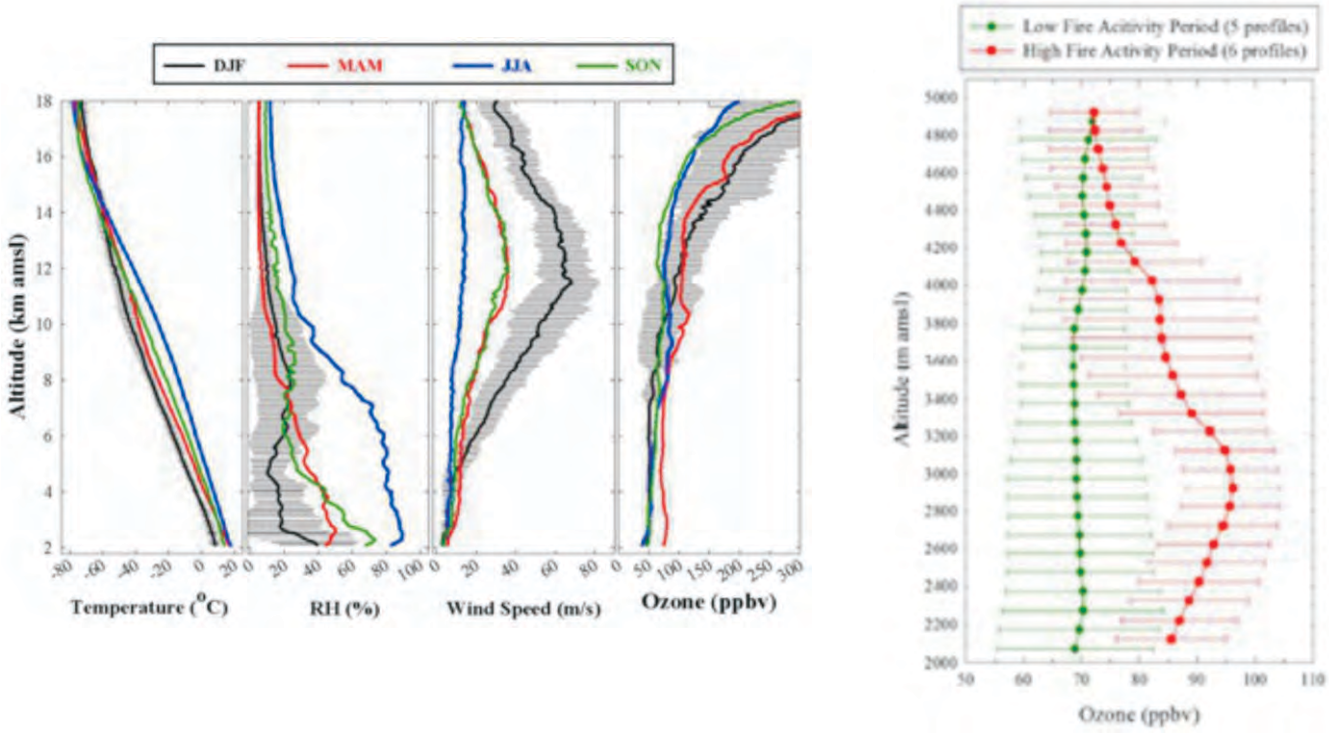

Figure 29. *Seasonal variations in the vertical distribution of Temeprature, relative humidity, wind speed and ozone. Ozone enhancement during fire activity period is also shown at right side.*

WFR-Chem simulation of a typical pre-monsoon dust storm

WRF-Chem model is used to study the impact of a typical pre-monsoon season dust storm event on the regional aerosol optical properties and radiation budget in northern India. Model estimated total dust emissions of 7.5 Tg over the model domain during an event in April 2010. Dust is shown to be transported from Thar Desert and loading in different sizes (representing accumulation, coarse and giant mode) is seen in the boundary layer and free troposphere **(Figure 30)**. Both, in situ and satellite observations show significant increase (>50%) in local to regional scale aerosol optical depth and decrease (>70%) in the Angström exponent during the event. The WRF-Chem model reproduced the spatial and temporal distributions of dust plumes and aerosol optical properties but generally underestimated the AOD. Model results show that dust particles cool the surface and the top of the atmosphere, and warm the atmosphere. The regionally averaged radiative perturbation due to dust aerosols is estimated as −2.0±3.0Wm−2 at the top of the atmosphere, 2.3±1.8Wm−2 in the atmosphere and −4.4±3.1Wm−2 at the surface.

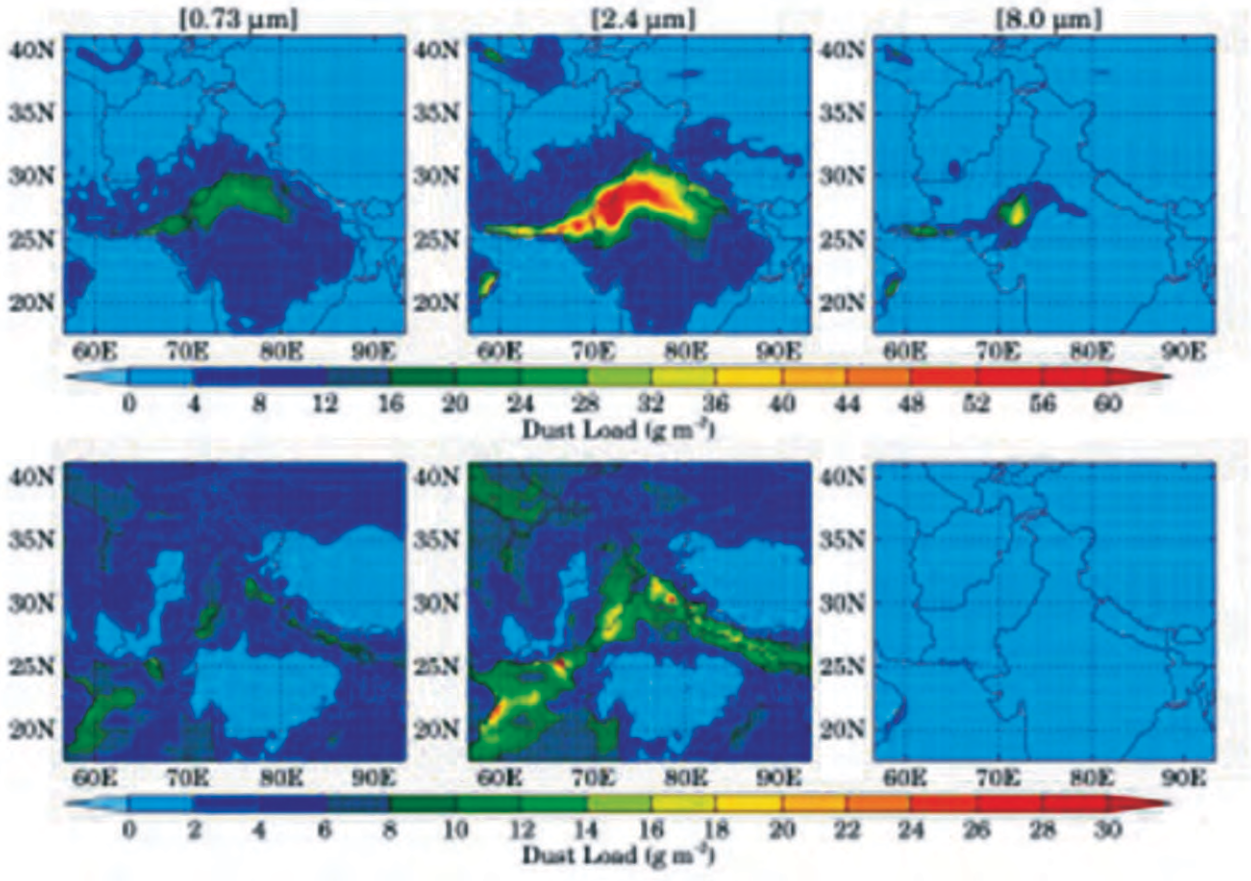

Figure 30. *WRF-Chem simulated accumulation, coarse and giant mode dust load in the boundary layer and free troposphere.*

List of Publications

Refereed Journals

1. Rani, B., et al. (including **Gupta, A. C.**). (2013). Radio to gamma-ray variability study of blazer S5 0716+714. *Astron. Astrophy., 552*, A11.

2. **Srivastava, A. K.,** Dwivedi, B. N. & Kumar, M. (2013). Observations of intensity oscillations in a prominence-like cool loop system as observed by SDO/AIA: evidence of multiple harmonics of fast magnetoacoustic waves. *Astrophy. Space Sci.*, *345,* 25-32.

3. **Kumar**, **Brajesh,** et al. (including **Pandey, S. B., Kumar, B., Bose, S., Roy, R.** & **Sagar, R.**) (2013). Light curve and spectral evolution of the type IIb supernova 2011fu. *Mon. Not. Roy. Astron. Soc., 431*, 308-321.

4. **Yadav, R. K. S., Sariya, Devesh P.** & **Sagar, R.** (2013). Proper motions and membership probabilities of stars in the region of open cluster NGC 3766, *Mon. Not. Roy. Astron. Soc. 430*, 3350-3358.

5. Patel, M. K., **Pandey**, **J. C.,** Savanov, I. S., Prasad, V. & Srivastava, D. C. (2013). Study of photospheric, chromospheric and coronal activities of V1147 Tau, *Mon. Not. Roy. Astron. Soc. 430,* 2154-2168.

6. Gopalswamy, N. et al. (including **Uddin**, **W., Srivastava, A. K.** & **Joshi, N. C.**) (2013). Height of shock formation in the solar corona inferred from observations of type II radio bursts and coronal mass ejections, *Advances in Space Research*, *51*, 1981-1989.

7. **Kayshap, P., Srivastava**, **A. K.,** Murawski, K. & Tripathi, D. (2013). Origin of macrospicule and jet in polar corona by a small-scale kinked flux tube, *Astrophy. Jr. Lett., 770*, L3.

8. **Joshi, N. C.,** et al. (including **Uddin, W., Srivastava, A. K. & Kayshap, P.**). (2013). A multiwavelength study of eruptive events on January 23, 2012 associated with a major solar energetic particle event, *Advances in Space Research*, *52*, 1-14.

9. **Joshi, N. C., Srivastava**, **A. K.,** Filippov, B., **Uddin, W., Kayshap, P.** & Chandra, R. (2013). A study of a failed coronal mass ejection core associated with an asymmetric filament eruption, *Astrophy. Jr., 771,* 65.

10. **Soam, A., Maheswar**, **G.,** Bhatt, H. C., Lee, C. W. & Ramaprakash, A. N. (2013). Magnetic fields in cometary globules-IV LBN. 437, *Mon. Not. Roy. Astron. Soc., 432*, 1502-1512.

11. Haarlem, M. P. van et al. (including **Omar, A.**). (2013). LOFAR: The low-Frequency ARray, *Astron. Astrophy., 556,* A2.

12. Bisht, D., **Yadav, R. K. S.** & Durgapal, A. K. (2013). Photometric studies of open star clusters Haffner 11 and Czernik 31, *New Astronomy, 25*, 103-108.

13. **Eswaraiah, C., Maheswar, G., Pandey, A. K., Jose, J.,** Ramprakash, A. N. & Bhatt, H. C. (2013). A study of the starless dark cloud LDN 1570: distance, dust properties and magnetic field geometry, *Astron. Astrophy., 556*, A65.

14. Malik, C., Lal, S., **Naja**, **M.,** Chand, D., Venkataramani, S., **Joshi**, **Hema** & **Pant**, **P.** (2013). Enhanced SO_2 concentrations observed over northern India: role of long-range transport, *International Jr. of Remote Sens., 34*, 2749-2762.

15. **Srivastava**, **A. K.,** Botha, G. J. J., Arber, T. D. & **Kayshap, P.** (2013). Simulation of the observed coronal kink instability and its implications for the SDO/AIA, *Adv. Space Rese., 52,* 15-21.

16. **Pandey, S. B. (2013).** Core-Collapse Supernovae and Gamma-Ray Bursts in TMT Era**,** *Jr. Astrophy. Astron.*, *34,* 157-173.

17. **Sagar**, **R. (2013).** The Thirty Meter Telescope – Observatory GenNext, *Jr. Astrophy. Astron.*, *34,* 75-80.

18. **Dumka**, **U. C.,** Manchand, R. K., Sinha, P. R., Sreenivasan, S., Moorthy, K. K. & Babu, S. S. (2013). Temporal variability and radiative impact of black carbon aerosol over tropical urban station Hyderabad, *Jr. Atmo. Solar-Terr. Phy.*, *105-106,* 81-90.

19. Mallik, C., Lal, S., Venkataramani, S., **Naja, M.** & **Ojha**, **N.** (2013). Variability in ozone and its precursors over the Bay of Bengal during post monsoon: Transport and emission effects, *Jr. Geophys. Res.: Atmosph. 118,* 1-20.

20. Choudhary, D. P., et al. (including **Uddin, W., Srivastava, A. K., Joshi, N. C.** & **Kashyap, P.**). (2013). Flux emergence, flux imbalance, magnetic free energy and solar flares. *Advances in Space Research*, *52,* 1561-1566.

21. **Jaiswal, S.** & **Omar**, **A.** (2013). Devasthal fast optical telescope observations of worlf-rayet dwarf galaxy Mrk 996. *Jr. Astrophys. Astr., 34,* 247-257.

22. Goyal, A., et al. (including **Sagar, R.**), (2013). On the photometric error calibration for the differential light curves of point-like active galactic nuclei. *Jr. Astrophys. Astr., 34,* 273-296.

23. **Srivastava, A. K.** & Goossens, M. (2013). X6.9-class flare-induced vertical kink oscillations in large-scale plasma curtain as observed by the solar dynamics observatory/atmospheric imagaing assembly. *Astrophy. Jr., 777,* 17 (9pp).

24. Goyal, A., Gopal-Krishna, Witta, P. J., Stalin, C. S. & **Sagar**, **R.** (2013). Improved characterization of intranight optical variability of prominent AGN Classes, *Mon. Not. Roy. Astron. Soc. 435,* 1300-1312.

25. Bhatta, G., et al. (including **Gupta, A. C.** & **Sagar, R.**). (2013). The 72-h WEBT microvariability observation of blazer S5 0716+714 in 2009, *Astron. Astrophy. 558*, A92.

26. **Roy**, **R.,** et al. (including **Kumar, Brijesh, Nandi, S., Mishra, K., Kumar, Brajesh, Pandey, S. B.** & **Sagar, R.**) (2013). SN 2007uy-metamorphosis of an aspheric type Ib explosion. *Mon. Not. Roy. Astron. Soc., 434,* 2032-2050.

27. **Bose, S.,** et al.(including **Kumar, Brijesh, Kumar, Brajesh, Roy, R., Pandey, S. B., Sagar, R.** & **Mishra, Kuntal**) (2013). Supernova 2012aw- a high energy clone of archetypal type IIP SN 1999em. *Mon. Not. Roy. Astron. Soc. 433*, 1871-1891.

28. **Srivastava**, **A. K.,** Lalitha, S. & **Pandey, J. C.** (2013). Evidence of multiple slow acoustic oscillations in the stellar flaring loops of proxima centauri. *Astrophy. Jr. Lett., 778,* L28.

29. **Kumar**, **Rajiv,** Singh, C. B., **Chattopadhyay, I.** & Chakrabarti, S. K. (2013). Effect of the flow composition on outflow rates from accretion discs around black holes. *Mon. Not. Roy. Astron. Soc., 436,* 2864-2873.

30. **Kumar**, **S.,** Singh, A. K. & Singh, R. P. (2013). Ionospheric response to total solar eclipse of 22 July 2009 in different Indian region, *Ann. Geophys. 31*, 1549-1558.

31. Das**,** H. S., **Medhi, B. J.,** Wolf, S., Bertrang, G., Roy, P. D. & Chakraborty, A. (2013). Polarimetric studies of comet C/2009 P1 (Garradd). *Mon. Not. Roy. Astron. Soc.,* 436, 3500-3506.

32. Bhatt**,** H., **Pandey**, **J. C.,** Singh, K. P., **Sagar, R.** & **Kumar**, **Brijesh. (2013).** X-ray observations of eight young open stat clusters: I. Membership and X-ray luminosity. *Jr. Astrophys. Astr., 34,* 393-429.

33. Tripathi, D., Reeves, K. K., Gibson, S. E., **Srivastava**, **A. K. & Joshi, N. C.** (2013). SDO/AIA observations of a partially erupting prominence. *Astrophy. Jr.,* 778, 142.

34. **Joshi, R.** & **Chand**, **H.** (2013). Intranight optical variability of radio-loud broad absorption line quasars, *Mon. Not. Roy. Astron. Soc., 429,* 1717-1724.

35. Sharma, M., Nath, B. B. & **Chand**, **H.** (2013). Signature of outflows in strong Mg II absorbers in quasar sightlines. *Mon. Not. Roy. Astron. Soc., 431,* L93-97.

36. **Joshi, R.** & **Chand**, **H.** (2013). Dependence of residual rotation measure (RRM) on intervening Mg II absorbers at cosmic distance, *Mon. Not. Roy. Astron. Soc., 434,* 3566-3571.

37. Tripathi, A., Pandey, U. S. & **Kumar**, **Brijesh.** (2013). Photometric study of galactic open cluster NGC 2129, NGC 1502 and King 12. *Bull. Astro. Soc. India*, *41,* 209-226.

38. Reddy, K., **Phanikumar**, **D. V.,** Ahammed, Y. N. & **Naja, M.** (2013). Aerosol vertical profiles strongly affect their radiative forcing uncertainties: study by using ground-based lidar and other measurements. *Remote Sens. Letts.*, *4,* 1018-1027.

39. Gopal-Krishan, **Joshi, R.** & **Chand**, **H.** (2013). Intranight optical variability of radio-quiet weak emission line quasars, *Mon. Not. Roy. Astron. Soc., 430*, 1302-1308.

40. **Kumar**, **S.,** Singh, A. K. & Singh, R. P. (2013). Ionospheric response to total soalr eclipse of 22 July 2009 in different Indian regions. *Ann. Geophys.*, *31,* 1549-1558.

41. Errmann, R. et. al. (including **Pandey, A. K**.). (2013). The stellar content of the young open cluster Trumpler 37**,** *Astron. Nachr. Soc., 334*, 673-681.

42. **Jose, J., Pandey, A. K.,** Samal, M. R., Ojha, D. K., Ogura, K., Kim, J. S., Kobayashi, N., Goyal, A., Chauhan, N. & **Eswaraiah, C.** (2013). Young stellar population and ongoing star formation in the H II complex Sh2-252, *Mon. Not. Roy. Astron. Soc., 432*, 3445-3461.

43. **Lata, S., Pandey, A. K., Sharma, S.,** Bonatto, C. and **Yadav**, **R. K.** (2014). Photometric study of five open star clusters. *New Astron., 26,* 77-85.

44. **Sariya, D. P., Lata, S.** & **Yadav**, **R. K. S. (2014).** Variable stars in the globular cluster NGC 4590 (M68), *New Astron., 27,* 56-62.

45. **Joshi, Y. C.,** Balona, L. A., **Joshi, S.** & **Kumar**, **B.** (2014). Photometric study of the open cluster-II. stellar population and dynamical evolution in NGC 559, *Mon. Not. Roy. Astron. Soc., 437,* 804-815.

46. **Gaur, H., Gupta**, **A. C.,** Wiita, P. J., Uemura, M., Itoh, R. & Sasada, M. (2014). Anti–correlated optical flux and polarization variability in BL LAC. *Astrophy. Jr. Lett.,* 781, L4 .

47. **Kumar, Rajiv, Chattopadhyay, I.** & Mandal, S. (2014). Radiatively and thermally driven self-consistent bipolar outflows from accreation disc around compact object, *Mon. Not. Roy. Astron. Soc., 437,* 2992-3003.

48. Chmielewski, P., **Srivastava, A. K.,** Murawski, K. & Musielak, Z. E. (2014). Impulsively generated linear and non-linear Alfve'n waves in the coronal funnels, *Acta Physica Polonica A, 125,* 158-164.

49. Gatakin, P. & **Kumar, Brijesh,** (2014). Dynamical modeling and resonance frequency analysis of 3.6-m optical telescope pier. *Int. Jr. Structural and Civil Engineering Research*, *3,* 1-10.

50. **Shukla, K. K., Phanikumar, D. V.,** Newsom, R. K., Kumar, K. N., Ratnam, M. V., **Naja, M.** & **Singh, N.** (2014). Estimation of the mixing layer

height over a high altitude site in Central Himalayan region by using Doppler lidar. *Jr. Atomsph. Solar-Tere. Phy., 109,* 48-53.

51. **Sarangi, T., Naja, M., Ojha, N.,** Kumar, R., Lal, S., Venkataramani, S., Kumar, A., **Sagar, R.** & Chandola, H. C. (2014). First simultaneous measurements of ozone, CO and NOy at a high-altitude regional representative site in the Central Himalayas. *Jr. Geophys. Res.: Atmosph., 119,* 1592-1611.

52. **Phanikumar, D. V.,** et al. (including **Shukla, K. K., Joshi, Hema** & **Naja, M.**). (2014). Signatures of Rossby wave modulation in aerosol optical depth over the Central Himalayan region. *Ann. Geophy., 32*, 175-180.

53. Wang, P. F., et al. (including **Pandey, A. K.**) (2014). Characterization of the praesepe star cluster by photometry and proper motions with 2MASSS, PPMx2 and Pan-starrs, *Astrophy. Jr., 784,* 57 (10pp).

54. **Soam, A., Maheswar, G. & Eswaraiah**, **C.** (2014). Additional polarized standards in the fields of known bright standard stars. *Astrophy. Space Science, 350,* 251-263.

55. Bhatt, H., **Pandey**, **J. C.,** Singh, K. P., **Sagar, R.** & **Kumar, Brijesh.** (2014). X-ray flares observed from six young stars located in the region of star clusters NGC 869 and IC 2602. *J. Astrophys. Astr.*, *35,* 39-54.

56. **Pandey**, **A. K.,** et al. (including **Yadav, R. K., Lata, S.** & **Pandey, J. C.**). (2014). Pre-main sequence population in NGC 1893 region: X-ray properties. *New Astron.,* 29, 18-24.

57. **Bose, S.** and **Kumar, B. (2014).** Distance determination to eight galaxies using expanding photosphere method. *Astrophy. Jr., 782,* 98 (12pp).

58. Reddy, K., Ahammed, Y. N. & **Phanikumar, D. V.** (2014). Effect of cloud reflection on direct aerosol radiative forcing: a modeling study based on lidar observations. *Remote Sens. Letts.*, *5,* 277-285.

59. Kumar, R., Barth, M. C., Pfister, G. G., **Naja, M.** & Brasseur, G. P. *(2014).* WRF-Chem simulations of typical pre-monsoon dust storm in northern India: influences on aerosol optical properties and radiation budget. *Atmos. Chem. Phys., 14,* 2131-2446.

60. **Kumar**, **S.,** Singh, A. K. & Lee, J. (2014). Equatorial Ionospheric Anomaly (EIA) and comparison with IRI model during descending phase of solar activity (2005-2009). *Adv. Space Res., 53,* 724-733.

Circulars/Bulletins/Conference Proceedings

1. Su, B. H., Chen, W. P., **Eswaraiah**, **C.,** Tamura, M. & Kandori, R. (2013). Magnetic field structure inferred by near infrared polarization in the Carina Nebula and RCW57. *AIP Conf. Proc., 1543*, 115 -119.

2. Chien-De L., **Eswaraiah, C., Pandey, A. K.** & Chen, W. (2013). A multiband optical polarimetric study of classical Be stars with exceptionally large near-infrared excess. *AIP Conf. Proc., 1543*, 129 -137.

3. **Eswaraiah, C., Pandey, A. K., Sharma, S.** & **Yadav, R. K. (2013).** Photometric and polarimetric studies towards NGC 1931. *AIP Conf. Proc., 1543*, 138-147.

4. **Yadav, R. K., Pandey**, **A. K., Sharma, S. & Eswaraiah, C. (2013).** Multiwavelength studies of H II region NGC 2467. *AIP Conf. Proc., 1543*, 148-156.

5. **Pandey, S. B.** & Zheng, W. (2013). Implications of early time observations of optical afterglows of GRBs. *EAS Publications Series, 61,* 203-209.

6. Castro-Tirado, A. J., et al. (including **Pandey, S. B.**). (2013). Millimetre observations of gamma-ray bursts at IRAM. *EAS Publications Series, 61,* 279-281.

7. **Kumar, Rajiv, Chattopadhyay, I.** & Mandal, S. (2013). Study of jet properties around compact object with the change in accretion disc parameters. *ASI Conf. Series.*, *8*, 147-150.

8. Mandal, S., **Kumar, Rajiv** & **Chattopadhyay**, **I. (2013).** Accretion disc spectrum in presence of mass outflow around black holes. *ASI Conf. Series., 8,* 45-50.

9. Das, S., **Chattopadhyay, I.** & Nandi, A. (2013). Formation of non-steady outflows and QPOs around black hole. *ASI Conf. Series.*, *8,* 31-36.

10. **Chattopadhyay, I.** & **Kumar, R. (2013).** Viscous accretion disc around black holes with variable adiabatic index. *ASI Conf. Series., 8,* 19-25.

11. **Chattopadhyaya**, **I.,** Ryu, D. & Jang, H. (2013). Numerical simulation of astrophysical plasma with relativistic equation of state. *ASI Conf. Series.*, *9,* 13-16.

Accepted Papers (Refereed Journals /Conference Proceedings Etc.) (in Press)

1. **Joshi**, **N. C.,** Srivastava, A. K., Filippov, B., **Kayshap, P., Uddin, W.,** Chandra, R., Choudhary, D. P. & Dwivedi, B. N. (2014). Confined partial filament eruption and its reformation within a stable mangnetic flux rope. *Astrophy. Jr.*

2. **Chand, H., Kumar, Parveen** & Gopal-Krishan, (2014). Intranight optical variability of radio-quiet weak emission line quasars – II. *Mon. Not. Roy. Astron. Soc.*

3. Sharma, M., Nath, B. B., **Chattopadhyay, I.** & Shchekinov, Y. (2014). Interaction of a galactic wind with halo gas and the origin of multiphase extraplanar material. *Mon. Not. Roy. Astron. Soc.*

4. **Dumka**, **U. C.,** et al. (including **Sagar, R.**). (2014). Latitudinal variation of aerosol properties from Indo- Gangetic Plain to central Himalayan foothills during TIGERZ campaign. *JGR: Atmosphere*.

5. **Joshi, Y. C.** & **Joshi**, **S.** (2014). Population I Cepheids and star formation history of the Large Magellanic Cloud, *New Astron.*

6. Vereshchagin, S. V., Chupina, N. V., **Sariya, D. P., Yadav, R. K. S.** & **Kumar, Brijesh.** (2014). Apex determination and detection of stellar clumps in the open cluster M 67. *New Astronomy*.

7. **Ojha , N., Naja, M., Sarangi, T.,** Kumar, R., **Bhardwaj**, **P.,** Lal, S., Venkataramani, S., **Sagar, R.,** Kumar, A. & Chandola, H. C. (2014). On the processes influencing the vertical distribution of ozone over the central Himalayas: Analysis of yearlong ozonesonde observations. *Atmo. Envi.*

8. Tripathi, A., Pandey, U. S. & **Kumar**, **Brijesh.** (2014). Structure and mass function of three young open clusters. *New Astron.*

Magazine/Book Chapter

1. Roy, A. D., Chakraborty, A., Das, H. S., **Medhi, B. J.,** Wolf, S. & Bertrang, G. (2013). Polarmetric Observation of comet C/2009 P1 Garradd, *Emerging Areas of Research and Development in Chemical and Physical Sciences in North East India* (pp. 3-7). Assam: Silchar Sungraphics.

Ph.D. Theses

Awarded

1. Study on star forming regions in wolf rayet galaxies, **Chrishphin Karthick, M.**, (Supervisors: **B. B. Sanwal** and S. Bisht), *Kumaun University,* April, 2013.
2. Large radio sources and episodic nuclear activity, **Sumana Nandi,** (Supervisors: H. C. Chandola, **Mahendra Singh** and D. J. Saikia), *Kumaun University,* August, 2013.
3. Investigation of energetic cosmic explosions and their after effects, **Rupak Roy,** (Supervisor & Co-Supervisor: **Brijesh Kumar** and H. C. Chandola), *Kumaun University,* December, 2013.
4. X-ray and optical studies of blazars, **Haritma Gaur**, (Supervisor & Co-Supervisor : **A. C. Gupta** and U. S. Pandy), *Deen Dayal Upadhyay Gorakhpur University,* September, 2013.
5. Multiwavelength studies of galactic star forming regions, **C. Eswaraiah,** (Supervisor & Co-Supervisor: **A. K Pandey** and H. C. Chandola), *Kumaun University,* September, 2013.
6. Large Radio Sources and their environment, **Akash Pirya,** (Supervisor & Co-Supervisor: H. C. Chandola and **Mahendra Singh**), *Kumaun University,* March, 2014.

Submitted

1. Study of ozone and other trace gases distribution in the lower atmosphere, **N. Ojha**, (Supervisors: **M. Naja** and H. C. Chandola), *Kumaun University,* May, 2013.
2. Variabilities in surface ozone and precursors at Nainital, **Tapaswini Sarangi,** (Supervisor & Co-Supervisor: **M. Naja** and H. C. Chandola), *Kumaun University,* March, 2014.

Summary

1.	Total number of Publications in Refereed Journals	60
2.	Total number of Publications in Press	8
3.	Number of Publications in Circulars/Bulletin	11
4.	Ph.D. Theses awarded	6
5.	Ph.D. Theses submitted	2

International and National Research Projects

During the year 2013-2014 following research projects were funded from outside agencies.

Project Title: Time resolved photometric and spectroscopic study of the chemically peculiar stars.
P.I.: Santosh Joshi
Funding Agency: Department of Science and Technology, Govt. of India.
Project Code: INT/RFBR/P-118

Project Title: Study of dynamical events in the solar atmosphere during maximum of Solar Cycle 24".
P.I.: A. K. Srivastava
Funding Agency: DST-RFBR.

Project Title: Multiwavelength Study of Solar Eruptive Phenomena and their Interplanetary Response
P.I.: Wahab Uddin
Funding Agency: IUSSTF

Project Title: Observations of trace gases at a high altitude site in the Central Himalayas.
P.I.: Manish Naja
Funding Agency: Indian Space Research Organization (ISRO), India.

Project Title: Surface observations of ozone at a rural location in Pantnagar.
P.I.: Manish Naja
Funding Agency: Indian Space Research Organization (ISRO), India.

Project Title: Vertical Distribution of Ozone and Meteorological Parameters in the Central Himalayas.
P.I.: Manish Naja
Funding Agency: Indian Space Research Organization (ISRO), India.

Project Title: Study of the aerosol characteristics over central Himalayas.
P.I.: Manish Naja
Funding Agency: Indian Space Research Organization (ISRO), India.

Title of Project: Star formation history of OB associations and characterization of global properties of young open clusters
Name of P.I.: A. K. Pandey
Funding Agency: DST, New Delhi
Project Code: DST/INT/JSPS/P-168/2013

Project Title: Photometrical and kinematical studies of galactic disc population
P.I.: Brijesh Kumar
Funding Agency: DST, New Delhi
Project Code: DST-ILTP (No. B 3.22)

Project Title: Magnetic activities in low mass stars
P.I.: Jeewan C. Pandey
Funding Agency: DST, New Delhi
Project Code: INT/RUS/RFBR/P-167

Project Title: Short term optical variability of various classes of luminous AGNs
P.I.: Alok C. Gupta
Funding Agency: DST, New Delhi
Project Code: INT/BULGARIA/B-5/08

Project Title: Multiwavelength observations of blazars
P.I.: Alok C. Gupta
Funding Agency: DST, New Delhi
Project Code: INT/UKR/2012/P-02

Project Title: Atmospheric boundary layer network and characterization (ABLN&C): ISROGBP-NOBLE.
P.I.: Narendra Singh
Funding Agency: Indian Space Research Organization (ISRO), India.

Project Title: Development of infrared camera for 3.6m Devasthal Optical Telescope.
Co-PI: Saurabh Sharma
Funding Agency: TIFR/ARIES

Project Title: Thirty Meter Telescope (TMT) Project.
Co-I: Wahab Uddin
Co-ordinator: S. B. Pandey
Funding Agency: DST/DAE

Important Highlights of International and National Projects

Time Resolved Photometric and Spectroscopic Study of the Chemically Peculiar Stars

Name of the P.I.: Santosh Joshi, ARIES, Nainital and Evgeny Semenko, SAO, RAS, Russia.

Report for the Period 01 April 2013-31 March 2014 on the Indo-Russian Project

A project entitled "Time Resolved Photometric and Spectroscopic Study of the Chemically Peculiar Stars " was sanctioned jointly by Department of Science and Technology, Govt of India and Russian Academy of Science. To achieve the goal of the project, a catalogue of 242 chemically peculiar (CP) stars was compiled from the existing photometric and spectroscopic catalogues for the observations from 1.3-m and 1.04-m telescopes of ARIES, Nainital-India and 6.0-m telescope of SAO, Russia.

1. During the financial year 2013-2014, 12 CP stars and 6 open star clusters were observed from Indian telescopes. The main aim was to search for such stars which are pulsationally unstable i.e. variable stars. The photometric data analysis of these objects are in progress. Five known pulsating CP stars were observed spectroscopically from Russian telescope and the analysis of Echelle spectra of these stars was used for the est estimation of the basic physical parameters such as effective temperature, surf gravity, rotational velocity and performed the abundance analysis. The combined photometric and spectroscopic analysis of these stars is being prepared for the publication.

2. Under this Indo-Russian RFBR project Mr. Rahul Aggrawal joined as a JRF in December 2013.

4. At ARIES a focal reducer and three channel time-series CCD photometer for the upcoming 3.6-m telescope are under development. Krishna Reddy visited INASAN, Russia and SAO Russia from 28-03-14 to 08-04-14 to review the optical design of these instruments. During this visit a special presentation was given briefing the status, present status of 3.6-m telescope and those first, second generations instruments which will be mounted on the telescope. Later, a presentation on optical design and analysis of single channel focal reducer and optical design of three channel focal reducer was given in front of optical engineer and few scientists associated with the INASAN and SAO.

Publication:

1. Submitted a paper in Proceedings IAU Symposium No. 307, 2014 G. Meynet, C. Georgy, J.H. Groh & Ph. Stee, eds.

2. Submitted a paper in JAA, Proceeding of the Indo-UK Seminar held at ARIES from 26-28 March 2014.

Star formation history of OB associations and characterization of global properties of young open clusters

Name of the P.I.: A. K. Pandey and N. Kobayashi, University of Tokyo, Japan

This project, in collaboration with Prof. N. Kobayashi, (Japan) and Prof. K. Ogura (Japan), aims to elucidate the global properties of young open clusters in the Galaxy as well as star formation history of the young open clusters/ OB associations associated with HII regions. The initial mass function (IMF), defined as the stellar mass distribution at the time of birth of a clusters, shall be

one of the points of the PI's main interests. They have paid special attention to the number and spatial distribution of low-mass stars. Low-mass members of open clusters/ associations are faint and usually widely distributed over their peripheries (often called as "coronae").

Since open clusters and OB associations are the major mode of star formation in the Galaxy, the distribution of low mas stars in the star forming regions is of crucial importance in understanding the star formation history of the region.

The PIs plan to fully sample the low-mass stars in a few star forming regions with the 2.1 deg square field of view (FOV) of the new CCD camera, KWFC, of the Kiso Schmidt (Japan), which is of the largest FOV in the world.

Highlights of the project

The PIs have carried out an extensive survey of the star-forming complex Sh2-252 an aim to explore its hidden young stellar population as well as to understand the structure and star formation history for the first time. This complex is composed of five prominent embedded clusters associated with the sub-regions A, C, E, NGC 2175s and Teu 136. Using the IR colour-colour criteria, we identified 577 YSOs, of which, 163 are Class I, 400 are Class II and 14 are transition disc YSOs, suggesting a moderately rich number of YSOs in this complex. Spatial distribution of the candidate YSOs shows that they are mostly clustered around the sub-regions in the western half of the complex, suggesting enhanced star formation activity towards its west. Morphology of the region in the 1.1 mm map shows a semicircular shaped molecular shell composed of several clumps and YSOs bordering the western ionization front of Sh2-252. Their analyses suggest that next generation star formation is currently under way along this border and that possibly fragmentation of the matter collected during the expansion of the H II region as one of the major processes is responsible for such stars.

Photometrical and kinematical studies of the galactic disc population

Name of PI : Brijesh Kumar (PI-India), A. E. Piskunov (PI-Russia), R. K. S. Yadav, Sneh Lata, A. Subramaniam, V. S. Avedisova, S. V. Vereschagin, V. V. Malkhov

DST Sanctioned this project on 4th June 2010 under Integrated long term program (ILTP) in Science and Technology between India and Russia. The project duration was for three years.

The project aims at investigating star clusters which are recognized as a valuable tools to understand the structure and evolution of galactic disc population. Two publications have resulted from this project. The fundamental parameters and mass function study of three star clusters NGC 2129, King 12 and NGC 1502 have been completed. The data were collected from 104-cm ARIES telescopes. The analysis shows that these are young star clusters with ages around 10 Myr and having differential interstellar reddening in the direction of all clusters.

In yet another study on the star cluster M67, PIs have determined the cluster's apex coordinates, studied the substructures and performed membership analysis in the central part 34x33 arc-min of the open cluster M 67. They used the individual stellar apexes method developed earlier and classical technique of proper motion diagrams in coordinate system connected with apex. The neighbor-to-neighbor distance technique was applied to detect space details. The membership list was corrected and some stars were excluded from the most probable members list. The apex

coordinates have been determined as: A0 = 132:97 ± 0:81 deg and D0 = 11:85 ± 0:90 deg. The 2D-space star density field was analyzed and high degree of in-homogeneity was found, indicating existence of substructure in the corona, see **Figure 31**.

Three visits, one from Russia to India in Nov 2010 by two Russian scientists and two from India to Russia in Mar 2011 and Mar 2013 by India scientists have been made.

1. UBVRI photometric studies of star clusters NGC 2129, King 12, NGC 1502Apara Tripathi, Brijesh Kumar, R.K.S. Yadav, U.S. Pandey 2011, Proceedings of the Astronomical Society Meeting, Raipur, 23-25 Feb

2. Apex determination and preliminary stellar clump determination in the core of M67 star clusterS. V. Vereschagin, N V Chupina, Devesh P. Sariya, R.K.S. Yadav, Brijesh Kumar,2014, New Astronomy, 31, 43-50

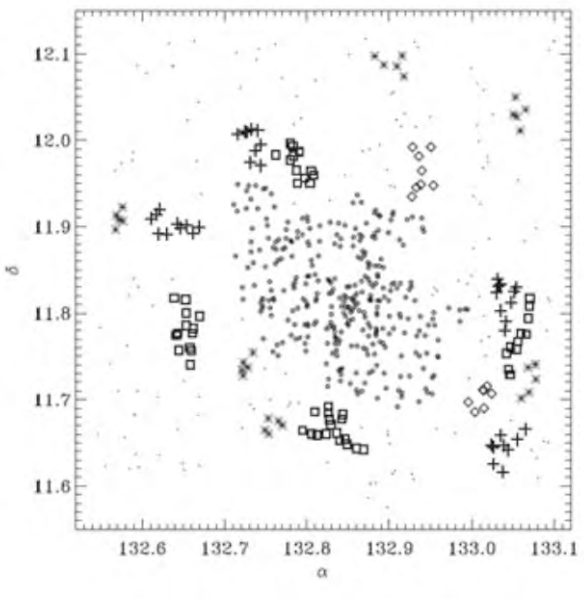

Figure 31. *The distribution of stars of M67 in the equatorial coordinate system. Different symbol designate group of stars obtained by different method.*

Short term optical variability of various classed of luminous AGNs

Name of P.I.: A. C. Gupta, ARIES, Nainital and E. Semkov, Institute of Astronomy and National Astronomical Observatory, Sofia, Bulgaria.

Results:

Blazars are a class of Active Galactic Nuclei (AGN) distinguished by the fact that their non-thermal, strongly anisotropic emission is believed to be coming from material moving at relativistic speed pointing in our direction. Blazars are at very large distances and it is hard to resolve their fine scale properties using the current and near future observing facilities. However, time scale of variability can be used to probe into the location and physical processes related to emission mechanisms at even finer scales.

X-ray emission region must be very close to the central engine by the light travel arguments. So, X-ray variability studies is very important in determining the size of the central engine. In this studies, the PIs have searched for the Intra-Day Variability (IDV) timescales in the X-ray Light Curves (LCs) to perhaps get information on the masses of the Super Massive Black Holes (SMBHs) in blazars. They analysed a sample of 24 XMM-Newton LCs of four blazars and found IDV time-scales in 8 LCs ranging from 15.7 ks to 46.8 ks. Also, we searched for the Quasi Periodic Oscillations (QPOs) in the X-Ray LCs as they shed new light on the physical processes of the source and associated X-Ray emission. We found a QPO of ~ 4.6 hours in one LC of blazar PKS 2155–304 and possible hints of QPOs in two other LCs. Assuming these oscillations are associated with the innermost portions of their accretion disk, they estimated their central black hole mass exceed 1.2 $\times 10^7$ M.

Optical IDV is very important to understand the sub-parsec scale structure of AGNs. Optical observations offer a wealth of information on the variability of different classes of blazars. In this work, they have studied the flux and the colour variations of blazars on short and IDV time-scales. They found that the blazars are highly variable and do show colour variations on short time-scales and can be attributed to the models involving shock propagating down the jets. It has been shown that BL Lacs show bluer-when-brighter trend whereas FSRQs (Flat Spectrum Radio Quasars) show redder-when-brighter trend. Also, they have studied optical IDV of a sample of HSP (High synchrotron Peaked) blazars which are not well studied in literature in optical bands. The PIs found that the HSP blazars are intrinsically less variable in optical bands as compared to LSP (Low Synchrotron Peaked) blazars.

Variability of the different wavelength regime can be used to examine connections between their emission mechanisms. Comparison of the amplitudes and time of peak flux of flares at different wavebands may be used to identify the location of relevant emission regions and are very necessary to constrain the existing models for X-ray and γ -ray emissions. So, they performed correlation between γ-ray, X-ray and optical band of the blazar 3C 454.3 and found strong correlation between γ -ray and optical bands but X-ray is not correlated with either of these. This result supports the external Compton model in which relativistic electrons in the jet radiate optical photons through synchrotron photons and then inverse Compton scatter optical photons to γ -ray energies.

The PIs studied the optical spectral indices of different classes of blazars (HSPs, LSPs (BL Lacs and FSRQs)) in order to examine the possible contaminations present in addition to the synchrotron component. They found the average optical spectral index of LSPs (BL Lacs) is ~1.5 and is in agreement with Synchrotron-Self-Compton models. LSPs (FSRQs) have a contribution from the thermal bump while optical spectra of HSPs indicates contamination of thermal as well as non-thermal components in addition to synchrotron component.

Thesis resulted from the project:

X-ray and optical studies of blazars**, Haritma Gaur**, (Supervisor & Co-Supervisor : **A. C. Gupta** and U. S. Pandy), *Deen Dayal Upadhyay Gorakhpur University,* February, 2013

Multiwavelength Study of Solar Eruptive Phenomena and their Interplanetary Response

Indian PI and Nodal Project Coordinator: Wahab Uddin, Aryabhatta Research Institute of Observational Sciences (ARIES), Manora Peak, Nainital, Uttarakhand, India

US PI: Dr. N. Gopalswamy, Astrophysicist, NASA Goddard Space Flight Center, Greenbelt, USA

This is an Indo-US Science and Technology Forum (IUSSTF) Joint Center Project on Solar Eruptive Phenomena ("IUSSTF/JC-Solar Eruptive Phenomena/99-2010/2011-2012") entitled "Multiwavelength Study of Solar Eruptive Phenomena and their Interplanetary Responses" funded by IUSSTF. Dr. Wahab Uddin is the P.I. and Nodal Project Coordinator from the nodal host institute Aryabhatta Research Institute of the Observational Sciences (ARIES), Manora Peak, Nainital, while Prof. Nat Gopalswamy is the US PI from GSFC-NASA. Other co-investigators are Dr. A.K. Srivastava (ARIES), Prof. Rajmal Jain (PRL,

Ahmadabad), Prof. P.K. Manoharan (RAC, NCRA-TIFR, Ooty), Dr. Ramesh Chandra (KU, Nainital), Prof. Debi Prasad Choudhary (The California State University, Northridge, LA, USA), Prof. Markus Aschwanden and Dr. N.V. Nitta (LMSAL), as well as various students and postdoctoral researchers from Indian and US sides.

Scientific Objectives of the Projects:

1. Origin of Eruptive Events (Initiation, Early acceleration, energy build-up and energy release processes in active region, waves and shocks).

2. Propagation of CMEs (Interplanetary Scintillations (IPS), IP type II bursts, in-situ observations of CMEs).

3. Geoimpact of Eruptive Events (Solar Energetic Particles, Energetic Storm Particles, Geomagnetic storms, and ionospheric effects, VLF propagation effects).

4. Impact on surrounding structures (coronal hole deflection and oscillation in active region loops, interaction of global EUV waves with coronal magnetic structures).

In the duration of the two years of the project (2011-2013), the various scientific research works have been carried out to understand the origin of solar eruptive events (e.g., solar flares, CMEs, eruptive prominences) and associated plasma processes, and their responses to the Earth's outer atmosphere under the prospective of the space weather. Several important papers have been published. Here we are presenting the main results of these various research works.

Scientific Results:

The observations of a confined partial eruption of a filament on 2012 August 4, which restores its initial shape within $\approx$ 2 hr after eruption were presented. From the Global Oscillation Network Group Hα observations, we find that the filament plasma turns into dynamic motion at around 11:20 UT from the middle part of the filament toward the northwest direction with an average speed of $\approx$ 105 km s^{-1}. A little brightening underneath the filament possibly shows the signature of low-altitude reconnection below the filament eruptive part. In Solar Dynamics Observatory/Atmospheric Imaging Assembly 171 Å images, an activation of right-handed helically twisted magnetic flux rope that contains the filament material and confines it during its dynamical motion was observed. The motion of cool filament plasma stops after traveling a distance of $\approx$ 215 Mm toward the northwest from the point of eruption. The plasma moves partly toward the right foot point of the flux rope, while most of the plasma returns after 12:20 UT toward the left foot point with an average speed of $\approx$ 60 km s^{-1} to reform the filament within the same stable magnetic structure. On the basis of the filament internal fine structure and its position relative to the photospheric magnetic fields, the filament chirality to be sinistral was found, while the activated enveloping flux rope shows a clear right-handed twist. Thus, this dynamic event is an apparent example of one-to-one correspondence between the filament chirality (sinistral) and the enveloping flux rope helicity (positive). From the coronal magnetic field decay index, n, calculation near the flux rope axis, it is evident that the whole filament axis lies within the domain of stability (i.e., $n < 1$), which provides the filament stability despite strong disturbances at its eastern foot point.

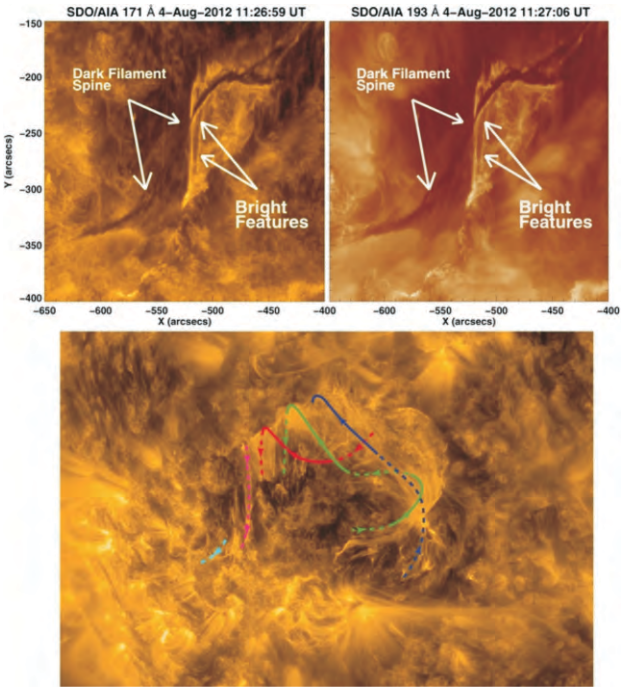

Figure 32. Upper panel: *SDO*/AIA 171 and 193 Å images at ≈ 11:27 UT, showing the crossing of dark (upper) and bright (below) threads. Bottom panel: *SDO*/AIA 171 Å image at 12:14:35 UT with drawn sections of flux rope field lines that can be followed from the visible threads. Field-line portions that lie above the flux rope axis are shown as solid lines, while those that lie below the flux rope axis are shown as dashed lines.

Publications:

1. Chandra, R., et. al. (including **Uddin, W., Srivastava, A. K.**, and **Joshi, N. C.**). Solar energetic particle events during the rise phases of solar cycles 23 and 24, *Advances in Space Research, 52,* 2102-2111.

2. **Joshi, N. C., et. al.** (including **Srivastava, A. K., Uddin, W. and Kayshap, P.).** A study of a failed coronal mass ejection core associated with an asymmetric filament eruption, *Astrophy. Jr., 771,* 65(13pp).

3. Choudhary, D. P., et al. (including **Uddin, W . , Srivastava, A. K., Joshi, N. C.** & **Kashyap, P.**). (2013). Flux emergence, flux imbalance, magnetic free energy and solar flares, *Advances in Space Research, 52,* 1561-1566.

4. **Joshi, N. C., Srivastava, A. K.**, Filippov, B., **Kayshap, P.**, **Uddin, W.**, Chandra, R., Choudhary, D. P. & Dwivedi, B. N. (2014). Confined partial filament eruption and its reformation within a stable mangnetic flux rope, *Astrophy. Jr., 787*, 11.

Atmospheric Chemistry Transport and Modeling (ATCTM) and Aerosols Radiative Forcing over India (ARFI) Projects under ISRO-GBP

Name of the P.I. – Manish Naja

Surface observations of ozone, CO and NOy are made for the first time over the central Himalaya during 2009-2011. It is shown that variabilities in these gases are mainly associated with meteorological and dynamical processes, while photochemistry is playing a least role. This is confirmed by slope values of ozone-CO and ozone-NOy, showing minimal influences of fresh emissions in this region. Enhancements in ozone, CO and NOy have been attributed mainly to regional pollution supplemented with northern Indian biomass burning. Nevertheless, contribution of downward transport from higher altitudes is noticed in case of ozone. Influence of northern Indian (60° to 95°E and 20° to 38°N) biomass burning on levels of observed trace gases at Nainital has been studied using MODIS-derived total fire counts. Explicitly, biomass burning activities over this region are observed to be highest during spring months. The major source of these activities is crop residue burning, with some

contribution from forest fires. The fire counts are very low during wet season (summer monsoon) as well as during winter. A secondary peak is also noticed during autumn that is less prominent in comparison with spring. The observations are segregated into the high and low fire activity periods. In this approach, the period during which the 3 day running mean of fire counts exceeds the median fire count of April–May are classified as "High Fire Activity Period" while the remaining are termed as "Low Fire Activity Period". In this way, high fire activity periods are identified as 18 April to 17 May in year 2009, 14 April to 16 May in year 2010, and 22 April to 22 May in year 2011. Furthermore, low fire activity periods are restricted to those prior to high fire activity periods, i.e., 1–17 April 2009, 1–13 April 2010, and 1–21 April 2011, respectively, so as to avoid the residual influence of the prior high fire activities. **Figure 33** shows time series of ozone, CO, and NOy at Nainital during April and May for the years 2009, 2010, and 2011. The estimated enhancements in ozone, CO, and NOy during high fire activity period are found to be 4–18%, 15–76%, and 35–51%, respectively.

For the first time, measurements of vertical distribution of ozone (ECC ozonesonde) and meteorological (iMet GPS radiosonde) parameters are made up to 30-35 km in the central Himalayan region. Lower tropospheric (up to 4 km) ozone shows a prominent seasonality with highest ozone levels in spring (70-100 ppbv) and lowest in summer-monsoon (20-50 ppbv) that is consistent with surface ozone observation. In-contrast, middle and upper tropospheric ozone show a broad maximum in late winter and spring. Similar to the ground based ozone observations, significant enhancement in ozone is observed from surface to 4-5 km region with value more than 20 ppbv during the springtime high fire activity period over this region. Few events of downward ozone transports are also studied using vertical ozone profiles. It is known that tropopause fold and stratosphere-troposphere exchanges are more frequent during winter and early spring, but these studies are sparse over the Indian region and leading to induce uncertainty in the tropospheric ozone budget. In the present work, stratospheric intrusion events are observed and show enhancement in ozone levels by ~180% in the middle-upper troposphere. Events of downward ozone transport are confirmed by the RH profiles, those show descend of dry air. Few events of secondary ozone peaks are also observed in middle-upper troposphere in all seasons **(Figure 34)**. Ozone profiles show layered structures of elevated ozone levels (140-250 ppbv) in 8-12 km region. The frequency of such events is higher in spring. A comparison is also made between ozone profiles at this Himalayan region and urbanized location (Ahmedabad). Ozone levels are observed to be more-or-less similar over both regions up to middle troposphere, except in spring when ozone levels are higher over Himalaya. This suggests the influences of pollution from IGP that is supplemented with the contribution of northern Indian biomass burning. It is envisaged that dynamical processes, including advection and downward transport from the stratosphere are playing major role in middle-upper tropospheric variations while, regional emissions and biomass burning processes play controlling role in the lower troposphere.

Impact of a typical pre-monsoon season dust storm event (April 2010) is assessed on the regional aerosol optical properties and radiation budget in northern India. Dust is shown to be transported from Thar Desert and loading in different sizes is seen in the boundary layer and free troposphere. Model estimated total dust emissions of 7.5 Tg over the model domain. Model reproduced the spatial and temporal distributions of dust plumes and aerosol optical properties but generally underestimated the AOD. Model results show that dust particles cool

the surface and the top of the atmosphere, and warm the atmosphere. The regionally averaged radiative perturbation due to dust aerosols is estimated as −2.0±3.0Wm−2 at the top of the atmosphere, 2.3±1.8Wm−2 in the atmosphere and −4.4±3.1Wm−2 at the surface.

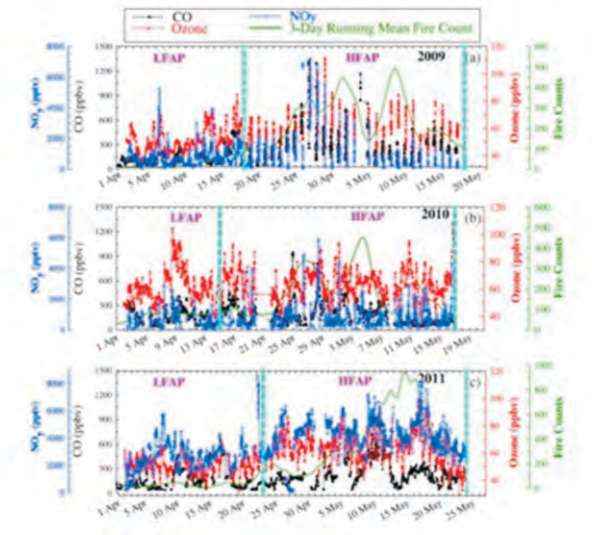

Figure 33. *Variations in ozone, CO and NOy during high fire activity and low fire activity periods during years 2009, 2010 and 2011.*

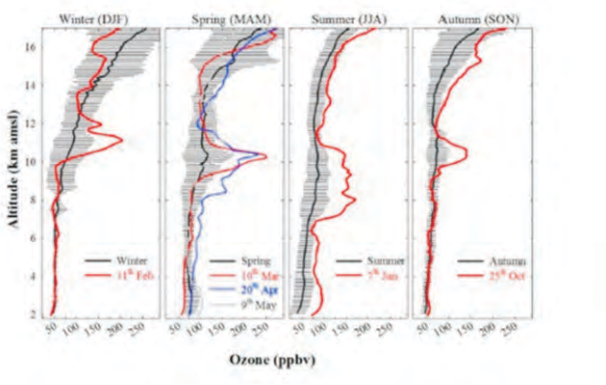

Figure 34. *Enhancements (secondary peak) in moddle-upper tropospheric ozone.*

Publication:

1. Sarangi T., **M. Naja**, N. Ojha, R. Kumar, S. Lal, S. Venkataramani, A. Kumar, R. Sagar and H. C. Chandola, First simultaneous measurements of ozone, CO and NO_y at a high altitude regional representative site in the central Himalayas, *J. Geophys. Res. Atmos.*, 119, doi:10.1002/2013JD020631, 2014. **[IF-3.17]**

2. N. Ojha, **M. Naja**, Sarangi T., R. Kumar, P. Bhardwaj, S. Lal, S. Venkataramani, R. Sagar, A. Kumar, and H. C. Chandola, On the processes influencing the vertical distribution of ozone over the central Himalayas: Analysis of yearlong ozonesonde observations, *Atmospheric Environment*,doi:10.1016/j.atmosenv.2014.01.031, 2014. **[IF-3.78]**

3. Kumar, R., M. C. Barth, G. G. Pfister, **M. Naja**, G. P. Brasseur, WRF-Chem simulations of a typical pre-monsoon dust storm in northern India: influences on aerosol optical properties and radiation budget, *Atmos. Chem. Phys*, 14, 2431-2446, 2014. **[IF-5.51]**

Micrometeorological observations over Manora peak

Name of the P.I.: Narendra Singh

Experimental exploration of ABL processes over mountainous region in the central Himalayas is being carried out at ARIES, Nainital, under the IGBP-NOBLE project. Extensive studies for characterization of boundary layer over Indian-subcontinent are lacking, therefore a network of observatories have been set-up, of which this site is a part representing mountainous region, which aims at characterizing the boundary layer and provide critical inputs for the modeling purpose.

Two Fast response ultrasonic sonic anemometers (METEK, Germany) are installed on a self supported meteorological tower at two levels (27 m and 12 m) above the ground. Measurement of three axis winds (basically all three components of the wind), temperature and humidity at a sampling rate of 25 Hz are active since 29 January 2013. These observations are subsequently used to determine, turbulent kinetic energy, surface layer turbulent fluxes of momentum and heat (*Stull, 1988*) and stability parameter (z/L). In general, defining characteristics of the Atmospheric Surface Layer (ASL) are its buoyant stability, the vertical variations of wind speed, temperature, relative humidity, and the related vertical fluxes. In order to understand diurnal variations of parameters being presented

Table 1. Specifications of Ultrasonic anemometer

Parameters	Measuring range	Resolution
Wind Speed	0 to 45 m/s; (For raw data) 0 ... 60 m/s (averages > 60 seconds	0.02 m/s [1*] -or- 0.01 m/s [2**] [1*] for instantaneous data 2* for averages (⩾ 1s)
Wind direction	0 to 360 degree	1 degree
Wind components	-45 to +45 m/s; (for raw data) -60 to 60 m/s (averages > 60 seconds)	0.01 m/s
Temperature	-30 to +55 °C derived from the sound velocity, compares to the virtual temperature	0.01 K

over the month of a season, every 25 Hz archived data is averaged for half an hour during a given day resulting into a total of 48 data sets for the given cycle of 24 hours. Further, half an hour data of the same time, for all available days of a month, is utilized to generate a monthly mean over the diurnal cycle, and the statistics was applied on it to obtain mean and standard deviation.

Results

The study found that boundary layer in mountainous topography has complex behavior. Surface layer parameters were estimated with eddy-covariance method; z/L and vertical winds indicated diurnal variability in all seasons, but no diurnal variability was observed in MF and TKE except during the spring season. The wind direction also showed a gradual change in late morning hours from November to December, thereby illustrating the impact of mountainous terrain on wind flow over the site in calm wind conditions. In valley systems, the local wind system has a considerable impact on the measurements. The continuous wind along the valley axis, up-valley during the day and down-valley by night, certainly involves horizontal advection, however, over this in the spring season, consistent strong (>4m/s) north-westerly flow which hits the mountain slope resulting in strong upslope flow over the site.

The results obtained in this study provide supporting evidence on the effect of slope winds on the temperature variability and the stability parameter. The slope winds cause convergence (divergence) of air mass in day (night) reducing the amplitude of air diurnal cycle temperature mountain peak, which shows that orographic wind flows govern the diurnal cycles of air temperature in a region of complex topography. The surface layer shows transition from stable layer to unstable layer in the morning hours and the return from unstable to stable (stratified)

state in the evening, during all seasons, however the stability in nigh-time is not very strong (almost neutral with z/L values nearly approaching zero) especially during the spring and monsoon season.

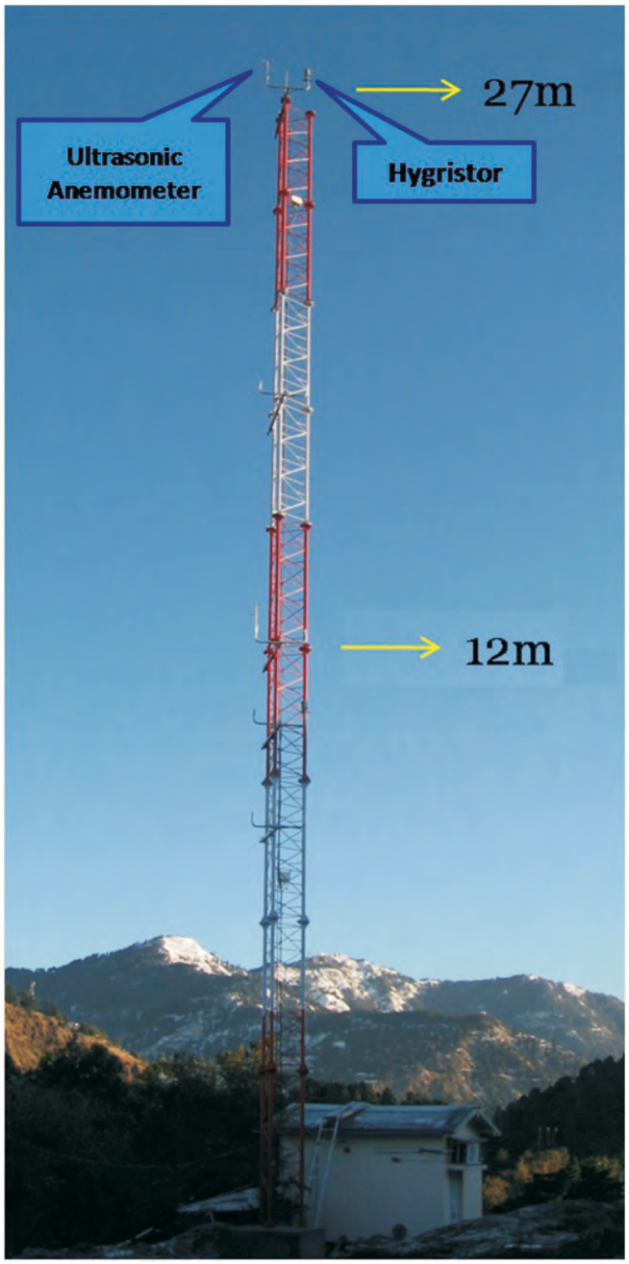

Figure 35. Self-supported meteorological tower at ARIES, Manora Peak, Nainital.

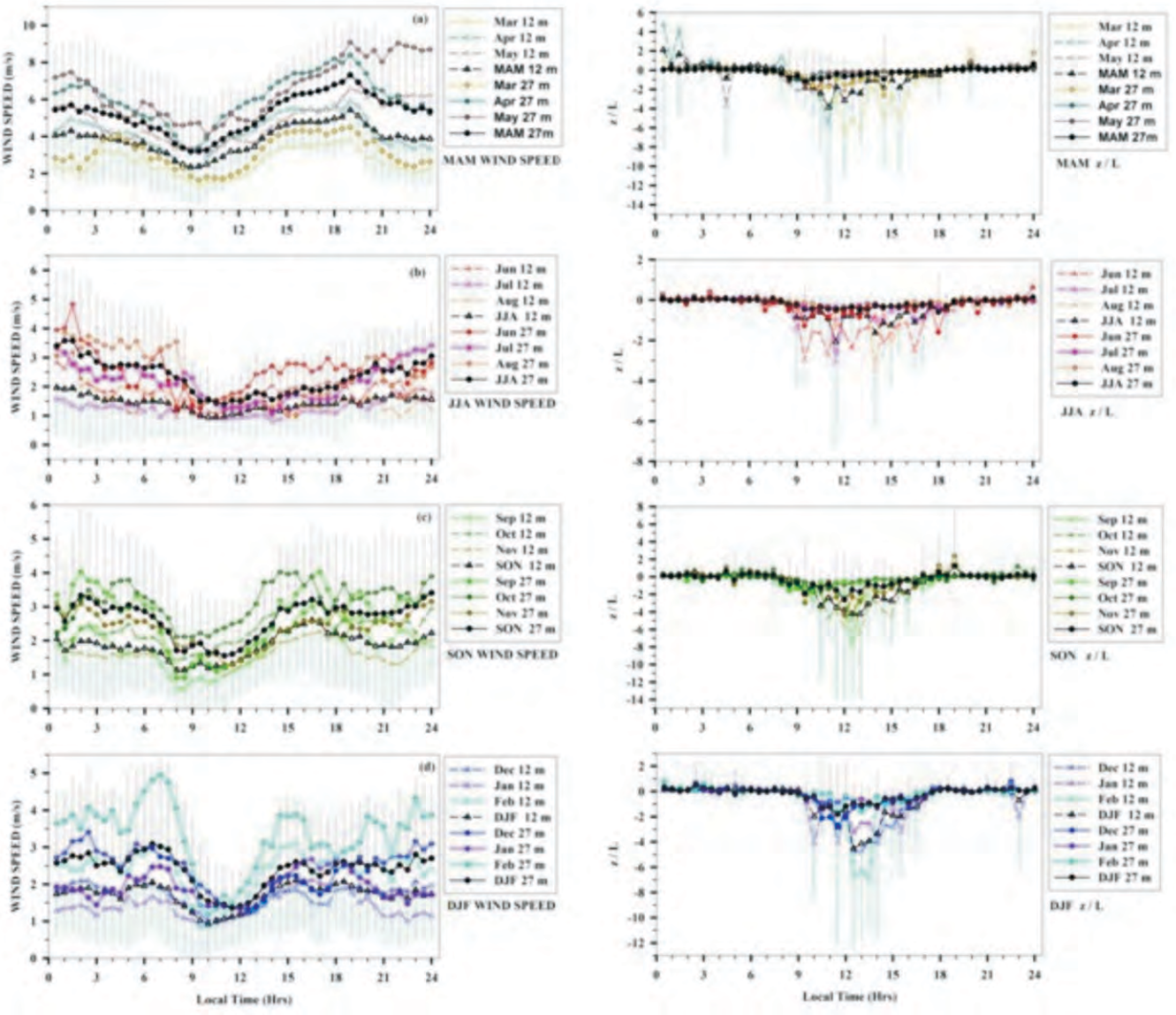

Figure 36. *The panel on left shows daily variability in wind speed over the site in different seasons of the year, similarly the panel on the right depicts the diurnal variability in stability parameter in different seasons. The vertical bars denote the standard deviation in observations.*

Instruments Facility and Design Laboratory (IFDL)

A modern instrument facility and design laboratory has been established in the institute, with capabilities of performing sensitive optics and electronics experiments, and assembling the optical and opto-electronics instruments in a clean environment. Several vibration free tables, metrological instruments such as laser interferometer, phase contrast interferometer for optical profiling, coordinate measurement machine (CMM), laboratory spectrometers and several light sources have been made operational. A computer numerical control (CNC) machine for manufacturing of mechanical parts has been established. The mechanical workshop has been upgraded to perform maintenance of the facilities in the institute. A set up for measuring absolute reflectivity of coated samples has been designed and built by the institute. A class 10,000 clean room providing a dust free environment has been created so that sensitive electronics equipment like charge coupled device cameras and optical instruments can be assembled within the institute. The laboratory is also equipped with all necessary capabilities to perform designing of complex instruments. Several instruments such as faint object spectrograph and camera (FOSC), High resolution spectrograph (HRS), and multi-channel fast photometer for the 3.6 meter optical telescope have been designed within the institute. The electronics lab has made setups for performing experiments on advanced motion control of telescope systems and embedded systems. Several MoU programs have been established with IITs, research institutes in India and abroad (such as Canada, Belgium, Russia) for instrument development. The laboratory is also providing consultancy and training to students from various Indian universities and national engineering colleges for academic and research purpose, in the field of optical design and instrumentation.

Major Highlights from laboratories:

Optics Laboratory: Optics section is actively involved in the instrumentation activities related to various projects. To support different instrumentation activities, optics section has installed some new facilities/ instruments for aligning, testing, integrating etc. of optics/optical system. The detail of the new facilities / instruments installed is as below:

Clean Room Facility: A class-10,000 clean room with a laminar flow unit providing air with class-100 specifications has been installed in the optics lab. The clean room has a vibration isolated optical table of 12 x 9 x 9 feet dimension. This facility is used for assembly of optics and electronics (CCD camera etc.) related to the instrumentation programs.

Figure 37. *The class 10,000 clean room facility with vibration free table installed at optics lab, ARIES, Nainital.*

Metrology instruments: Several metrological instruments were procured:

(i) A laser interferometer (Agilent 5530/5519A) has been procured. It will be used for micron level measurements (linear/angular alignments, vibrations etc.) of mechanical and opto-mechanical systems of the 3.6 meter telescope during installation and further maintenance of its active optics system.

(ii) An optical profiler cum phase shift interferometer has been procured. It can measure surface roughness and shape profiles of optical elements, step height of metal/dielectric coatings on mirror, lenses as well as can perform any kind of 3D surface profile analyses.

(iii) A handheld UV-VIS-NIR spectrometer has been procured to measure transmission/reflectance of materials such as glass, mirrors etc.

(iv) A coordinate measurement machine (CMM) has been installed. It is used for precise (~10 micron accuracy) metrology measurements of mechanical components manufactured in house and verification of similar components procured from outside. It can also be used for doing reverse engineering of components.

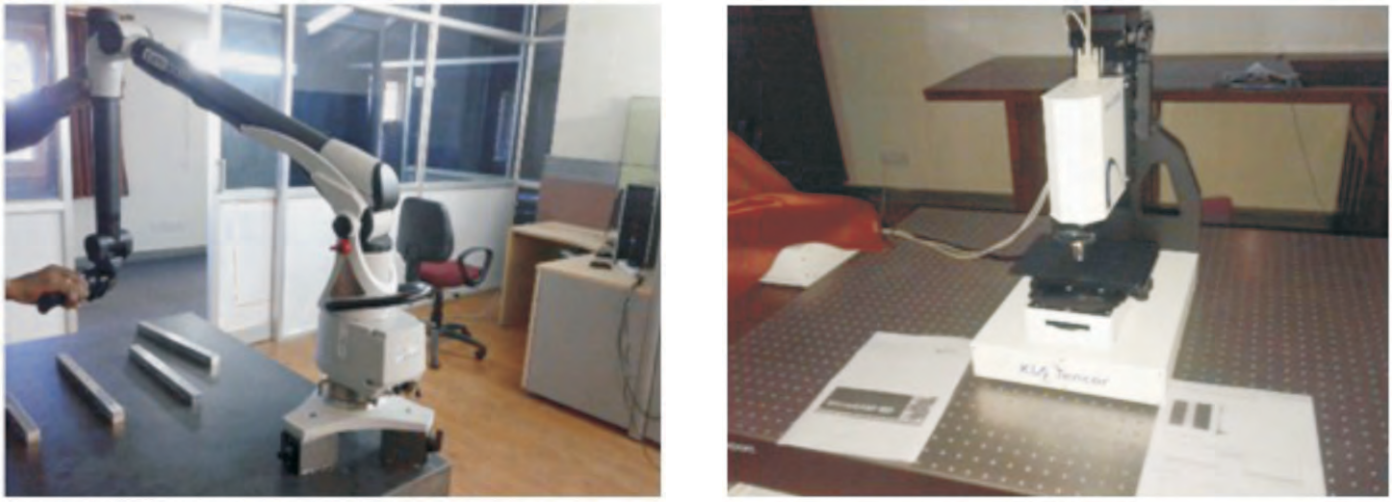

Figure 38. *(left) The coordinate measurement machine (right) optical profiler acquired in the optics lab, ARIES, Nainital.*

In addition to these, design section of optics laboratory was actively involved in the optical designing of various instruments under different projects. Testing, verification of various instruments was carried out in the laboratory. Optical alignment of instruments/ telescopes image quality testing was also carried out. The major achievements in 2013-2014 are:

(i) The optics of the Faint Object Spectrograph and Camera (FOSC), the first science instrument on the 3.6 meter telescope, was designed by ARIES. The manufacturing of the optics has been completed. The optics was tested and after being found to conform with specifications, was delivered to ARIES. The test results on individual elements and overall image quality were highly satisfactory.

(ii) Optical design work for next generation instrument e.g. high resolution spectrograph, wide field polarimeter, fast photometer etc. is in progress. Optical cleaning, alignment and image quality testing of 130 cm primary mirror and 104 cm primary mirror were also carried out.

Development of this new competitive 0.8 - 2.5 micron medium resolution spectrograph /imager for the ARIES 3.6 meter Devasthal optical telescope:

There is a very large class of problems of astrophysical interest, in which the NIR observations play an crucial role. Spectroscopic surveys of astronomical sources in NIR wavelength are practically negligible due to its complexity in instrumentation. Development of a new NIR spectrograph is in its advance stage. Development of this new competitive 0.8-2.5 micron medium resolution spectrograph/imager for the ARIES 3.6 meter Devasthal optical telescope would give enormous in-house instrumentation development opportunity and manpower development in India as well as high class data very useful for the various astronomical studies.

Figure 39. *A view of Optics Building*

Status of a new Near Infrared Spectrograph for 3.6-m DOT

There is a growing demand for the near infrared (NIR) studies for star forming regions/brown dwarfs/AGNs active galaxies etc for which the NIR observations play an crucial role. Spectroscopic surveys of these astronomical sources in NIR wavelength are practically negligible in our country due to its complexity in instrumentation. , Tata Institute of Fundamental Research, Mumbai, India (DAA-TIFR) and the Aryabhatta Research Institute of Observational Sciences, Nainital, India (ARIES) are jointly developing an Infrared medium resolution Spectrometer for the 3.6m Devasthal Optical Telescope.

The cost involved in the building of this medium resolution spectrometer will be equally borne by DAA-TIFR and ARIES. The total cost of the project is expected to be approximately Rs. 20 Crores during the 12th Plan period. The contribution of DAA-TIFR and ARIES will be 50% of the total amount each during the 12th Plan period. The verification of the design suitability, testing and qualifying the spectrometer will be done jointly by DAA-TIFR and ARIES. If found feasible, the capabilities of TIFR and ARIES in the areas of mechanical construction, electronics design and software design will be utilized to complement the efforts of the contractor in realizing the spectrometer.

The responsibility of ARIES includes,

- All hardware, software, and operational specifications and requirements related to the telescope and the observatory.
- Integration of the instrument control and data acquisition system with the telescope and observatory control system.
- Operation and Routine maintenance of the instrument.
- Power, network, electrical, mechanical and optical interfaces on the telescope and observatory side.

The project is planned to be completed in three years comprised of approximately one year for the design and finalization of the optical components, electronics and mechanical parts and two years for the building and testing.

Detailed review of the feasibility of the project and the science goal has been carried out. The team involved in the project has generated science cases of the instrument and after the formal approval of the project, they have worked out the technical details of the instrument based on the financial constrains and the science goals. The current status of the project is as given below:

1. The project has been approved by TIFR in July 2012.
2. Final Instrument specification is going to be a 0.8 to 2.5 micron spectrometer with slit viewer within the available budget.
3. Making of a preliminary design of the instrument is in progress.
4. First draft of the MoU between ARIES and TIFR has been made on 19 March 2013 and currently under review.
5. A MoU defining work-packages and responsibilities for this instruments has been signed between ARIES and TIFR on 26th August 2013

6. Public Tender has been floated for Spectrograph on 18th October 2013.

7. The technical bids of the Public Tender for the TIFR-ARIES Near Infrared Spectrometer (TANSPEC) were opened on 25th November 2013.

8. Based on the comments from the national and international experts, technical evolution committee (9th January 2014) has found Mauna Kea Infrared LLC suitable for developing the instrument.

9. Briefly, this spectrograph will consists of two modes of observations:

   (a) Cross dispersed high resolution mode with resolving power of ~2000 – 3000 at the narrowest slit position

   (b) Low resolution mode with resolving power of ~100.

It will also have an infra-red field viewer with field of view of 1 x 1 arcmin square.

Status Report on the Upcoming Major Facilities

1. Devasthal Optical Telescope (DOT) (3.6-m Aperture):

ARIES is establishing a national facility in optical astronomy at Devasthal to fulfil the major aspirations of the Indian astronomical community. This facility consists of a modern 3.6 meter optical new technology telescope, a suite of instruments, an observatory with a coating plant, a control room and a data center. The 3.6-m Devasthal Optical Telescope (DOT) will have a number of instruments providing high resolution spectral and imaging capabilities at visible and near-infrared bands. In addition to optical studies of a wide variety of astronomical topics, it will be used for follow-up studies of sources identified in the radio region by GMRT and UV/X-ray by ASTROSAT.

The 3.6-m DOT project is monitored and advised periodically by a nine member Project Management Board (PMB) chaired by Professor P.C. Agrawal. The day-to-day activities related to scientific, technical and financial aspect of the project is executed by a project implementation team (PIT) and eight project working groups (PWG) under the guidance of the project director and project manager. The PMB, PIT and PWGs met at several occasions to monitor the progress of the project. During Apr 2013 – Mar 2014, most of the scheduled project activities were carried out successfully.

Manufacturing of 3.6m aperture optical telescope has been completed and the telescope parts were transported from AMOS Belgium to the Devasthal site, India in March 2013. The work on enclosure which will house the telescope is in advanced stage.

Telescope enclosure and auxiliary building : For 'Manufacture, supply, erection and commissioning of telescope enclosure structure and equipments for the 3.6m Devasthal Optical Telescope', a contract agreement has been signed with the M/s Pedvak Hyderabad. The work was divided into three parts – extension building structure, dome support structure and dome structure.

Extension building : The extension building has size of 24m x 12.25m and it is designed to house coating plant. Total structure weighs about 118 Ton. Erection of the entire extension building was completed. Rolling shutters, heavy duty exhaust fans, windows and doors were installed. Sheeting work of the extension building was also completed. Rails and ground trolley were also installed and commissioned.

Dome support structure: The stationary dome support structure of the telescope building has shape of a cylinder with inner diameter of 16.5m and a height of 15 m. Total structure weighs about 123T including a lift and staircase. Erection of entire dome support structure was completed. Several subsystems – such as circular ring beams, dome drive assembly, 11m platform, 12 ventilation fans, and exhaust fans of technical room, platform for pier were successfully installed and commissioned.

Dome structure: The rotating dome of the 3.6m telescope building is a circular steel structure of 16.5m diameter and 13.9 meter heigh. The rotating dome weighs around 175 Ton and it is the most critical part of the building. It also houses 4.2m wide slit doors and a wind screed. Several subsystems of the dome, such as dome drive assembly, wind screen assembly, slit doors, ome columns, sheeting of the dome, were successfully installed and commissioned. About ninety percent of the dome structure work was completed till 31st March 2013. A picture of the dome is shown in **Figure 40**.

Figure 40. *Picture of Dome of 3.6m telescope taken on 19th March 2014.*

Figure 41. *Picture of 3.6m building taken on 30th March 2014. Dome support and extension building is completed. Dome structure is nearly complete.*

2. ARIES Stratosphere Troposphere Radar (@ 206.5 MHZ)

The Stratosphere Troposphere (ST) Radar being established at ARIES, Nainital to provide continuous vertical profile of winds with high temporal and spatial (vertical) resolution, under all weather conditions, in the central Himalayan region. The radar system is configured as an active phased array using state-of-art solid state Transmit Receive Module (TRM) and Digital Signal Processing (DSP) techniques (**Figure 42 'a' and 'b'**) to obtain the end product. This system has an array of 588 Yagi (3-elements) in a circular aperture on equilateral triangular grid arrangement with the inter element spacing of 0.7'λ. This radar system is indigenously developed in India and antennae array is installed on a roof top for the first time (**Figure 43**).

ARIES ST Radar (ASTRAD) project is monitored and advised periodically by a Project Management Committee chaired by Professor B. M. Reddy. Test and Evaluation meeting for DSP systems was carried out during 6-7 Oct, 2013 at ARIES, Nainital. The radar was operated with a sub-array of initial 49 elements consisting the central cluster of the system. Several experiments have been conducted and test profiles are available now using one cluster (group of 49 TRMs and Antennae) to seven clusters. Work is also in progress to fine-tune remaining clusters. An uninterrupted power supply unit (3x200 KVA) along with its panels is now available at the radar site.

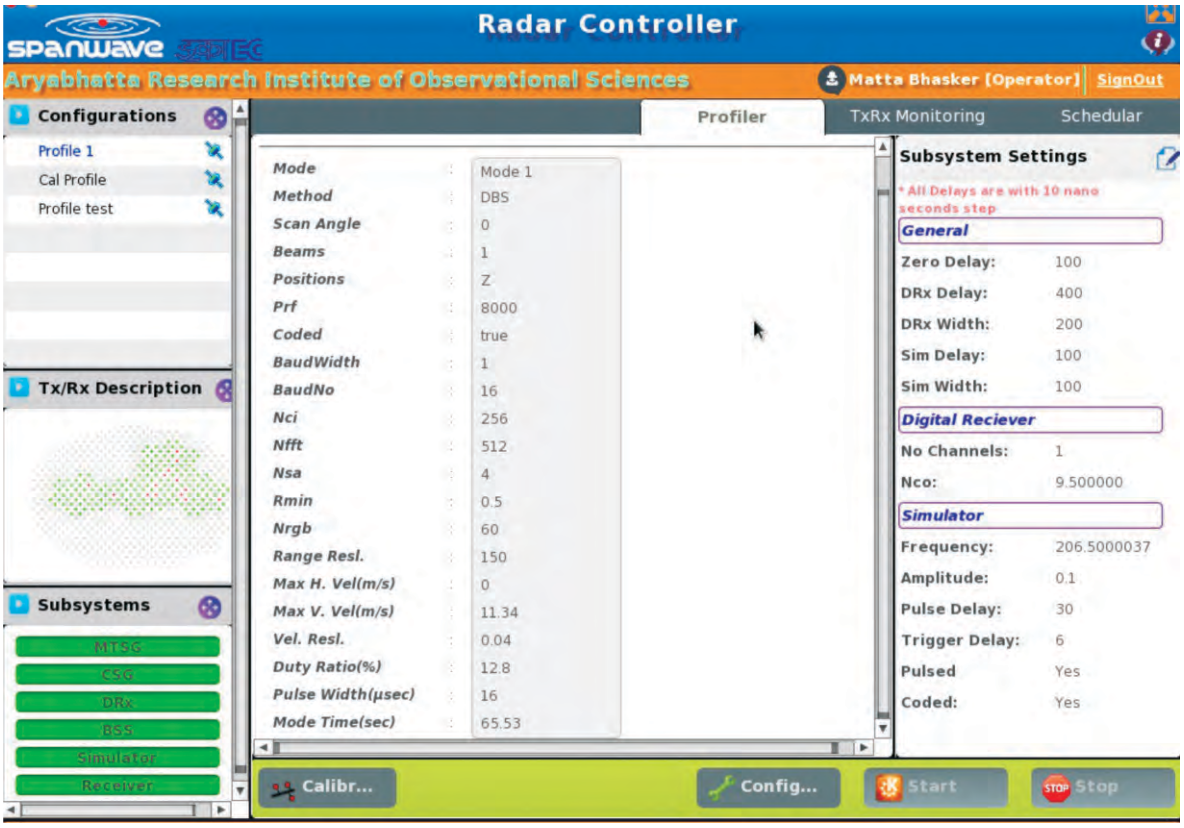

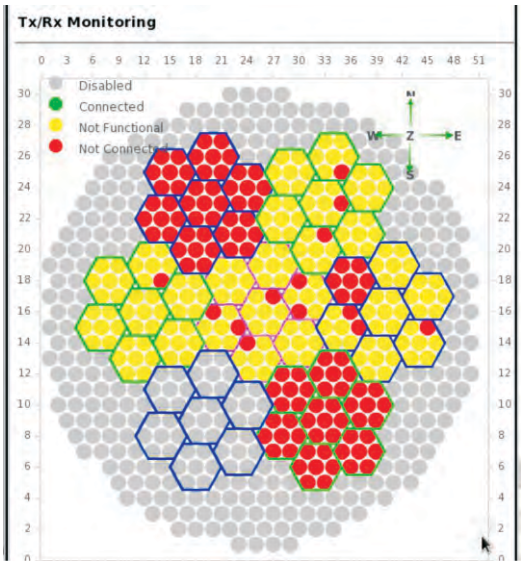

Figure 42. *(a) A typical experimental specification and control panel of radar controller system, in operation with few clusters of the array. (b) Status of some of the TRMs received by the radar controller.*

Figure 43. *Panoramic view of the Antenna array installed over the roof-top of ARIES ST Radar building.*

Characteristics of as-built 3.6m telescope pier

The pier is an important building block of large optical telescopes. There are several sources of vibrations all around the optical telescope. A large height makes it vulnerable to low frequency oscillations, both as surface waves, as well as bulk oscillations which may be transferred to the optical system. It mainly happens through the pier, since it is directly connected to the telescope. In order to avoid enhanced transfer of energy between pier and optical system, it is necessary to ensure that the resonance frequency of the pier and the telescope fixtures are fairly separated. In this work, the as-built

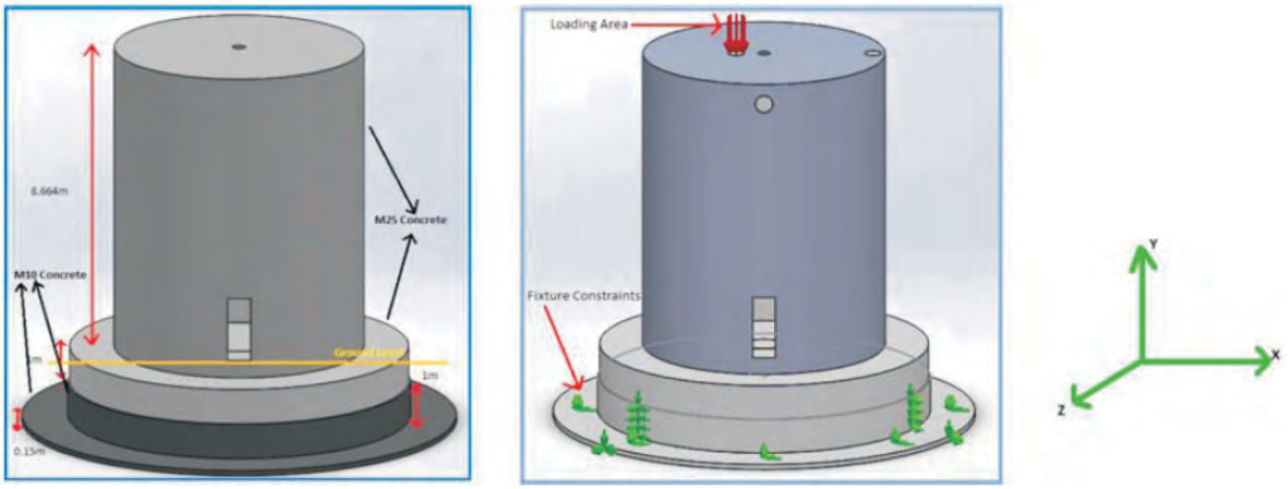

Figure 44. *A- pier model as constructed, B- loaded telescope pier for impacting, C- the coordinate system used.*

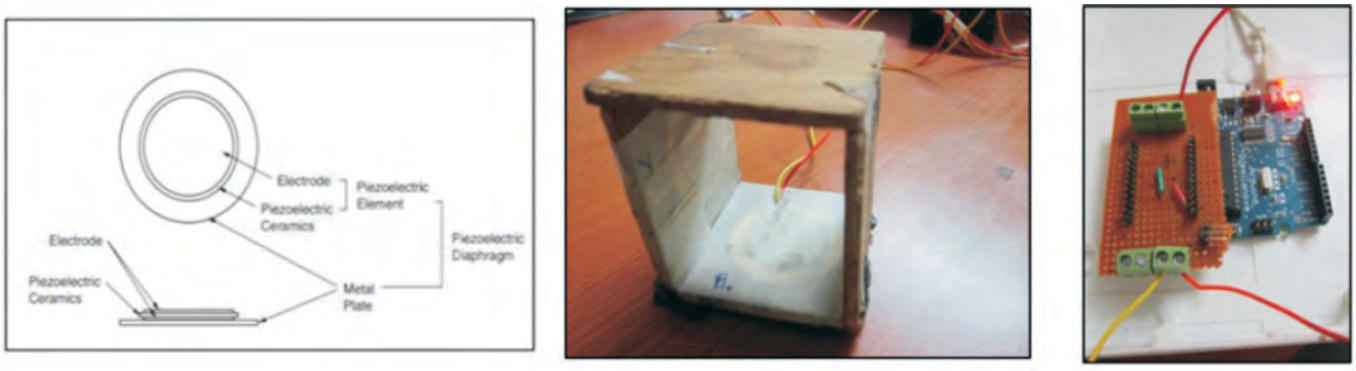

Figure 45. *Piezoelectric sensor block diagram.*

structure of telescope pier was simulated using FEM analysis for finding the resonating modes, see **Figure 44**. Various test procedures were defined and on-site testing was done using 3C geophones and piezoelectric sensors to closely observe response of the pier, **Figure 45 and 46**. The main mode in low frequency regime was found to occur at approximately 22±2 Hz by both testing and simulations. Theoretical supports are also provided for observed modes. A proof of concept was demonstrated for impulse response based resonance frequency determination. It was also demonstrated that a low-cost piezoelectric sensor based test-bench can be used for finding the resonating modes, compared to expensive 3C geophones.

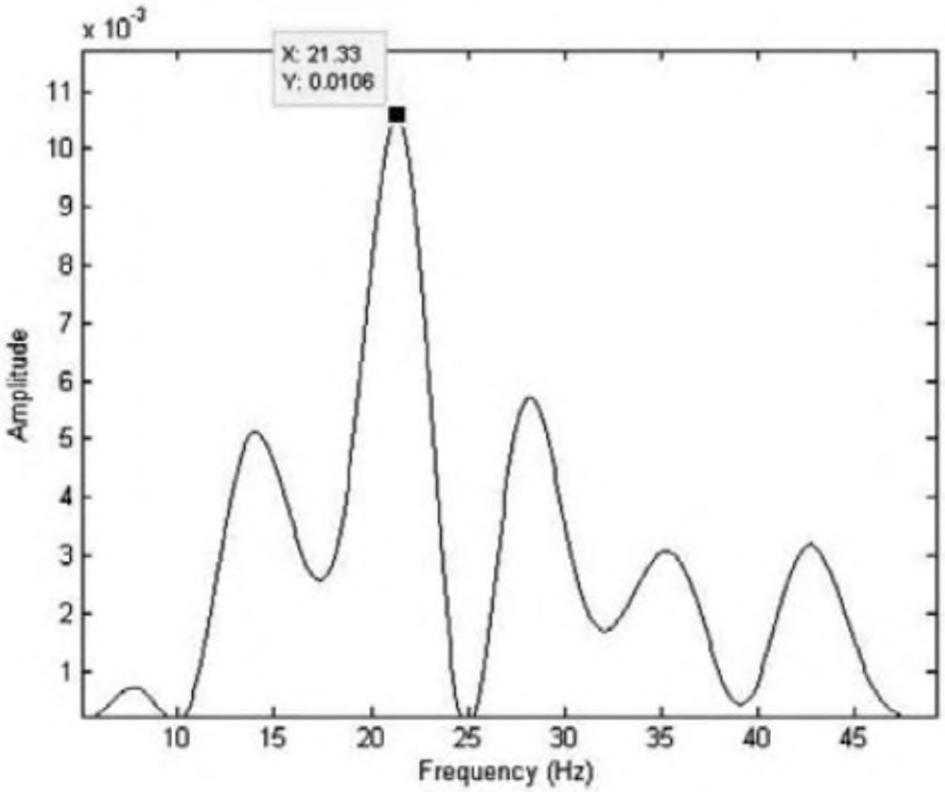

Figure 46. *FFT of Y-axis response.*

A Decade of Optical Polarimetry with AIMPOL: 2004 – 2014

In Astronomy, our endeavor is to detect polarized fraction of light originating from the celestial sources. Now it is beyond any doubt that polarimetry of celestial sources play an important role either in its own right, or in combination with other observational tools to understand the behavior of celestial sources. It is a tool to gain information on the geometry of astrophysical sources, and on the environments giving rise to polarized radiation.

In India, efforts for making polarimetric observations of celestial objects began in 1985 when M. R. Deshpande of Physical Research Laboratory made the first polarimeter. The instrument, which is still in use, is a two-channel photopolarimeter capable of measuring polarization down to 0.03% for a 5th magnitude star on 1-m telescope. Photomultiplier tubes are used as detectors to measure intensities of the ordinary and extra-ordinary rays produced by a Wollaston prism and modulated by a rotatable half-wave retarder. Taking advantage of the advances in array detector technology, A. N. Ramprakash of Inter University Centre for Astronomy and Astrophysics in 1998 made the first imaging polarimeter (IMPOL) for measuring linear polarization in the wavelength band from 400 - 800 nm. Again, a Wollaston prism is used as the analyzer to measure simultaneously the two orthogonal polarization components that define a Stoke's parameter. An achromatic half-wave plate is used to rotate the plane of polarization with respect to the axis of the analyzer so that the second Stoke's parameter also can be determined. The optical design from the above instrument was adopted by B. S. Rautela to construct one more imaging polarimeter called ARIES imaging polarimeter (AIMPOL) which is being used on 104-cm Sampurnanand telescope, Nainital since it's commissioning in 2004. It has the largest field-of-view among the polarimeters available in the country at present (8 arc min in diameter) (see **Figure 47**). The mechanical fabrication of the instrument was done in the institute workshop.

Figure 47. *ARIES Imaging Polarimeter (AIMPOL) attached with 104-cm Sampurnanand Telescope.*

From 2004 onwards, the instrument is available for regularly observations with the 104-cm telescope. From comets to clusters and from individual stars to the follow-up observations of supernova, AIMPOL has been used by astronomers of ARIES to address various issues related to astronomy and astrophysics. The demand for the instrument is a growing, for instance, in 2013-14, 40% of the total time allotted for the telescope was for AIMPOL. A list of publications resulted from the data obtained from AIMPOL since 2004 is given below.

1. Broad-band polarimetric follow-up of Type IIP SN 2012aw, 2014, **MNRAS**, 442, 2, Kumar,

Brajesh, Pandey, S. B., Eswaraiah, C., Gorosabel, J.

2. Additional polarised standards in the fields of known bright standard stars, 2014, Ap&SS, Soam, A., Maheswar, G., Eswaraiah, C.

3. Polarimetric studies of Comet C/2009 P1 (Garradd), 2013, **MNRAS**, 436, 3500, Das, H. S., Medhi, B. J., Wolf, S., Bertrang, G., Roy, P. Deb, Chakraborty, A.

4. Cluster membership probability: polarimetric approach, 2013, **MNRAS**, 430, 1334, Medhi, Biman J., Tamura, Motohide

5. A study of the starless dark cloud LDN 1570: Distance, dust properties, and magnetic field geometry, 2013, **A&A**, 556, 65, Eswaraiah, C., Maheswar, G., Pandey, A. K., Jose, J., Ramaprakash, A. N., Bhatt, H. C.

6. Magnetic fields in cometary globules - IV. LBN 437, 2013, **MNRAS**, 432, 1502, Soam, A., Maheswar, G., Bhatt, H. C., Lee, Chang Won, Ramaprakash, A. N.

7. BVRI photometric and polarimetric studies of W UMa type eclipsing binary FO Hydra 2013, NewA, 20, 52, Prasad, Vinod, Pandey, J. C., Patel, Manoj K., Srivastava, D. C.

8. Study of photospheric, chromospheric and coronal activities of V1147 Tau, 2013, **MNRAS**, 430, 2154, Patel, Manoj K., Pandey, J. C., Savanov, Igor S., Prasad, Vinod, Srivastava, D. C.

9.Broad-band optical polarimetric studies towards the Galactic young star cluster Berkeley 59, 2012, **MNRAS**, 419, 2587, Eswaraiah, C., Pandey, A. K., Maheswar, G., Chen, W. P., Ojha, D. K., Chandola, H. C.

10.A multiwavelength polarimetric study towards the open cluster NGC 1893, 2011, **MNRAS**, 411, 1418, Eswaraiah, C., Pandey, A. K., Maheswar, G., Medhi, Biman J., Pandey, J. C., Ojha, D. K., Chen, W. P.

11.Polarization towards the young open cluster NGC 6823, 2010, **MNRAS**, 403, 1577, Medhi, Biman J., Maheswar G., Pandey, J. C., Tamura, Motohide, Sagar, R.

12.LO Pegasi: an investigation of multiband optical polarization, 2009, **MNRAS**, 396, 1004 Pandey, J. C., Medhi, Biman J., Sagar, R., Pandey, A. K.

13.Optical polarimetric study of open clusters: distribution of interstellar matter towards NGC 654, 2008, **MNRAS**, 388, 105, Medhi, Biman J., Maheswar, G., Pandey, J. C., Kumar, T. S., Sagar, Ram

14.Broad-band optical polarimetric study of IC 1805, 2007, **MNRAS**, 378, 881, Medhi, Biman J., Maheswar, G., Brijesh, K., Pandey, J. C., Kumar, T. S., Sagar, R.

15.ARIES imaging polarimeter, 2004, BASI, 32, 159, Rautela, B. S., Joshi, G. C., Pandey, J. C.

S. No:	Refereed Journal	No: of Publications
1	MNRAS	11
2	A&A	1
3	New Astronomy	1
4	BASI	1
5	Ap&SS	1

Development of New Softwares for the Upcoming Observing Facilities

Observatory Control Software for 3.6m Devasthal Optical Telescope (August, 2013 to March, 2014)

A new GUI of Observatory Control Software (OCS) for 3.6m Devasthal Optical Telescope has been developed and its interface with the TCS has been tested using the Telescope Control System (TCS) Simulator. OCS is a software system which provides interface to generate and send commands to Telescope Control System, Instrument Control System and Dome Control System etc. It also provides remote access interface and receives information from Weather Monitoring System. It receives the status information from various systems and update the status on OCS GUI window.

This version of the OCS provides interface to the telescope Control system using GUI as well as Command Interface. GUI for ICS and DCS have also been integrated with this version of OCS.

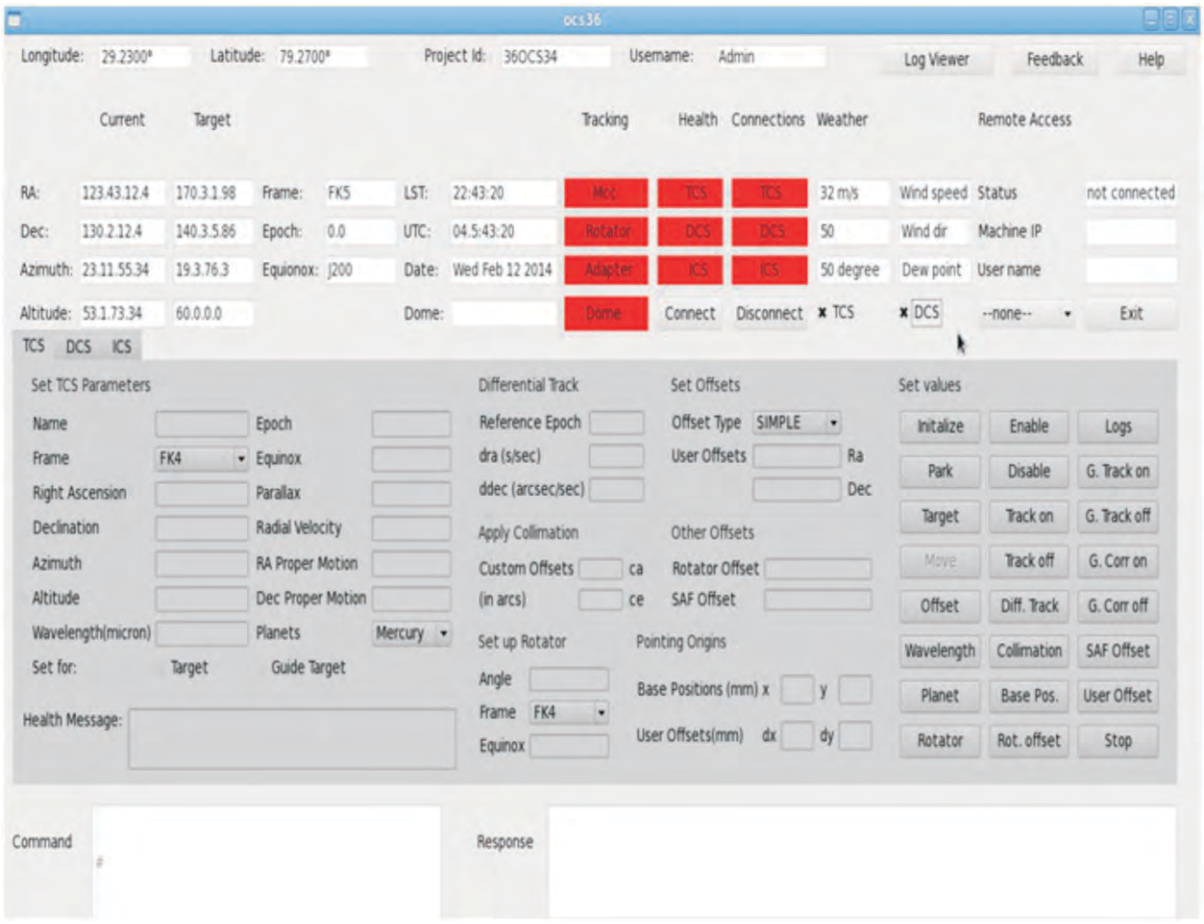

Figure 48. *A snapshot of the GUI of the Observatory control system.*

Platform: Fedora Linux Version 16
Framework: Qt 4.8 Framework (C / C++)

ARIES PARTICIPATION TO THE THIRTY METER TELESCOPE PROJECT, STATUS REPORT 2013-14

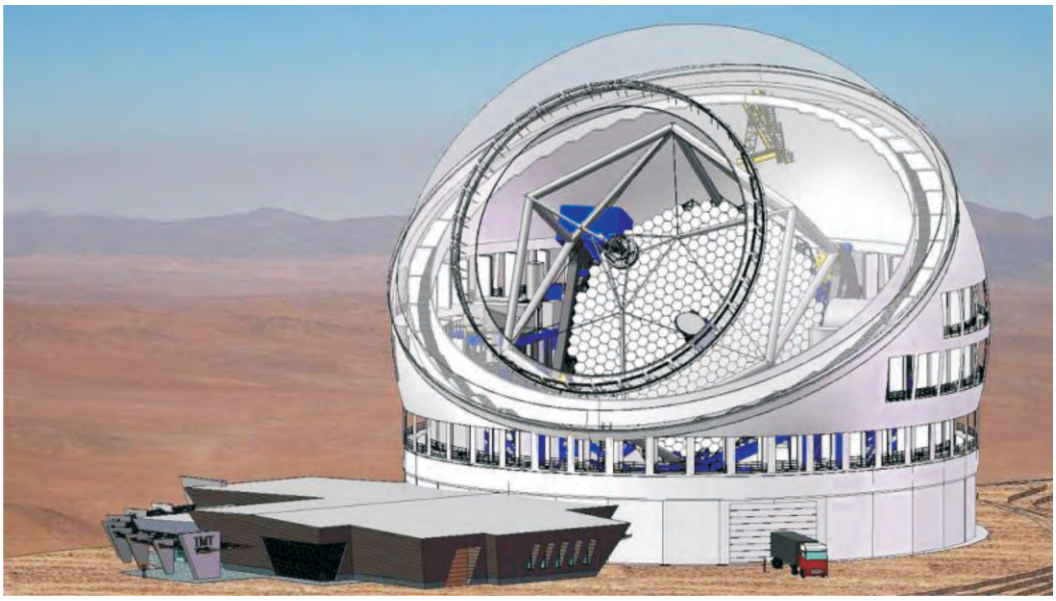

Figure 49. *Thirty Meter Telescope: enclosure with all vents open (Image source: Google)*

The primary mirror ("M1") of the Thirty Meter Telescope (TMT) is comprised of 492 hexagonal mirror Segments. Each mirror segment is 1.44 meters measured across corners These segments need to be maintained at the required surface accuracy and stability, against structural deformations caused by temperature, gravity, wind and seismic vibrations. For this each segment is actively controlled by three actuators and passively controlled by the Segment Support Assemblies (SSA). SSAs, thus support each mirror segment with minimum deformations to the optical surface under variable environments and therefore form an important component of the primary mirror cells **(see Figure 50).**

ARIES, one of the participating institutes to ITCC in collaboration with the TMT head-office, intends to engage two separate vendors in the execution of this work, i.e. “Fabrication and delivery of 6 version-3 segment support assemblies, assembly tooling and test-bed hardware” each vendor performing approximately half of the work. The Vendor(s) is expected to fabricate, assemble and deliver hardware including six SSAs, various tooling and other hardware for the purpose of supply chain development & vendor qualification. The prototypes will be delivered to ITCC and TMT project for qualification testing and demonstration. ITCC and the TMT project shall provide all of the drawings, specifications, and assembly procedures, making this primarily a build-to-print effort. The vendor has to provide a list of suppliers from whom the bought out items are being planned to be procured and confirm the availability of the required quantity from the vendor and include the same in the quotation. Because this work-scope includes supply chain development and cost estimating for the production

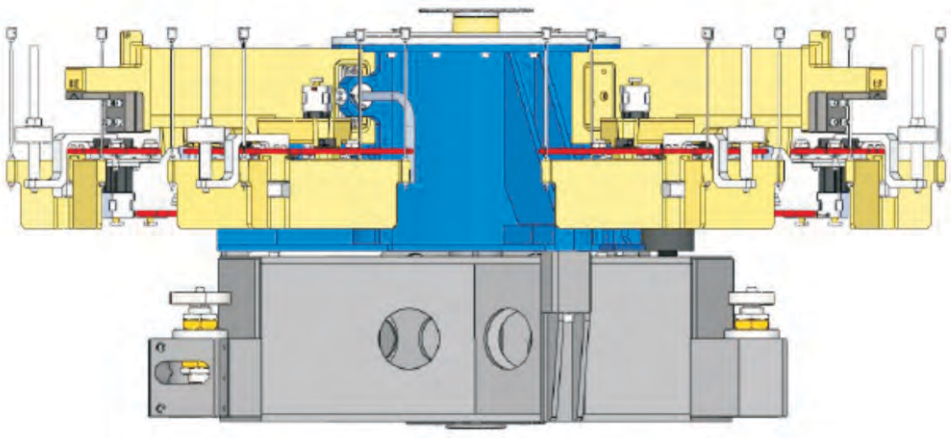

Figure 50. *Complete Segment Support Assemblies (SSA) module with the sub-assemblies.*

program (580 SSAs), it is necessary that the respondents either have the existing capability for performing the production work, or a credible plan for performing the production work, in order to be qualified for this work.

Director ARIES (ex-officio Co-I of the India-TMT related activities) constituted a high level committee on 04/10/12 under the chairman-ship of Prof. Ramesh Koul from BARC Mumbai and other members from the participating institute to evaluate the technical proposals to award the contract and monitor the manufacturing of prototypes of SSAs. The contract of prototyping of SSAs was awarded in September 2013 to two companies namely Avasarala Tech Ltd. and Godrej. The manufacturing work at both the firms is going on as per schedule in consultation with the project office.

ARIES scientists and engineers are also involved towards other ongoing work-packages i.e. polarimetric modelling of the Thirty Metrer Telescope, manufacturing of the leaf-springs for SSAs, involvement in the Telescope Control software, first generation back-end instruments etc.

Dr. S. B. Pandey from ARIES is nominated as member of the Scientific Advisory Committee along with other members for the TMT project.

Devasthal – An Observatory in Making

Devasthal is the second campus of ARIES. It is located about 50 km by road towards east of Nainital.The altitude of 2540 m of the Devasthal site makes it one of the most promising high-altitude sites of India. The site offers excellent dark skies (darkness per square arc sec sky, V~21.8 mag) due to the lack of large scale human settlements. With the installation of 1.3m telescope, the Devasthal site has become an observatory. With the installation of 3.6-m telescope, the observatory will be housing India's biggest telescope.

A number of developmental activities have taken place during last one year. The 3.6-m telescope enclosure building is now complete. We are gearing up for the installation of the telescope inside the building. A computer center has been setup which includes office space for the eight staff members who are posted at Devasthal. Several new facilities are planned for the site. For instance, a new 160 kva generator, interlinking 400 and 160 kva generators, lightening arresters and proper earthing are some of them. Recently a new microwave terminal has been installed to improve connectivity between Manora Peak and Devasthal campuses. This is in addition to the 20 mbps connection that was available already.

The new microwave link is operating at 5.4 Ghz band and is weather proof. Throughput of this device is 110 Mbps in 20 MHz channel bandwidth and Ethernet output is 1000 Base T(RJ45). System supports range of 54 kilometers in 20 MHz channel bandwidth and typical latency of radio is up to 10 ms round trip. It can be monitored using web-based system(GUI).

The eight staff members who are posted at Devasthal are to maintain and run facilities. Of there three are related to computer hardware and software, three are for electrical and electronic related work and one is for mechanical. One person is looking into the maintenance of 130-cm telescope. Setting up of a small workshop and an electronics lab is also planned. The observatory is guarded by security personals.

Devasthal has a guest house with 4 rooms. It can accommodates a total of 8 persons. A canteen runs on no loss and no profit basis.

Figure 51. *New microwave tower installed at* Devasthal.

Report on the Existing Observing Facilities

104 cm Sampurnanand Telescope

From 1972 onwards, the 104-cm Sampurnanand Telescope (ST) is utilized as the main observing facility to carry-out research in the optical domain by the students and scientists. The preventive maintenance and the image quality tests were carried out regularly by the scientists and the engineering staff of the ST.

The two of the major back-end instruments Wright 2K CCD, Tek 1K CCD and ARIES Imaging Polarimeter (AIMPOL) were working satisfactorily. Various scientific programs such as; study of star-clusters, star-forming regions, AGNs, optical counterpart of Gamma-ray-bursts and supernovae, polarimetric studies of star-forming regions and late type stars etc. were carried out using this facility.

Figure 52. *The optical 104-cm Sampurnanand telescope at ARIES.*

Statistics of Observations

Joint Time Allocation Committee (JTAC) allotted approximately 50% of time for CCD imaging, 40% of time for imaging polarimetry and 10% of time reserve for Target of Opportunity (ToO) as well as for Time Critical Observation (TCO). During the period of 2013 – 2014, out of 273 allotted nights, nearly 160 nights were clear for observations. There were 12 publications in refereed journals and 2 in conference proceeding based on the data taken from ST.

130 cm Devasthal Fast Optical Telescope

Various photometric programs were carried out using 130 cm Devasthal Fast Optical Telescope (DFOT). Recently, the filter wheel was made automatic so that the filters can be selected from the console room itself. This was developed in-house by our engineers. The dome of this telescope retracts fully making it a open roof telescope. A new observatory control system (OCS) has been developed for the 1.3m telescope observations. This OCS will have arrangement to operate the telescope along with the instrument operation and filter movement. Now this is ready and observations from the telescope can be remotely done by any computer connected through internet. A data archive system has been developed which can be accessible on the internet so that the observers can download the data taken from telescope, based on a number of search criteria such as object name, their coordinates, observer name etc.. All the observing log of the observations is now maintained online. A new website of telescope is maintained with all the necessary information regarding the telescope, its publications, its build, its operation as well as the details of various camera's which are being used on the telescope. An automatic weather station and all sky camera installed on the building provides necessary inputs on the sky and weather conditions for the observers.

Statistics of Observations

JTAC has allotted a total of 142 nights for various photometric projects to be carried out using this telescope. Of which 39 nights were lost due to bad weather and 30 nights were lost due to technical problems. A total of 73 nights were observed. There were 05 publications in refereed journals based on the data obtained from this telescope during 2013-14.

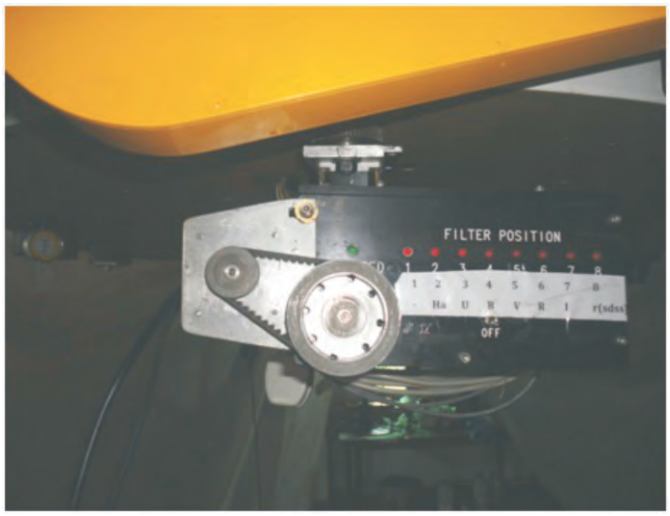

Figure 53. *Automatic filter wheel assembly used in 130 cm telescope*

The 15 inch Solar Telescope

The main solar observing facility at ARIES is 15-cm, f/15 Coudé Solar Tower Telescope equipped with Hα filter, and CCD camera (1K×1K, 13 μ2, 16 bit, 10 MHz read out rate, frame transfer, back Illuminated). It has a spatial resolution of 0.58" per pixel. It is an automatic Hα flare patrolling system, which takes fast sequence of images in the flare mode observations. The main objective of the group is to observe the solar eruptive events (e.g., solar flares, filaments and prominences eruptions, surges etc.). The group also has FeX 6374 Å, FeXIV 5303 Å, FeXI 7892 Å filters to observe the corona during total solar eclipse. The space based advanced data acquisition and analysis environments are also available to pursue solar research.

The Manora Peak site where the telescope is commissioned, is a reasonable site with good observing conditions especially in first half of the day. The total clear observing days are approx. 250 per year.

Figure 54. *15-cm Coude Solar tower telescope for solar observations.*

Atmospheric Sciences Observing facilities

Main focus of atmospheric sciences group at ARIES is in the lower atmosphere and it has facilities for observations of various trace gases, optical and physical properties of aerosols and meteorological parameters. Aerosols (AOD) observations are made since January 2002 and later on observations of black carbon and aerosols number concentrations were added. Instruments for observations of different trace gases (ozone, CO, NO, NO_y, and SO_2) were also installed in late 2006. Additionally, air sampling for the analysis of greenhouse gases (GHGs) were initiated in late 2006. Recently, nephelometer and aerodynamic particle sizer have also been installed. Apart from these surface based observations, facility has been setup for balloon-borne **(Figure 55)** vertical profiling of ozone together with meteorological parameters and Lidar based aerosols profiling.

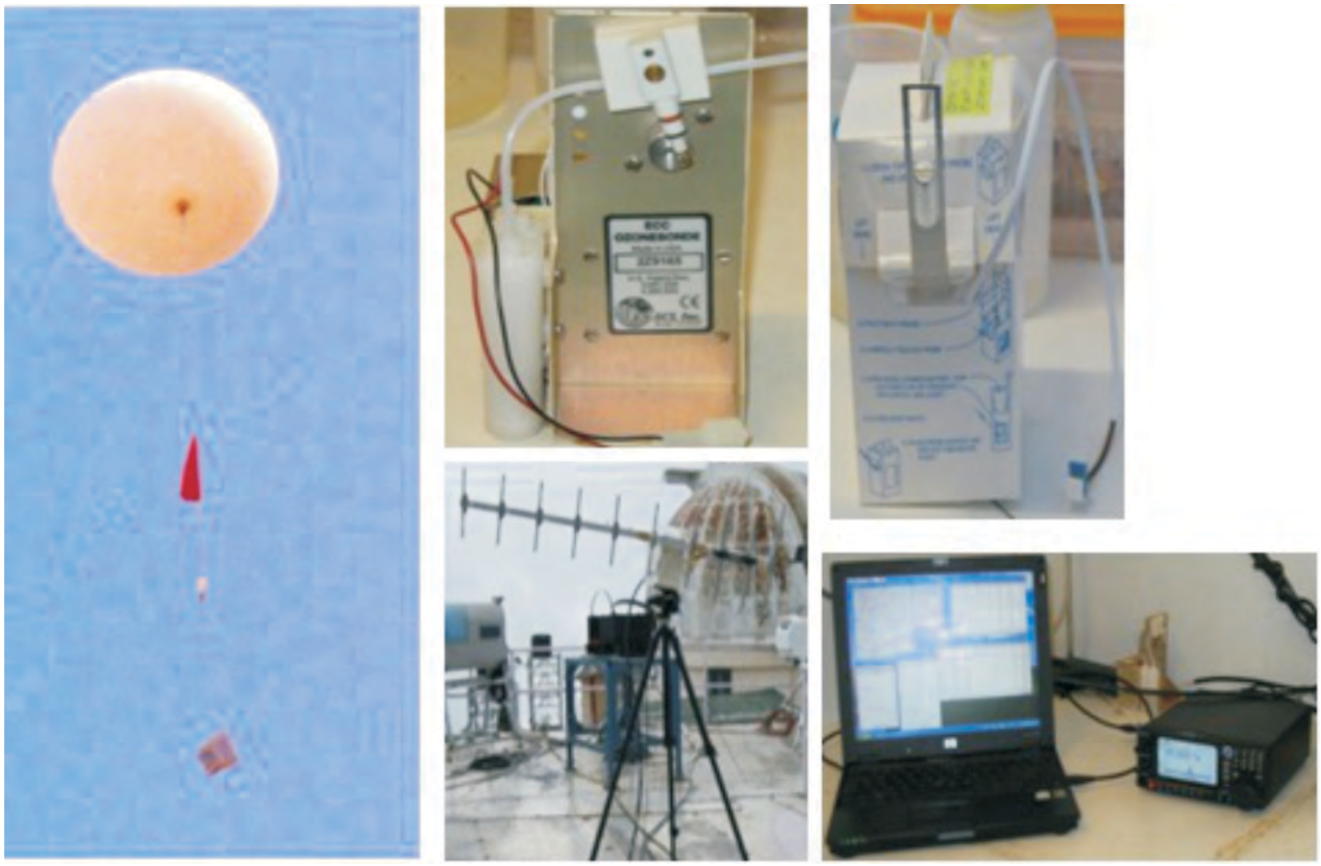

Figure 55. *Balloon-borne experiment for observations of ozone and meteorological parameters. (a) Complete setup with balloon, parachute, reel and sensors, (b) ozonesonde (c) radiosonde (d) Antenna (3) data acquisition system are also shown.*

Knowledge Resource Centre (KRC)/Library

Institute has a well stocked automated library which is named as Knowledge Resource Centre (KRC). It is facilitated with Wi-Fi connectivity. The ARIES KRC acquires books and journals mainly related to Astronomy & Astrophysics and Atmospheric Sciences. The KRC also acquires reference books at time to time. The ARIES KRC is a member of FORSA (Forum for Resource Sharing in Astronomy and Astrophysics), which was established by Indian Astronomy Librarians in 1979. The ARIES KRC is also a member of National Knowledge Resource Consortium (NKRC). NKRC provides free access of Subscribed Online Databases to DST and CSIR institutions.

KRC Resource Development

During the period 2013 – 2014, the following information resources were added:-

Books	:57
Subscription to Journals	:66 (Print + Online) + 14 Full Text Databases
Publications in refereed journals	: 61
Theses awarded	: 06
The collection at the end of the period is Books	: 10,565
Bound volumes of Journals	: 11,205

Apart from books and journals, non-book materials such as slides, charts, maps, diskettes, CD-ROMs, etc. are also available in the KRC. During 2012 – 13, the LIBSYS 4.0 software of the KRC was upgraded to LIBSYS 7.0. The new features of Online Catalogue are available at Web-OPAC on ARIES home page. DSpace, an open source software is used for the digital repository of ARIES, where KRC preserves Scientific documents, Academic Reports, Photographs of special events, Newspaper Clippings, etc.

Figure 56. *KRC Main Reading Hall.*

Academic Programmes of ARIES

The Academic Committee (AC) of ARIES is pursuing a goal to invigorate the academic endeavours of the Institute. The present members of the committee are: [1] Dr. I. Chattopadhyay (Chariman); [2] Dr. A. C. Gupta; [3] Dr. J. C. Pandey; [4] Dr. A. K. Srivastava; [5] Dr. Hum Chand; and [6] Dr. D. V. Phanikumar. Mr. V. K. Singh acts as the AC secretary.

Major activities of AC in 2013-2014 are listed below:

(A) Joint Entrance Screening Examination (JEST) :

One member of Academic Committee (Dr. D. V. Phani Kumar) managed the JEST 2014 examination at Nainital centre. AC also participates actively in over all planning of JEST on the behalf of ARIES.

(B) PhD entrance interviews :

AC organizes the interviews every year to select PhD students as Junior Research Fellows in ARIES. Dr. J. C. Pandey through his tireless efforts arranged the pre-PhD entrance interview in May 2013. Students who are MSc in physics/astrophysics and have qualified JEST/ NET/ GATE are invited to appear in an interview. Candidates who have successfully qualified the interview are selected as Junior Research Fellows and are inducted in the pre-PhD course work. In the year 2013, 3 students entered ARIES pre-PhD coursework, but one eventually left.

(C) Summer Project Students :

The summer project internship is one of the significant endeavors of the academic committee which provides training to Bachelor/Master level students from various universities and provides glimpses in cutting-edge research and development activities of the Institute. Dr. Hum Chand is in overall management and planning and execution of the visiting students programme. In the summer of 2013-14, many summer project students have been selected for pursuing the project at ARIES followed by submission of their project report and evaluation as well as open oral talks.

(D) Conducting the Course Work of ARIES Post Graduate School :

Academic Committee has made the detailed course work structure in Astronomy & Astrophysics, and Atmospheric Science for the students joining the ARIES. Committee conducts the trimester pattern followed by three months project in the specialized area of the basic research.

The extensive course work is followed by rigorous examination. Each instructor takes the examination under the supervision of the AC, and evaluate the students as per the criteria made by the AC. The project related evaluations, commissioning of respective committees and experts, and arrangements of the project talks, are also executed by AC. In 2013-2014, AC conducted the examination and project presentations of the first year batch 2012-13. Following students successfully negotiated course work 2012-13, and entered the main PhD programme of ARIES:

[1] Ms. Abha Monga

[2] Ms. Aditi Agarwal

[3] Ms. Arti Joshi

[3] Mr. Parveen Kumar

(E) PhD Thesis awarded:

As many as four students of ARIES defended their PhD thesis during April 2013-March 2014. And they are:

a) Dr. Rupak Roy,

b) Dr. C. Eswaraiah,

c) Dr. Haritma Gaur

d) Dr. Sumana Nandi

All of them are currently post-docs abroad.

Moreover, Ms. Tapaswini Sarangi submitted her PhD thesis.

(F) Conducting/Managing Post Doctoral Fellows:

All the applications related to postdoctoral fellows are processed throughout the year by AC. Under the guidance of the Director, the AC arranges the expert committee for the post doctoral position and the interview cum talk of the applicants. AC also manages the annual reviews of the post-doctoral fellows. Three ARIES students joined as Post docs in ARIES, after submission of their thesis and fulfilling the norms of the Institute and they are:

1. Narendra Ojha

2. Sumana Nandi

3. Akash Priya.

And Post-doctoral Fellows who joined other Institutes during their period were:

Dr. Bharat Kumar Yerra

Dr. Rupak Roy,

Dr. Hartima Gaur

Dr. C. Eshwariah

Dr. Narendra Ojha

Dr. Sanjay Kumar

Dr. Sumana Nandi

Two existing Post-doctoral fellows:

I. Dr. Navin C. Joshi

II. Dr. Akash Priya

(G) Conducting the Annual Student/Postdoc Reviews :

Every year around the month of July/August, AC under the guidance of the Director, forms the expert panels , select the examiners, and furnish the details of the Junior and Senior Research Fellows of the Institute to conduct their annual review process. The recommendations on upgrading their fellowships, thesis submissions etc are based on the significant review process organized by the committee. In 2013 the following students have been promoted to SRF after the review process :

[1] Mr. Abhishek Paswan

[2] Ms. Neha Sharma

[3] Mr. Subhajit Karmakar

Public Outreach Programmes

Over view of the facilities and regular activities

For the purpose of disseminating scientific information to the public as a part of the public outreach program, ARIES has set-up a science center comprising of one virtual lecture hall equipped with 44inch LED display for online courses, and a video-cum lecture hall with capacity of about 40 students. Beside this an exhibition hall is set-up to display the science model and posters to the school students. In addition to these a small 14 inch telescope has been installed to facilitate live night sky visual observations for the general public every Tuesday and Thursday.

Recently, a digital planetarium of 5m diameter has been installed in the science center. In this planetarium a collection of about 2 dozen videos with full dome shows, where students and general public get almost real night sky 3D feeling of astronomical phenomenon. This has become a major source of attraction particularly for students from various schools who visit ARIES.

ARIES science center is open to public on all the working days.

Popular science program at ARIES

ARIES Training School of Observational Astronomy:

ARIES Training School of Observational Astronomy (ATOSA) is a annual program in which about 30-40 post graduate students with post-graduate science background from different universities/Institution participate to get trained in observational Astronomy in optical domain. This year it was held between March 3rd -12th , 2014. The school consist of about 30 lectures and about 8-10 half days data analysis sessions. The total number of participants were about 35, mostly from post-graduate levels. The total number of application received this year was about 450.

Premier of Popular science Film :

Premier show of Nobel at nineteen (a popular science Film based on work and life of S. Chandrasekhar) Produced by Vigyan Prasar was organized by ARIES on 4th April 2013. In this show about 200 students from different school of Nainital and its nearby area were invited to watch the film along with a popular talk delivered by ARIES scientist.

Virtual observations session: IIT Roorkee

In association with IIT Roorkee astro-club, ARIES outreach group has organized a live “VIRTUAL OBSERVATION” events on 28th September 2013, through the state of art ARIES 1.3m Devasthal telescope to experience the glorious experience of observations. The live telecast was done with state of art video facility.

Popular science program outside ARIES

ARIES also participate in many outside campus activity by providing the support as resource persons. Few of them are listed as below.

- Vigyan Jagrukta Adhiveshan at Vashist Nagar, Gorakhpur
- 3rd vision Uttrakhand-2013 Exhibition at Ramnagar (17th - 19th May 2013)
- 7th Science & Technology Expo 2013 at Bhimtal

- (6^{th} - 8^{th} June 2013)
- Cosmos from my terrace at K R Manglam School, Gurgaon (9-10 September 2013)
- Telescope assembling Workshop at Guru Govind Singh College, Chandigarh (24^{th} -25^{th} February 2014)
- Astronomy workshop for Teachers at Alligarh (4^{th} -6^{th} December 2013)

Working model of 3.6 m telescope

As part of the public outreach activities, a working model of 3.6 m telescope has been made to display them at various locations for the visitors who visit ARIES. This model was made using wood material and runs on motors operated remotely. The scale of the model is 1:24.

Figure 57. *A working model of 3.6m optical telescope.*

Indo-UK seminar at ARIES

Summary of Workshop

The Indo-UK seminar was held at ARIES during 26-28 March 2014. The seminar was sponsored by DST Govt, of India and the Royal Society U. K. The theme of seminar was "plasma processes in the Solar and Space plasma at diverse spatio-temporal scales: upcoming challenges in the science and instrumentation". Total 35 Scientists, PDFs and PhD students from U.K. and India have participated in the seminar. During the seminar, total 22 talks and 8 posters were presented. Most of the talks were review talks and duration of each talk was 45 minutes. At the end of each day a session was devoted to the discussion on outcomes and collaborations. The outcomes of this seminar were manifold like research, innovation and training. The seminar have provided a basis for further collaborations that will enable a major leap towards finding of MHD waves and related phenomenon in the Sun and Sun-like stars . Further, it was an excellent platform for PhD students to develop their research skill. It was also decided that the talks delivered by invited speaker will be published as review article in special issue of Journal of Astronomy and Astrophysics.

Figure 58. *Participants at ATSOA-2014 school during 3rd -12th March 2014.*

Figure 59. *Lecture session during Astrophysics workshop at DAV College, Amritsar*

Figure 60. *Night SkyWatching during Telescope Assembling workshop at GGS College, Chandigarh*

Figure 61. *Releasing of the Cd's of the Popular Science Film - Noble at nineteen*

Figure 62. *Popular science film show during Astronomy workshop for Teachers at Alligarh*

Figure 63. *A student interacting with audience during Virtual observation programme.*

Figure 64. *Demonstration session during Cosmos from my terrace at K R Manglam School, Gurgaon.*

Figure 65. *Prize distribution during Vigyan Jagrukta Adhiveshan at Vashist Nagar, Gorakhpur*

Figure 66. *Sunspots watching during Cosmos from my terrace at K R Manglam School, Gurgaon*

Figure 67. *Inauguration of Two days workshop on Astrophysics at DAV college Amritsar.*

Abbreviations

AC	Academic Committee
ADFOSC	ARIES Devasthal Faint Object Spectrograph and Camera
AGN	Active Galactic Nuclei
AIA	Atmospheric Imaging Assembly
AIM	ARIES In-house Meeting
AIMPOL	ARIES Imaging Polarimeter
AMOS	Advanced Mechanical and Optical Systems
AOD	Aerosols Optical Depth
ASTROSAT	Indian Satellite Mission for Multiwavelength Astronomy
ATSOA	ARIES Training school in Observational Astronomy
BAL	Broad Absorption Line
BL Lac	BL Lacertae
BVR	Blue-Violet-Red
BVRI	Blue violet Red Infrared
CCD	Charged Coupled Device
CME	Coronal Mass Ejection
CNC	Computer Numerical Control
COSPAR	Committee On Space Research
CTIO	Cerro Tololo Inter-American Observatory
DC	Duty Cycle
DCS	Dome Control System
DDRGs	Double-double Radio Galaxies
DOT	Devasthal Optical Telescope
DSP	Digital signal processor
DU	Dobson Units
ECIL	Electronics Corporation of India Limited
EUV	Extreme ultraviolet
FCS	Filter Control System
FOSC	Faint Object Spectrograph and Camera
FSRQs	Flat-Spectrum Radio-Loud Quasars
GATE	Graduate Aptitude test in Engineering

GBM	Gamma-ray Burst Monitor
GCs	Globular Clusters
GMRT	Giant Meterwave Radio telescope
GRB	Gamma-Ray Burst
GRS	Global Positioning System
GUI	Graphic User Interface
HMI	Hydrargyrum medium-arc
ICS	Instrument Control System
IFDL	Instruments Facility and Development Laboratory
IGP	Indo-Gangetic Plane
INOV	Intranight Optical Variability
IRAC	Infrared Array Camera
ISS	Interstellar Scintillation Studies
IUCAA	Inter-University Centre for Astronomy and Astrophysics
JEST	Joint Entrance Screening Test
KRC	Knowledge Resource Centre
LAT	large Area Telescope
LIDAR	Light Detection and Ranging
LSPs	Layered Service Provider
MDI	Michelson Doppler Imager
MHD	Magnetohydrodynamic
MIR	Mid Infra Red
MOPITT	Measurement of Pollution in the Troposphere
MST	Mesosphere-Stratosphere-Troposphere
NARL	National Atmospheric Research Laboratory
NERC	Natural Environment Research Council
NET	National Eligibility Test
NGC	New General Catalog
NIR	Near Infra Red
NKRC	National Knowledge Resource Consortium
NLSy1	Narrow-line Seyfert1
NOAA	National Observatory of Astronomy and Astrophysics
OCS	Optical Control System

OMI	Ozone monitoring Instrument
OPAC	Online Public Access Catalogue
PIT	Project Implementation Team
PMB	Project Management Board
PWG	Project Working Groups
QSO	Quasi-Stellar Object
RL-BALQSOs	Radio-Loud Broad Absorption Lines
RRTMG	Rapid Radiative Transfer Model
SAC	Scientific Advisory Committee
SAO	Smithsonian Astrophysical Observatory
SAT	Site Acceptance Test
SDO	Solar Dynamics Observatory
SLL	Side Lobe Level
SOHO	Solar and Heliospheric Observatory
SQL	Structured Query Language
ST Radar	Stratosphere Troposphere Radar
ST	Sampurnanand Telescope
STA	Semiconductor Technology Associates
TIG	Tungsten Inert Gas
TMT	Thirty Meter Telescope
UBVRI	Ultraviolet-Blue-Visual-Red-Infrared
UHF	Ultra high frequency
UV	Ultra Violet
YSO	Young Stellar Object